Optimising canine olfactory ensheathing cell therapy using tissue engineering tools

Alexander Michael Delaney

Thesis submitted for Master of Philosophy in Neuroscience

October 2016

Keele University

[Declaration]

Bursaries and awards received during MPhil

1. **Awarded the Wolfson Foundation intercalated award 2015**

   An annual national competitive bursary for which intercalating medical students nominated by their medical school may compete, Royal College of Physicians, July 2015.

2. **Awarded the Comparative Clinical Science Foundation Intercalated Award 2015**

   An annual national competitive bursary awarded to one intercalating medical student and one intercalating veterinary science student in order to encourage communication and collaboration between the two disciplines, One Medicine by the CCSF, July 2015.

Abstract

The adult mammalian spinal cord is incapable of significant regeneration following injury. As such, spinal injury is a lifelong debilitating condition which represents a significant burden on healthcare globally. Olfactory ensheathing cells (OECs) have been reported to promote axonal regeneration and improve locomotor function when transplanted into the injured spinal cord. A recent clinical trial demonstrated improved motor function in companion dogs following autologous transplantation of OECs derived from the olfactory mucosa (olfactory mucosal cells; OMCs). Their utility in canine subjects offers considerable promise to human translation, as dogs are highly comparable to human patients in terms of spinal lesion heterogeneity, genetic/environmental variation and management strategies. Moreover, the autologous, minimally invasive derivation of OMCs makes them an attractive cellular therapy for spinal injury in human patients. However, translating this therapy to human patients requires that two key limitations be addressed: (i) incomplete corticospinal tract (CST) regeneration; (ii) cell loss due to mechanical stress and aggregation in injection fluid.

In this regard, this thesis will test the hypothesis that OMCs are amenable to two specific tissue engineering strategies in order to address these barriers to translation: specifically, whether magnetic particles (MPs) in combination with an applied magnetic field can deliver genes encoding therapeutic biomolecules to canine OMCs (cOMCs) in order to enhance their regenerative capabilities in the injured cord. Secondly, whether 3-D hydrogel technology could function as a protective cell delivery system for cOMCs. This is with a view to the eventual development of an implantable hydrogel construct impregnated with genetically

engineered OMCs.

In this thesis, it is shown that MPs in combination with an applied magnetic field can mediate safe and efficient delivery of genes encoding a major neurotrophic factor to cOMCs, with a maximum transfection efficiency of 57%. This thesis also reports that cOMC populations can be safely grown in implantable hydrogels, which could be tissue-matched to recipients non-invasively, using a clinically available imaging technique termed ultrasound elastography (USE). The results support the concept of generating a tissue-matched, nano-engineered "plug" of genetically enhanced cOMCs for delivery to sites of spinal cord injury (SCI). Moreover, the use of cells derived from a clinically relevant transplant population indicates a strong translational potential for this approach.

Table of Contents

Acknowledgements

First and foremost, I am indebted to my lead supervisor, Professor Divya Chari, for her tireless support in every aspect of my work this year, and for teaching me what it means to produce and present work to a high standard. Also, for teaching me that success and happiness are not mutually excusive, and that it's okay to give yourself a break every once in a while. To my co-supervisor Dr Chris Adams, a constant source of ideas and advice relating to my project and someone without whose input I simply would not have succeeded. To my co-supervisor Dr Nicolas Granger, for providing the cells needed to make this project happen, for inviting me to spend time at his clinic in Bristol and for helping me to identify what can be done to improve the quality of the treatments that his patients may ultimately receive, and to his PhD student Mr Darren Carwardine for his advice relating to OEC culture.

I have been fortunate to work in an incredibly friendly and supportive environment at the Harvey Lab this year, and every member of the team has done their upmost to make me feel welcome. Thank you to Arwa Al-Shakli for her hours spent teaching me cell culture technique, Dr Alinda Fernandes for teaching me the molecular biology of minicircles and providing the DNA constructs used for my research, Dr Stuart Jenkins for his advice and ideas relating to data presentation, and Jacqueline Tickle for her frankly saint-like patience in teaching me lab protocol.

I received advice relating to the clinical aspects of spinal injury from the staff at the neurosurgery department of the Royal Stoke University Hospital. Special thanks to neurosurgery registrar Mr Jon Sen for his advice in this regard.

I have also been aided and advised by numerous members of ISTM throughout my project, whose intelligent insights were an on going source of ideas. Rawaa Al-Mayyahi, Sile Griffen, George Joseph, Yolanda Gomez, Dr Paul Horrocks, Dr Heidi Fuller, James Allen, Eshan Mazumdar and Olivia Walsh. Also thanks to previous MPhil student Dr Daniel Weinberg for his advice relating to the course, and for not talking me out of it.

Thank you to the staff of the Life Sciences building. Chris and Phil, for keeping the lab spotless. Christine Bain, Jane Bromley and Ian Wright for keeping everything running smoothly.

Finally, thank you to my family for all of their support this year, and to my partner Rebecca, for her unwavering belief that this is something I could do.

Abbreviations

ASIA	American spinal injury association
BBB	Basso, Beattie and Bresnahan
BDNF	Brain-derived neurotrophic factor
ChABC	Chondroitinase ABC
CNS	Central nervous system
cOMC	Canine olfactory mucosal cells
CSPGs	Chondroitin sulphate proteoglycans
CST	Corticospinal tract
DMEM	Dulbecco's modified Eagle medium
DREZ	Dorsal route entry zone
DRG	Dorsal route ganglion
ECM	Extracellular matrix
EF1a	Elongation factor 1-alpha
ELISA	Enzyme-linked immunosorbent assay
ESC	Embryonic stem cell
EtH	Ethidium homodimer
Fn	Fibronectin
GFAP	Glial fibrillary acidic protein
GFP	Green fluorescent protein
GvHD	Graft vs. host disease
iPSC	Induced pluripotent stem cells
IRES	Internal ribosome entry site
LP-OEC	Lamina propria-derived olfactory ensheathing cell
MAG	Myelin-associated glycoprotein
MP	Magnetic particle
MRI	Magnetic resonance imaging
MSC	Mesenchymal stem cell
NF	No field
NGF	Nerve growth factor
NgR1	Nogo-66 receptor 1
NSC	Neural stem cell
NT-3	Neurotrophin 3
OB-OEC	Olfactory bulb-derived olfactory ensheathing cell
OEC	Olfactory ensheathing cell
OM	Olfactory mucosa
OMC	Olfactory mucosal cell
OMgo	Oligodendrocyte myelin glycoprotein
OP-1	Bone morphogenic protein-7
ORN	Olfactory receptor neuron
PBS	Phosphate buffer solution
PNS	Peripheral nervous system
PoA	Plane of analysis

PP	Parental plasmid
RT	Room temperature
SCI	Spinal cord injury
SEM	Standard error of the mean
USE	Ultrasound elastography

Chapter 1: General introduction

1.1 Pathology of spinal cord injuries and current therapeutic strategies

1.1.1 Traumatic spinal cord injury is a significant burden on healthcare globally

The annualised incidence of SCI is around 16 per million in Western Europe (1), with approximately 50,000 people believed to be currently living with SCI in the UK. Males are almost twice as likely to incur spinal injury as females (2). The most common mechanism of SCI is work-related accident, followed closely by motor vehicle accident; combined these cause more than 50% of spinal injuries (2). Moreover, spinal injury is the second leading cause of paralysis after stroke and represents a cost of around £1 billion annually to the UK (3). It is clear therefore that SCI presents an enormous personal burden on the afflicted, their carers and family, as well as significant financial burden on the healthcare system as a whole, an issue compounded by increasing life expectancy for spinal injury patients (4). As such, there is great drive in the scientific community to investigate emerging therapies that might offer novel solutions to ameliorate the devastating effects of SCI, with the potential to also benefit patients paralysed from stroke or traumatic brain injury.

1.1.2 Basic structure and function of the spinal cord

An understanding of the gross structure and cellular components of the spinal cord is necessary to identify therapeutic targets. The spinal cord is the component of the central nervous system

which acts as the intermediary between peripherally innervated tissues and the brain. It comprises a tubular bundle of nervous tissue which occupies the vertebral canal, extending from its origin at the foramen magnum to the conus medullaris where it terminates at the L1/L2 vertebral level. It is approximately 45cm long in the adult and is comprised of cervical, thoracic and lumbar segments.

The cord is comprised of a central body of grey matter containing predominantly neuronal cell bodies, surrounded by ascending and descending white matter tracts made up of sensory and motor fibres, respectively. Afferent sensory fibres and efferent motor fibres communicate with the spinal cord through dorsal and ventral nerve roots, respectively. The spinal cord has a total of 31 pairs of spinal nerves distributed along its length each of which is comprised of motor and sensory fibres which exit the cord through vertebral foraminae formed from the superior and inferior vertebral bodies. These nerve roots are named according to the foramina through which they pass such that the 4th thoracic spinal nerves (T4) pass between the 4th and 5th thoracic vertebrae. As the cord is shorter than the vertebral column, lower lumbar and sacral nerve roots form the cauda equina (literally “horse tail”) as they continue to associate with vertebral foramina below the conus medullaris. In total there are 8 pairs of cervical nerves, 12 thoracic, 5 lumbar, 5 sacral and 1 coccygeal pair. Spinal nerves are associated with discrete sensory areas of skin (‘dermatomes’), and groups of muscle (‘myotomes’).

The cord has three dural layers, from inner to outer: pia, arachnoid and dura mater. The subarachnoid space contains blood vessels which supply the spine and allows CSF to circulate

within it. The blood supply of the cord is derived from one anterior and a pair of posterior spinal arteries, which travel longitudinally along the length of the cord. This is in addition to radicular arteries derived from the descending aorta, which continue to supply the spinal cord throughout its length through major branches, such as the arteria radicularis magna (of Adamkiewicz) (5).

In addition to neuronal components, there exists a complement of non-neuronal cells within the brain and spinal cord. These cells, known as “neuroglia”, perform various protective and supportive functions in the cord, a brief outline of which is provided here. Neuroglia (or “glial cells”) within the CNS can be divided in to three major classes: (i) oligodendrocytes, derived from the neuroepithelium are the primary myelinating cells within the brain and spinal cord, (ii) microglia, which perform immune functions within the CNS analogous to that of macrophages peripherally, (iii) astrocytes, which have been proposed to perform many functions. Astrocytes maintain homeostasis within the CNS through regulation of the chemical composition of the extracellular compartment, act as an intermediary between neutrons and their relevant vasculature, and in doing so maintain the blood-brain barrier, and regulate synaptic transmission through maintenance of efficient synaptic metabolism (6). In addition, ependymal cells which line the ventricular components of the brain and the central canal of the spinal cord are responsible for the production of CSF. Recent studies have also suggested that these cells may also act as a source of stem cells of glial lineage (7).

1.1.2 Classification of SCI

Spinal injury can be broadly classified according to the affected region of body function, and by its extent and modality. All spinal injuries are classified based on the vertebral segment at which they occur, but additional terminology is used in order to further classify the extent of the injury. For example, loss of functionality as a result of damage to spinal cord between the thoracic segments and cauda equina (but excluding cervical segments) is termed "paraplegia", manifesting itself as dysfunction of the trunk, legs or pelvic organs. Damage to the cervical spinal cord may manifest as "tetraplegia", causing dysfunction of both the upper and lower limbs. Moreover, the specific site of the lesion within the cord at any given segment can affect the symptomatology. For example, damage to motor fibres on one side of the spinal cord manifests as hemiparesis, whereas damage to sensory fibres manifests as subjective altered sensation. Finally, the extent of the sensorimotor deficit can be used to classify a lesion as "complete" or "incomplete", based on the relative preservations of various sensory and motor components. A classification system has been developed based on the relative levels of impairment caused by the various injuries. The American spinal injury association (ASIA) impairment scale uses the clinical neurological examination to grade the severity of a patients' neurological deficit. This grade has prognostic value, as will be outlined below, and is used to monitor any changes in a patient's neurological status (8). A summary of the AISA impairment scale is presented in **Table 1**.

ASIA Scoring System	
A = Complete	No sensory function is preserved in sacral segments S4-5.
B = Sensory incomplete	Sensory but no motor function is preserved below the neurological level and includes the sacral segments S4-5 (light touch or pin prick at S4-5 or deep anal pressure) AND no motor function is preserved more than three levels below the motor level on either side of the body.
C = Motor incomplete	Motor function is preserved below the neurological level, and more than half of key muscle functions below the neurological level of injury (NLI) have muscle grade 0-2
D = Motor incomplete	Motor function is preserved below the neurological level, and at least half of key muscle functions below the NLI have muscle grade ≥3.
E = Normal	If sensation and motor function are graded normal in all segments, and the patient had prior deficits, then the ASIA grade is E. Someone without an initial SCI does not receive an ASIA grade.

Table 1: ASIA impairment scale for scoring the severity of spinal injury. *Adapted from* (9).

Further, spinal injury can be classified based on the mechanism by which it is incurred. These can be considered broadly as traumatic and non-traumatic injuries. The aetiology of non-traumatic SCI is broad, and can be derived from every major organ system. For example, this can be primarily neurological, such as some rare tumors of the cord, or can manifest as a sequela of non-neurological primary pathology, such as degenerative disease of a vertebra and its discs, vascular occlusion from thromboembolic disease, spinal metastasis of distant primary cancers, or autoimmune pathology, such as multiple sclerosis. Due to the diverse aetological nature of SCI, data regarding incidence of paralysis due to non-traumatic causes are limited and as such, statistics regarding prevalence of SCI may not be representative of non-traumatic causes (10). Finally, there exist a collection of discrete spinal syndromes which

themselves represent further sub-classifications of SCI. **Table 2** provides a summary of the major cord syndromes.

Spinal Syndromes	*Aetiology*	*Symptoms*
Anterior cord	Anterior compression, flexion injury to cervical spine, thrombosis of anterior spinal artery.	Loss of pain and temperature sensation with variable paralysis. Dorsal columns preserved.
Central cord	Hyperextension injuries, spinal cord ischaemia, cervical spine stenosis.	Motor weakness greater in the upper than lower extremities and worse distally than proximally, variable sensory loss.
Brown-Séquard	Hemitransection, unilateral compression.	Ipsilateral spastic paresis and loss of proprioception and vibration sense.
Cauda Equina	Compression of cord below L1/2 vertebral level.	Variable asymmetrical weakness, bowel/bladder/sexual dysfunction, perianal anaesthesia, saddle anaesthesia.

Table 2: Major cord syndromes. *Adapted from (11).*

1.1.3 Cellular and molecular therapeutic targets.

Initial traumatic lesion and the secondary injury process

The sequelae of traumatic SCI begin at the time of injury, and can extend well in to the chronic phase. The mechanism of injury is usually traumatic insult to the vertebral column and surrounding structures, leading to vertebral fracture subluxation and/or traumatic extrusion of intervertebral discs into the vertebral canal (12). This causes traumatic loss of neurons, oligodendrocytes and astrocytes through various forms of mechanical trauma including compression, distraction and shearing force, causing membrane rupture, and then anoxic injury through primary disruption of relevant spinal vasculature. Diversity in mechanical forces commonly results in a lesion with varying degrees of contusion and laceration, with complete spinal transection injuries being relatively less common (12). This initial traumatic damage to the spinal parenchyma has been referred to as the "primary injury".

The secondary injury process occurs as the result of ongoing deleterious processes triggered by the primary injury (13). Post-mortem studies demonstrate anatomical sparing of neural circuits in patients deemed to have clinically complete SCI (14), suggesting much axonal damage occurs after the traumatic injury as a result of the ongoing inflammatory response, and renders anatomically complete circuitry non-functional. Indeed, the gross appearance of the spinal cord may not appear different until many hours after the primary injury (15), when

the visible tissue damage will extend for several vertebral segments rostrocaudally, injuring spared tracts via the cumulative effects of several proposed injury processes.

Ongoing vascular changes such as vasospasm of intact vessels, compression from reactive oedema, and a fall in mean arterial pressure from autonomic dysfunction causes ongoing anoxic injury. Toxic metabolites such as oxygen free radicals and glutamate accumulate in the tissue. Free radical accumulation causes further injury through lipid peroxidation (16), particularly in the event of a reperfusion injury to uninjured regions of the cord (17). Accumulation of glutamate leads to aberrant excitation of NMDA receptors (18). These extracellular triggers of injury converge eventually on an influx of calcium, triggering apoptotic pathways (19). In the event that the blood-brain barrier is disrupted, inflammatory cell infiltrates release lytic enzymes and initiate the inflammatory cascade. The net result of this is ongoing necrotic and apoptotic cell death. Necrotic cell death perpetuates the accumulation of toxic cellular components, and ongoing apoptotic cell death causes further functional loss (20).

Molecular regulation of spinal repair and key barriers to regeneration

Following injury, the adult spinal cord is incapable of significant regeneration. Studies which demonstrate the growth of central nervous system (CNS) axons into transplanted peripheral nervous system (PNS) tissue indicate the presence of site-specific inhibitory factors/phenomena (21). One such factor is the development of the astrocytic scar (22)

(**Figure 1a**). Following injury, resident astrocytes begin to divide and hypertrophy (23). These 'reactive' astrocytes begin to clear cellular debris fragments from the injury site as they form a capsular border around the lesion, leaving behind a cystic cavity (24). The surrounding scar forms as the astrocytes enmesh their processes, and secrete extracellular matrix (ECM) components.

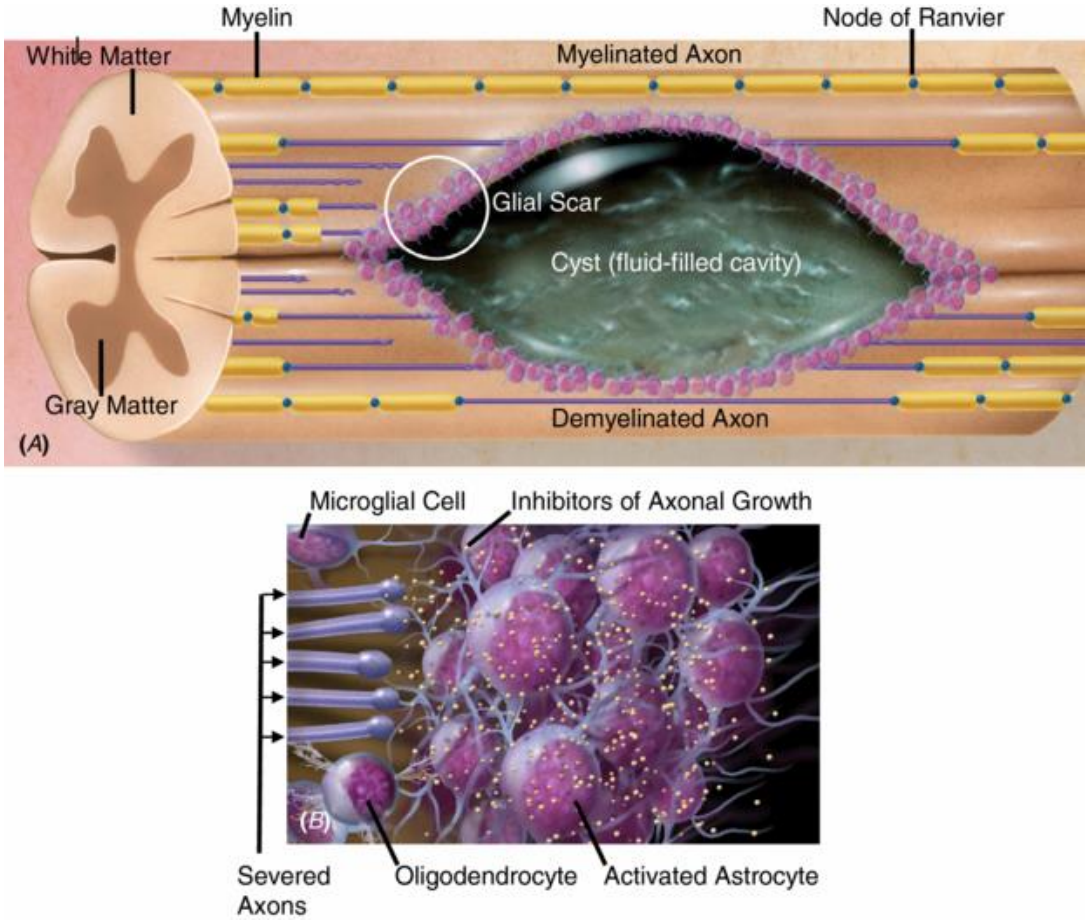

Figure 1a: Site-specific inhibitory components of the injured cord. *Following injury reactive glial astrocytes form a capsular border around the lesion, clearing debris and leaving behind a cystic cavity. Reactive glial astrocytes secrete inhibitory ECM components, while myelin breakdown produces a complement of further growth-restricting molecules, which prevent regeneration of injured axons across the lesion site. (Adapted from (24))*

While the glial scar may serve supportive functions in the cord, such as containing the inflammatory response (25), it contains many different inhibitory molecules. Some of the most studied of these are the chondroitin sulphate proteoglycans (CSPGs), ECM components with well-documented growth-restricting effects *in vivo* and *in vitro* (26). Naturally, CSPGs have been identified as a key molecular target for regenerative therapies. In 2002, Bradbury demonstrated regeneration of sensorimotor axons and recovery of locomotor and proprioceptive function in adult rats treated with intrathecal administration of the enzyme chondroitinase ABC (ChABC) (27). Since then, research using animal models has continued to test the potential for ChABC as a therapy for SCI, both alone and in combination with other therapeutic strategies such as cell therapy and rehabilitation (28,29). The promising results of this treatment have meant that the therapy is now being investigated in large animal models as part of a phase II clinical trial (30).

In addition to the inhibitory effects of ECM components, myelin is known to express numerous growth-restricting compounds. Studies of the non-permissive characteristics of myelin led to the identification of three key myelin-associated inhibitors of neuronal regeneration: Nogo, myelin-associated glycoprotein (MAG) and oligodendrocyte myelin glycoprotein (OMgp), whose inhibitory mechanisms converge on the Nogo-66 receptor (NgR1) (31). The deleterious effects of myelin-derived proteins are compounded in the CNS by the rate of debris clearance, which proceeds relatively slowly in the CNS compared with the PNS, as resident microglia respond less rapidly to traumatic insult than do peripheral macrophages (32).

Nogo demonstrates growth-restricting properties *in vitro* (33). Moreover, *in vivo* studies have demonstrated enhanced axonal regeneration if Nogo is attenuated either genetically or pharmacologically (34,35). The evidence for Nogo as a potent inhibitor of neural growth is strengthened by the observation that Nogo is present in CNS but not PNS myelin (36). A multi-centre phase I clinical trial into the efficacy of Anti-Nogo antibodies in human SCI subjects concluded in 2011, although no data has yet been published (37).

Finally, there exists a class of signaling molecule known as the neurotrophins that exert some control over the regeneration of the spinal circuitry through action on receptor tyrosine kinases. The first to be discovered was nerve growth factor (NGF) by Levi-Montalcini in 1951, noted for its growth-promoting effect on sympathetic and sensory neurons in rodent models (38). This was followed by the discovery of brain-derived neurotrophic factor (BDNF), and later neurotrophin-3 (NT-3) (39,40). As will be described in **Section 1.3.1**, these factors are strong candidates for use in combinatorial strategies in spinal repair and regeneration.

The complex sequelae of SCI therefore represents a collection of potential targets for neural regeneration research (**Figure 1b**): The breakdown of the glial scar, the regrowth of spinal vasculature and the regeneration of damaged axons are among these. However, a consensus is emerging in regenerative medicine that addressing only one of these targets is unlikely to be sufficient. There is a move therefore to the development of so-called 'combinatorial strategies', which combine more than one regenerative treatment in order to address

multiple facets of the injury process simultaneously (41). These will be described further in subsequent sections.

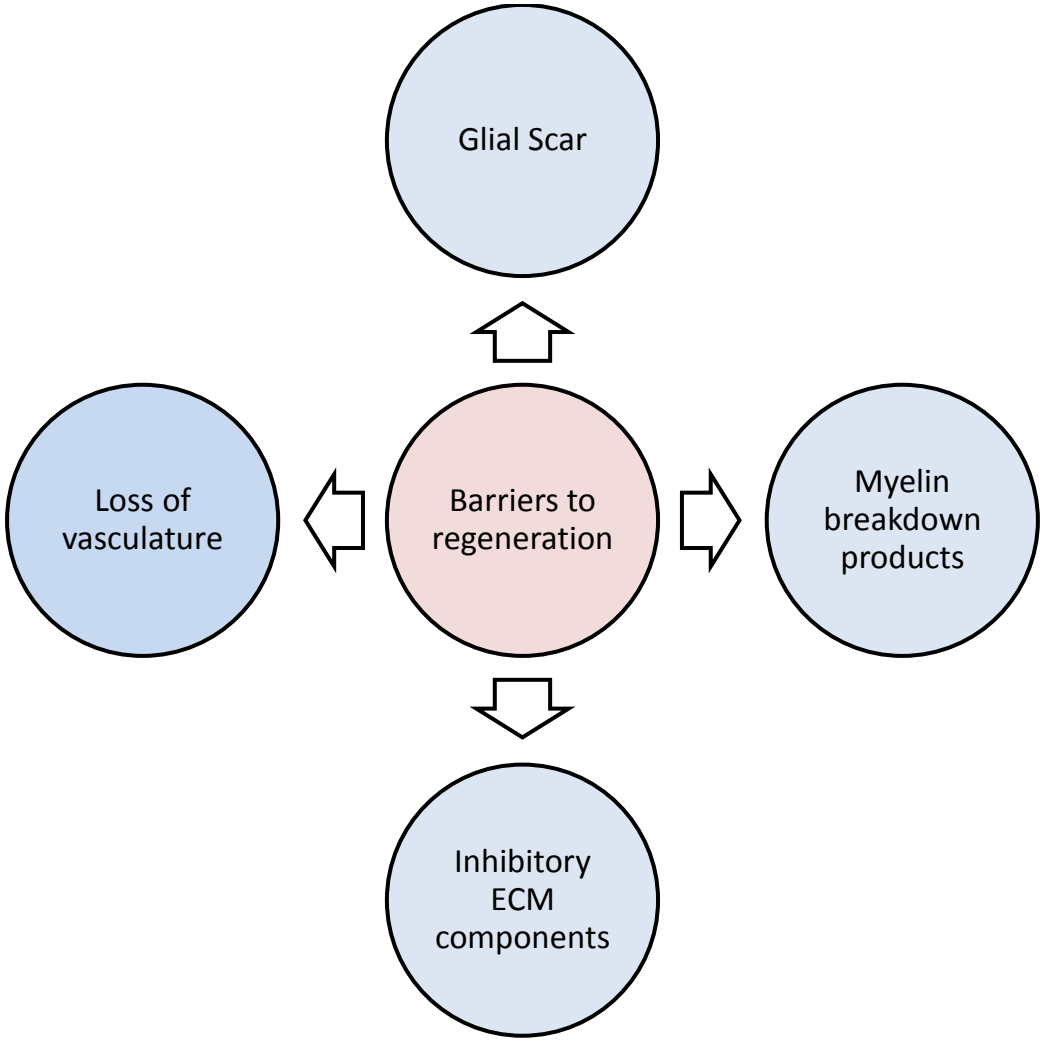

Figure 1b: Barriers to regeneration in SCI. *This figure represents four key biomolecular barriers to the regeneration of the injured spinal cord. The primary injury disrupts spinal vasculature, leading to anoxic injury. Reactive glial astrocytes form scar tissue which prevent*

the infiltration of regenerating neurons and secrete inhibitory ECM components. On going damage to oligodendrocytes leads to accumulation of inhibitory myelin derivatives.

1.1.4 There is no clinical treatment which can regenerate the chronically injured cord

SCI is a lifelong condition. Treatment begins with immediate life-saving trauma management and appropriately timed surgical interventions. This is followed by treatment of sensorimotor and autonomic dysfunction through rehabilitative therapy, use of assistive technologies and thereafter the myriad of domestic, professional and psychosocial adaptations which comprise community care. Presented here is an overview of the current principles of management of SCI.

The principles of acute management are firstly life-saving manoeuvres and stabilisation of the patient to maintain tissue perfusion and prevent further injury. The patient's airway is secured, the cervical spine immobilised, intravenous access gained, and appropriate analgesia administered. On arrival at the nearest appropriate facility, the patient is surveyed and treated according to the principles of advanced trauma life support. Once stable, the patient undergoes a full neurological examination and their initial status is recorded. Complications in the early stages of spinal injury can manifest in almost any organ system. As such, high-level nursing care is essential. For example, regular turning to prevent pressure ulcers, bladder catheterisation and monitoring of fluid balance, an appropriate bowel regime to prevent ileus, and cardiac monitoring to identify neurogenic shock from unopposed vagal

tone.

With regards to the spine itself, management focuses on prevention of secondary injury and stabilisation of the spine to facilitate engagement in rehabilitation. Early decompressive surgery may prevent secondary injury by relieving pressure in the vertebral canal from oedema and haematoma (42). However, clinical trials in human patients have yielded conflicting results, with some reporting shorter hospital stays, lower complication rates and better neurological outcomes, but others reporting no difference when compared with late surgical intervention (43). This data is further confounded by the lack of consensus regarding what constitutes early intervention, with definitions ranging from 8 hours to 4 days (42). Therefore, in clinical practice the decision as to when to intervene and to what extent is made on a case-by-case basis, with reference to imaging studies and neurological status. For example, there would be a strong case for decompressive surgery in a patient with a large spinal haematoma and deteriorating neurological function (42). There is currently no widely accepted pharmacological therapy for SCI. Corticosteroids have been investigated for their anti-inflammatory properties, however these are considered to be of marginal value (44). Indeed, a 2000 meta analysis of experimental data derived from clinical trials and experimental models relating to methylprednisolone administration for acute spinal injury determined that the results of these studies supported the exclusion of methylprednisolone from the acute management protocol, citing in particular concerns over the significance of experimental results (45).

The bulk of current therapy therefore comprises rehabilitation, beginning soon after injury and extending for years after discharge across a widely variable time frame: for some patients this could be a few years, for others a lifetime. The ultimate aim is to maximise patients' independence. Rehabilitation begins with active and passive limb and trunk exercises, often while the patient is still bed bound. This strengthens spared muscle groups, allowing them to compensate for denervated myotomes, and prevents the development of contractures, present in 66% of patients at 1 year (46). These initial exercises can provide patients with the strength and postural control necessary for manual transfer, wheelchair use, dressing and personal hygiene.

The act of ambulation is believed to restore lost sensorimotor function by optimising the functionality of remaining neurons through a set of processes collectively referred to as *'neuroplasticity'*. This term describes the changes which occur in spared neuronal circuits following insult to the nervous system and can occur in the spinal cord, brainstem and cerebral cortex (47). This phenomenon is believed to occur as a result of a combination of synaptic reorganisation, collateral axonal sprouting and up-regulation of neurotrophic factors (48). The net result can be measured through monitoring neurological status and electrophysiological assessment (49). However, in the absence of concurrent rehabilitation, functional gains are small (50), suggesting that physical therapy plays a role in facilitating the inherent neuroplastic properties of the spinal cord.

Locomotor training involves the patient walking with the body weight partially or fully

supported in order to stimulate reflex walking pathways which can operate independently of descending cortical input. This can be done either on a treadmill or over ground, and both are equally effective (51,52). Sensory input is preserved despite loss of brain-body communication, and movement of the legs is believed to preserve automatic pathways and restore reflex limb movement, contributing to restoration of mobility. However, how these mechanisms contribute to recovery is unclear. Rodent studies have demonstrated increased levels of BDNF below the level of the lesion in subjects undergoing locomotor training (53), suggesting this might contribute to the regenerative effect in humans.

Given the limited regenerative capacity currently available from conventional therapy, there is a large component of rehabilitative therapy which focuses on maximising functional ability for a given level of neurological deficit through the use of assistive devices. At their most basic, these devices comprise crutches, walking frames, wheelchairs and mechanical orthoses. However, there is a rapidly expanding area of research aimed at utilising human-machine interface technology to facilitate the use of more advanced assistive devices, some of which are already in clinical use (54). Functional electrical stimulation (FES) is one such form of assistive technology, which can be used to restore movement to certain key muscle groups through direct stimulation of the relevant neuromuscular pathway. Such devices can range from surface electrodes, which while inexpensive, provide non-specific stimulation which may be painful, to implantable devices which directly stimulate the appropriate nerve, and may restore or improve respiratory, bowel, bladder and sexual function (55). The remainder of available therapy focuses on maximising patients' functionality within their own

homes and workplace to restore independence, and minimising the emergence of long-term complications. Occupational health teams work with patients to make adjustments to the home and, where applicable, work spaces.

1.1.5 The prognosis following SCI is poor

At present, when considered across all injury types, the scope for patients with SCI to make a full recovery is limited, with the vast majority of functional gains occurring in the first 3 months post-injury (56). However, there are a number of prognostic factors that might predict the likelihood of recovery of the various functions affected in SCI. These are described below.

Among the most commonly used outcome measures is walking, as the ability to walk is rated as a priority for recovery among paralysed patients (57). The initial clinical examination of neurological status is considered a valuable prognostic indicator (58). The capacity for functional recovery in patients with complete injuries is very limited, with around 85% of those with complete motor injuries (ASIA A) unable to progress from wheelchair use to assisted walking methods (59). When compared to complete injuries, incomplete injuries (ASIA B and below) offer greater chances of functional recovery, with patients ASIA B or C having a 33% and 72% chance of regaining walking function, respectively (58).

Aside from the significant physical burden, there are also considerable psychological and social consequences. Spinal injury represents a significant upheaval of the lifestyle of the

affected. As one might predict, there is strong evidence for a link between psychological morbidity and SCI. In a 2009 systematic review, Craig et al found that of patients affected by SCI, up to 30% are at an increased risk of depressive illness, with higher incidence during the acute rehabilitation phase (60) and this remained present in 20% of patients at 1 year post-injury (61). There is also some evidence for a link between SCI and psychoactive substance abuse (62,63).

It is clear then that current clinical treatments for SCI are inadequate. This is particularly apparent when we consider the chronic phase of the injury process, in which the likelihood of a patient regaining any significant degree of functionality in very small (56). While in the acute phase there are some active steps that can be taken to minimise secondary injury and prevent complications, management in the chronic phase consists almost exclusively of on-going rehabilitation and assistive devices. There is currently no treatment in clinical practice that can regenerate spinal axons in the chronic phase. There is a clinical need then to explore emerging therapies which could regenerate damaged spinal tissue, and restore motor, sensory and autonomic function in patients with established spinal injuries.

1.2 Cellular transplantation as a regenerative therapy for SCI

1.2.1 Strategies to improve cell transplantation therapy are required

The scientific rationale for the modern emergence of cell-based therapies is twofold: (i) Repair of damaged cells by transplant populations through the release of neuroregenerative factors such as neurotrophins, and (ii) the direct replacement of lost or damaged cells (64). In the first decade of this century, more than 2700 clinical trials of cell therapies were initiated (65). Indeed, there are currently a variety of cell types under investigation for their neuroregenerative properties. An overview of key cell populations currently under investigation for spinal regeneration is provided here.

Embryonic stem cells (ESCs): ESCs are derived from the inner cell mass of the pre-implantation blastocyst, and human ESCs were first characterised by Thomson et al in 1998 (66). As a pluripotent cell type, they are capable of dividing in to any of the three germ layers, the progeny of all adult tissues (67). Moreover, they are capable of indefinite self-renewal *in vitro*, making them effectively immortal (68). As such, they have significant value in neuroregeneration. However, the derivation pluripotent ESCs necessitates the destruction of the embryo, and as such raises significant ethical concerns over their use (67). Moreover, their pluripotent nature confers the risk of teratoma (a tumor containing all three germ layers) formation at sites of transplantation (69). ESCs must now be pre-differentiated prior

to implantation to mitigate teratogenic risks. Finally, all ESC derivatives must be allografted (transplanted from a donor to a separate recipient), which risks graft vs. host disease (GvHD). However it must be remembered that the CNS is an immune privileged site, and the risk of GvHD is therefore lower than in peripheral tissues. The first trial to investigate the value of human ESCs by Geron Inc. was terminated when the company discontinued cell therapy research to focus on cancer therapy (70). Of the five patients treated, none showed adverse findings at a dose of ESCs below that expected to confer significant recovery (71). A phase I/II clinical trial is currently ongoing however, under the direction of Asterius Biotherapeutics (see www.clinicaltrials.gov, trial number NCT02302157).

Mesenchymal stem cells (MSCs): MSCs have the advantage of being derived from autologous adult sources such as bone marrow, adipose tissue and spinal cord and their safety in humans has been established by their use to treat blood-borne cancers. They have anti-inflammatory and neuroprotective properties believed to be mediated by paracrine and cell-cell contact mechanisms in response to host tissue injury, and a recent meta-analysis cited a mean improvement in Basso, Beattie and Bresnahan score (A widely used 21-point score of locomotor function) of 3.9 in MSC recipients (72), although whether this would translate to similar functional gain in human patients remains unclear. Rarity of appropriate cells in adults (around 1 in 100,000 in bone marrow) (73) does not represent a barrier to generation of sufficient numbers of cells for clinical investigation. Indeed, 493 MSC-based trials have been undertaken to date, making them the most widely investigated adult stem cell-based therapy in this regard (74).

Induced pluripotent stem cells (iPSCs): iPSCs are adult cell populations exposed to factors *ex vivo* which enforce expression of four key genes, thereby converting them to pluripotent cell lineages (75). They therefore share advantages with ESCs, but are not associated with any of the ethical restrictions. They can also be derived autologously from minimally invasive procedures (67). However, they cannot yet be generated efficiently enough for any widespread translational benefit to be feasible (76).

Neural stem cells (NSCs): NSCs are able to differentiate into any of the major neural cell types. They can be derived from differentiation of pluripotent stem cells, or can be isolated from certain regions of the adult CNS: The subventricular zone of the forebrain, the dentate gyrus of the hippocampus and the periventricular region of the spinal cord (77). When isolated, these cells can be propagated in defined culture media that uses a specific complement of growth factors to selectively expand the NSCs, either in free-floating clusters of cells known as neurospheres, or as adherent monolayers. Indeed, NSCs have demonstrated significant neuroprotective and neuroregenerative potential experimentally. For example, when transplanted in to a transecting injury model, NSCs were associated with axonal growth of up to 25 mm (78). It has been suggested that their pro-regenerative effects are due to the secretion of neurotrophic factors such as NT-3, NGF and glial-derived neurotrophic factor (GDNF) (79). Moreover, the culture conditions can be adjusted in order to direct differentiation in to precursor cells of any of the three major neural cell types. However, differentiation of this cell type is difficult to control as they tend towards glial

lineage, and there have been some reports of allodynia in transplant recipients (80). That said, Phase I/II clinical trials for the treatment of spinal cord injury in sub-acute stage patients were recently completed, under the direction of the company Stem Cells Inc. (see www.clinicaltrials.gov, trial number NCT01321333).

Schwann Cells: The observation that peripheral nerves spontaneously regenerate and remyelinate is the rationale behind the ongoing investigation of Schwann cells as a potential transplant population. Historical success in peripheral nerve regeneration using Schwann cell transplants (81) and the discovery of specific neurotrophic factors, cell adhesion molecules and basement membrane components (82) produced by Schwann cells has led to grafts being tested and refined in animal models more than any other cell-based treatment (83). Moreover, FDA approval has meant that human clinical trials have begun, and these cells are the focus of ongoing investigation by the 'Miami Project to Cure Paralysis' (84) (See www.clinicaltrials.gov, trial number 01739023). Schwann cells are obtained autologously and pose little risk of GvHD or teratogenicity; however significant translational barriers still remain: Schwann cells must be acquired invasively with the potential for neurological deficit at the donor site (85), and they have shown poor integration with astrocytes (86), which reduces the potential for long-distance axonal regeneration across lesion sites. As such, a cell population with similar regenerative properties without the translational limitations of Schwann cells is required.

1.2.2 OECs as a transplant population - a solution to translational barriers?

OECs are a specialised neural glial cell located in the olfactory system which support the growth of olfactory receptor neurons (ORNs) (87). Primary olfactory neurons must be continuously generated throughout adult life, possibly due to oxidative stress secondary to exposure to the air. Therefore after injury (or indeed during normal cell turnover) new olfactory receptor neurons are generated from basal stem cells in the olfactory epithelium, which then extend axons through the cribriform plate and in to the olfactory bulb (88). It is believed that this capacity for neuroregeneration is due in part to the properties of OECs, which ensheath bundles of ORN axons as they pass from their origins in the olfactory epithelium of the PNS to their synaptic targets in the glomeruli of the olfactory bulb within the CNS (89).

OECs are the only glial cell population that continue to ensheath axons from the PNS as they enter the CNS throughout adult life (90), forming a continuous supportive pathway from peripheral to central nervous system along which the olfactory axons can grow. OECs produce growth factors such as NGF and BDNF, and ECM proteins such as fibronectin and type IV collagen to promote axonal outgrowth and guide axons to their synaptic targets (91). Their structure therefore forms an effective 'track' along which olfactory axons grow, and within which a permissive growth environment can be manufactured (**Figure 2**).

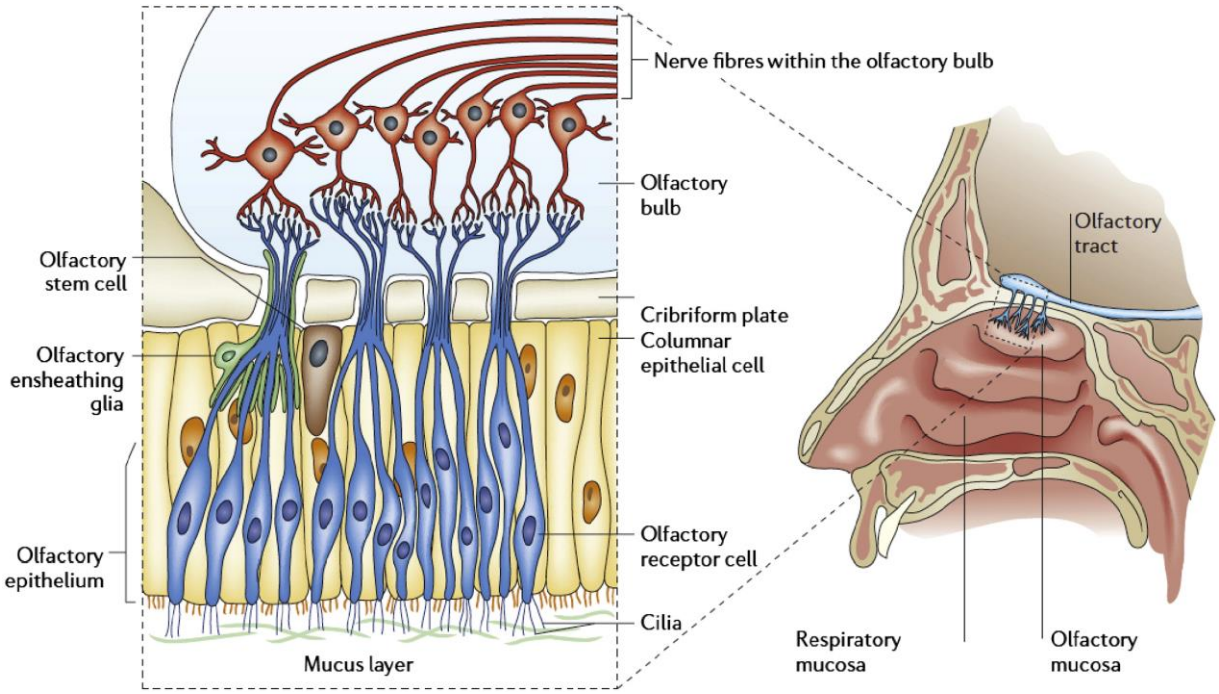

Figure 2: OECs support the regeneration of primary olfactory neurons throughout adult life. *Illustration of the cellular components of the olfactory system in humans. Primary olfactory neurons continually regenerate from basal stem cells; bundles of axons are ensheathed by OECs as they extend from the olfactory epithelium to the olfactory bulb. It is believed that this regenerative capacity relies on the capacity of OECs to manufacture a permissive growth environment within the olfactory system. Adapted from (89).*

OECs share phenotypical similarities with other glial cell types. They were initially believed to be Schwann cells specific to the olfactory system due to their morphology and anatomical location (92,93). However, immunocytochemical studies later revealed expression of the astrocyte marker glial fibrilary acidic protein (GFAP), leading to the hypothesis that they were more closely related to astrocytes (94,95). Subsequent studies revealed expression of the low-affinity NGF receptor p75, a marker for non-myelinating type Schwann cells (96,97). OECs are now known to be capable of expressing a range of antigenic markers in common with astrocytes and Schwann cells, and are currently considered as being a distinct cell type sharing similarities with both. Indeed, they are classified morphologically as being 'astrocyte-like', with comparatively shorter, randomly oriented processes and flattened morphology, or Schwann cell-like, with a long fusiform bipolar morphology. Recent work using cell fate-mapping techniques in chicken embryos has suggested that OECs share a common embryological origin in the neural crest with Schwann cells. This may mean that the similarities between these two cell types extends further than adult phenotype, but rather they may originate from a common progenitor (98).

OECs were further classified based by Au and Roskams based on their site of origin. 2 subtypes of OEC were recognised: those harvested from the olfactory bulb (OB-OECs), and those harvested from the lamina propria of the olfactory mucosa (LP-OECs) (90). There is evidence that LP-OECs express the same characteristic proteins as OB-OECs *in vivo* and *in vitro*, and so this may not represent two distinct glial cell types, and the two are now collectively referred to as OECs (99).

1.2.3 OECs for neurological injury

The unique regenerative properties of the adult olfactory system have been known for some time (91). Indeed, the observed permissivity of the adult olfactory bulb to the ingrowth of olfactory axons prompted the first reported experiment into the regenerative properties of OECs by Ramón-Cueto and Nieto-Sampedro in 1994 (100). This group performed autologous transplantation of rodent OECs into a rhizotomised spinal cord segment. The entry point of the dorsal root ganglia (DRG) was identified via laminectomy at the T10 vertebral level before being completely transected and then microsurgically anastomosed to the root stump. A purified OEC suspension was then added to the lesion site. This study demonstrated regrowth of severed dorsal root axons within 3 weeks of transplantation, concluding that OEC transplantation was associated with axonal regrowth in the DRG and that this might be generalisable to other CNS injuries, laying the groundwork for numerous studies into OEC transplantation over the next two decades. Presented here is a review of significant studies of OECs in model lesions and a discussion of human and animal trials.

1.2.4 OECs in laboratory models of SCI

Several laboratories have further substantiated the initial findings that OECs can establish synaptic continuity between the periphery and brain (101,102). The Raisman group was able to successfully restore goal-directed forepaw movement in rodent models of brachial plexus avulsion injuries (103). Here, researchers transected the dorsal roots of C6-T1 before

transplanting OEC populations into the lesion site. Behavioral assessment revealed progressive improvement in forepaw function in those rats which received OEC transplantation. Moreover, electrophysiological assessment of subjects demonstrated restored impulse transmission. Post-mortem histological examination of specimens demonstrated regrowth of axons and invasion of OECs into the dorsal route entry zone (DREZ). The additional validity gained by the use of three separate measures to assess the degree of recovery adds confidence to this groups' suggestion that functional recovery was due to OEC implantation.

However, if OECs are to be considered a viable translational therapy for SCI then their benefits in centrally occurring lesions must be demonstrated. In addition to DRG injury models, the regenerative properties of OECs have been tested in numerous other models of SCI. Indeed, OECs have been shown to promote axonal regrowth and restore function in both transection and contusion SCI models (104,105). In 2000, Ramón-Cueto's group successfully restored functionality in paraplegic rats in a complete spinal cord transection model (106). This study demonstrated restoration of sensorimotor reflexes, voluntary movement and proprioception. All experimental conditions in this study demonstrated at least some functional improvement compared to the control group. A further study by Li et al in 2003 into motor recovery following cervical hemisection injury demonstrated that subjects regained supraspinal control of respiratory function in addition to motor function, which has significant implications for human patients with high cervical lesions (107). OECs have also been demonstrated to remyelinate demyelinated axons in the spinal cord (108),

demonstrating their efficacy in a range of lesion modalities.

1.2.5 OECs in pre-clinical studies

Due to the relative success of autologous OEC transplantation in experimental "proof-of-concept" models of SCI, there has been an initiative to undertake trials which assess their value in clinical cases. In 2012, Granger et al performed autologous intraspinal transplantation of OECs derived from cultured olfactory mucosal tissue in companion dogs with chronic SCI in a double-blind randomised control trial (109). Dogs in the experimental condition demonstrated significantly greater fore-hind limb coordination after transplantation. Granger concluded that autologous OMC transplantation is associated with improved locomotor function in chronic spinal injury, noting particularly that there was improved functionality in dogs that had been paraplegic for over 12 months, the period in which significant recovery would be expected (56).

This study is of particular interest to human applications, as the use of companion canines as a large animal model of spinal injury offers distinct similarities to human pathology. For example, cells derived from companion dogs have comparable genetic variation and environmental conditions to their human counterparts. This is in contrast to purpose-bred animal and *in vitro* models which lack the genetic and environmental heterogeneity of human patients (110). Moreover, the mechanism of injury and pathological sequelae which result in lesion heterogeneity, as well as the diagnostic, therapeutic and rehabilitative

strategies employed are all comparable to humans (111). This means that when developing therapies in this population, any clinically detectable recovery observed is likely to translate to comparable benefits in human patients (112). As such, conclusions drawn from canine subjects are likely to have greater relevance to human therapies.

1.2.6 OECs in human trials

In addition to the steps forward taken in animal trials, there have been several promising trials which have established the safety and feasibility of autologous OMC grafts in human patients suffering from chronic SCI (113–116). One of the earliest trials began in Australia in 2002 (117). 3 adult male patients with chronic stable thoracic spinal injuries (ASIA A) received autologous olfactory mucosal grafts of differing total cell number (2, 24 and 28 million) via syringe injection directly in to the healthy cord adjacent to the lesion. At one year (113) and three years (114) post-transplantation, there was no deterioration in sensorimotor function or new neuropathic pain, nor was there any radiological evidence of lesion deterioration.

More recently, Huang et al conducted a retrospective study of 108 patients with chronic SCI who had received autologous intraspinal OEC therapy (118). Here, mean motor scores were seen to improve significantly ($p<0.01$) and 34 patients with ASIA A were reclassified to a less severe score. Tabakow et al reported improvements in motor function in a 38 year old male patient with a complete transecting model of spinal injury (ASIA A) (119). Here, the glial scar of the patient was resected and a mixed OEC and olfactory nerve fibroblast populations

derived from the OB were delivered via injection to both lesion stumps, and the 8 mm gap bridged by sural nerve autograft. No negative outcomes were reported in the immediate or long-term postoperative period. The patient improved from ASIA A to ASIA C, and electrophysiological studies confirmed that long tract continuity across the lesion had been restored. However, the absence of a control group in the study by Huang makes drawing conclusions about the extent of the recovery that was due to OEC implantation difficult. Similarly, Tabakow reported on a single patient, and it is difficult to establish if the patient would have improved without intervention. Moreover, injuries of this nature (complete transection secondary to knife wound) are very uncommon, and as such results may be unlikely in patients with more typical, heterogeneous lesions.

1.2.7 Controversies surrounding OECs as a transplant population

Despite the promising results of multiple trials, the precise mechanism by which OECs exert their therapeutic effect remains unclear. The most widely accepted hypothesis is the production of a permissive growth environment within the lesion site analogous to that seen in their anatomical location (108). This is likely to be supported by the local secretion of neurotrophic factors and the remyelination of axons (89). Additional studies have suggested that OECs can modulate the immune response and alter glial scarring (120). There is also significant evidence that OECs might recruit Schwann cells to the lesion site in order to mediate repair (121). It is clear that additional research is needed if the precise underlying mechanism of OEC-based therapies is to be elucidated.

A recent case report of a patient who developed neuropathic pain following autologous olfactory mucosal tissue autograft 8 years previously must also be considered (122). Imaging studies revealed the source of the pain to be a cystic intramedullary mass at the graft site that required resection. Histological analysis of the resected tissue revealed the presence of respiratory epithelium, confirming that the graft tissue was the source. However, in this study mucosal tissue was grafted directly into the lesion site. More recent trials purify the olfactory cell population to mitigate the risk of transplantation of respiratory epithelium or native tissue stem cells (99). In any case, long-term follow up of all patients engaged in trials is therefore essential if this therapy is to be considered safe for clinical implementation, as at present few of these studies exist beyond initial feasibility and outcome reports.

Moreover, the number of negative studies in to OEC-based therapies means that conclusions regarding their viability as a translational therapy must be drawn tentatively. In particular, despite reports of greater efficacy of LP-OECs when compared to OB-OECs and Schwann cells (121,123), some studies into the benefits of peripherally-derived OECs have demonstrated limited regenerative benefit in rodent injury models. For example, Lu et al in 2006 did not find any benefits to axonal regeneration from LP-OECs when compared to other grafted cell types such as fibroblasts, bone marrow stromal cells or Schwann cells, nor did they find that OECs supported any axonal regeneration in the CST, suggesting instead that previous studies which did report regeneration might instead have observed spared rather than regenerating axons (124). In this study, the authors were also unable to replicate the migratory properties

of OECs towards sites of axonal injury that had previously been reported, instead concluding that observed OEC tracts were in fact pressure phenomena extending from the injection site. In corroboration with this, two studies compared the effects of transplanting olfactory mucosal lamina propria into complete transection models of rodent spinal injury using respiratory lamina propria, which should not contain any OECs, as the control condition (125,126). While one study did report recovery in motor function in both the control and experimental condition, neither reported any significant difference between the transplantation of olfactory and respiratory lamina propria.

It is unclear why this variability in experimental findings exists. The sheer volume of literature supporting a positive regenerative effect makes it unlikely that these are, as Lu postulated, due to misidentification of residual axons and artifact caused by experimental technique. Due to the relative novelty of OECs as a therapeutic strategy there is no widely accepted method of identifying and culturing cells. As a result, the culture techniques and purity of cultures differs between groups. It is possible therefore that differences in cell culture methodology and duration may be responsible in part for inconsistencies in experimental results.

1.2.8 Advantages of OECs over other transplant populations

The concept of cell transplant populations as a potential therapy for axonal injury is not a new one, and numerous cell types have been extensively investigated to this end **(Section**

1.2.1). Despite this, no cell type to date has been able to amount to an effective therapy, as evidenced by the lack of widespread clinical use of any cell type in SCI. The rise in interest in OECs as an alternative cell therapy in the last two decades may therefore be due to the distinct advantages these cells possess as a transplant population, when compared to other cell types: (i) OECs can be derived autologously, with minimal negative side-effects from donor sites, and therefore do not have the ethical and immunological implications associated with other cell types (127). (ii) OECs can be derived non-invasively from the lamina propria of the olfactory mucosa (128), providing a very low-risk source of cells when compared to the OECs of the olfactory bulb, located behind the cribriform plate. (iii) OECs are able to integrate with reactive glial astrocytes, a significant advantage when compared to Schwann cells, which have been shown to be incapable of invading reactive astrocytic tissue both *in vitro* and *in vivo* (127).

1.3 Combinatorial strategies are needed to address regenerative barriers

As discussed above, traumatic SCI is a complex pathological process, which presents a number of regenerative barriers. Transplantation of OMC grafts to spinal injury foci is a promising strategy to encourage regeneration in the chronically injured spinal cord, as a recent clinical trial demonstrated (102; **Section 1.2.5**). However, in this trial the researchers reported that not all canine subjects responded to OMC therapy. Moreover, in those subjects that did respond, recovery was incomplete. The researchers have identified two key domains

which may account for these results: (1) cOMC transplantation alone may be insufficient to regenerate CST axons in the chronically injured cord; (2) Cell loss during tranplantation due to mechanical stress during injection and clumping in the injection fluid may lead to a therapeutically inadequate number of cells being delivered to spinal injury foci. These limitations will be discussed further in **Sections 1.3.2** and **1.3.4**, respectively.

The remaining sections of this chapter will discuss two neural tissue engineering strategies that may be used to enhance cOMC transplantation in order to address these deficits. First, MPs complexed with genes encoding therapeutic biomolecules could be used to genetically engineer cOMCs as a way of augmenting their therapeutic efficacy, enabling them to act as "biopumps" for the release of therapeutic factors at the lesion site. Second, hydrogels could be used to encapsulate cOMCs in to 3-D implantable, mouldable, protective cell delivery devices, which can then be administered to spinal injury foci to maximise the number of viable cells being delivered. Presented here is the rationale for why these strategies are needed, and the specific properties they possess that make them suitable for incorporation in to a combinatorial approach to spinal regeneration.

1.3.1 Genetically engineering OMCs could address limitations in OMC transplantation therapy

Autologous cOMC transplantation in domestic canines for the treatment of spinal injury is not associated with restoration of cortical control of motor function (109). In the trial described above **(Section 1.2.5)**, secondary outcome measures including somatosensory evoked potentials and transcranial magnetic motor-evoked potentials indicated that the significant recovery of walking function seen may have been due to improved local connections across the lesion site, and not representative of CST regeneration. This is in keeping with the findings of previous studies by Yamamoto, Raisman and colleagues. In the initial studies, adult OB-OECs were transplanted in to an upper cervical hemisection model of spinal injury in rodents (129,130). In both cases, the results of behavioral analyses identified restoration of goal-directed motor function, and histological analyses confirmed that these observations were the result of restored continuity in the CST. However, following the discovery that OECs could be derived from the lamina propria of the olfactory mucosa, subsequent studies compared the regenerative function of OM-OECs in an identical lesion in terms of both functional recovery and CST regeneration (131). Again, the researchers found that goal-directed motor function was restored. Crucially, however, the results of histological analyses revealed that this was not the result of CST regeneration across the lesion site, and was in fact more likely to be the result of regeneration of local axonal circuitry.

Human spinal injury patients most highly rate the restoration of arm, bladder and sexual function in terms of recovery priorities (132). All of these functions are dependent on CST continuity, and as such the restoration of these tracts in the injured cord is a key goal for spinal injury research. However, derivation of OECs without the need to breach the cranial vault would of course be preferable in terms of clinical applications, as it avoids the inherent risks of an additional neurosurgical procedure (133). Therefore, incorporation of mucosa-derived OECs in to a combinatorial approach, whereby their regenerative function is enhanced through the delivery of genes encoding neurotrophic factors, may represent a solution to this problem.

Genetic engineering is the process of manually altering an organism's genome. This process may: (i) add phenotypic traits not usually found in that organism, (ii) alter the expression of phenotypic traits that the organism already possesses. There has been some success in the delivery of genes to OECs in proof-of-concept demonstrations (134–138). These have included NT-3 (134,137), GDNF (135) and BDNF (136). In 2003, Ruitenberg et al used adenoviral vectors to successfully deliver genes encoding BDNF *ex vivo* to autologously derived OECs before implantation in to a transection model of spinal injury in rodents. Axonal regeneration and locomotor function was significantly greater in rats that received engineered OECs compared with those that received un-engineered OECs. In 2005, the same group used adenoviral vectors to deliver OECs engineered to secrete NT-3 to transecting cervical spinal injury models and demonstrated significant CST regeneration (137), highlighting the potential value of this strategy in terms of long tract regeneration. However,

current methods of OEC engineering rely almost exclusively on the use of viral vectors for gene delivery.

1.3.2 Disadvantages of viral vectors for gene delivery to transplant populations; consideration of non-viral alternatives

Viral vectors are amongst the most commonly used means of gene delivery for pre-clinical and *in vitro* studies, and have been the most widely investigated means of delivering genes to OECs. This technique utilises viral components that have been modified to minimise pathogenicity through limiting self-replicating capacity, whilst maintaining gene transfer properties. One of the key advantages of using viral vectors is their high rate of successful gene transfer. For example, when OECs were engineered to express NT-3 before transplantation into the transected cord, transfection efficiency was upwards of 95% (137). Moreover, the transgene expression of viral vectors is often very high, with some viruses able to confer permanent gene transfer to transplant populations (139).

However, certain key disadvantages prevent their widespread clinical use in regenerative neurology: (i) the risk of insertional mutagenesis in the host genome (140); (ii) immunogenicity increases the chance of host inflammatory response (141); (iii) limitations to the size of the gene to be delivered: larger genes cannot be transferred by conventional viral vectors (142); (iv) difficulties manufacturing viruses in the quantities necessary for large-scale

engineering of human cells in clinical applications (143). As such, a number of non-viral methods have been developed.

One of the most extensively studied non-viral gene delivery methods is lipofection. This process utilises a cationic liposome containing desired genes to transfect target cells (144). Similarly, electroporation utilises electric currents applied to cell membranes to induce transient pore formation, allowing negatively charged DNA into the cell where it becomes trapped when the current is withdrawn. There also exist a variety of techniques to transmit naked DNA directly into target cells either through direct manual or ballistic "gun" injection (145). However, the majority of these methodologies result in low transfection efficiency, which limits their clinical applicability (146). For example, Wu et al engineered OECs to express NT-3 using lipofection techniques (138). While this enhanced locomotor recovery and axonal sprouting when transplanted into the lesioned rodent cord compared to transplantation of un-engineered OECs, the transfection efficiency achieved was only 30%, much lower than that achieved through viral means. There is thus a need to develop a transfection technique that is efficient enough to enable delivery of therapeutic levels of genetic material, but is also safe.

1.3.3 MPs as safe and efficient gene vectors

In the context of gene delivery, MPs can offer a safe and efficient means of engineering transplant populations. They are comprised of three main components: (i) a magnetic core,

which allows the particle to be manipulated by magnetic field gradients; (ii) a protective coating, usually a biocompatible polymer; (iii) a functional biomolecule, in this case a gene. A schematic representation of the structure of a magnetic particle is provided in **Figure 3**.

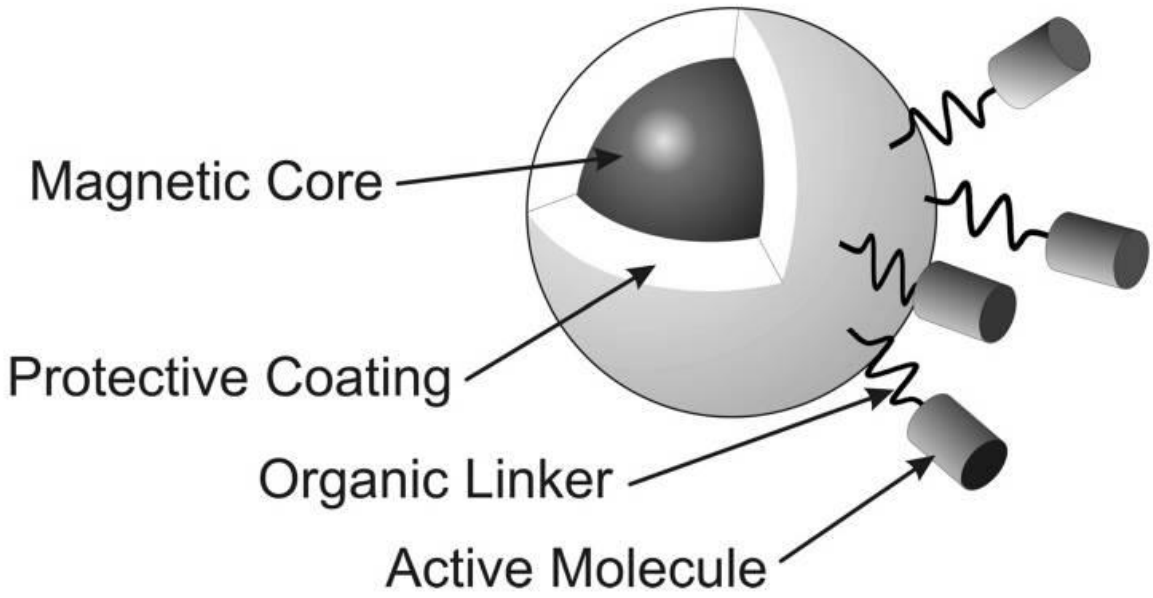

Figure 3: Schematic representation of a MP*. A typical magnetic particle is comprised of three key components. The magnetic core, most commonly made of iron oxide, imparts magnetic properties. The protective coating provides biocompatibility and facilitates the incorporation of organic linker molecules. Active biomolecules such as gene vectors, immunomodulatory agents or slow-release drugs can then be incorporated in to the particle. Adapted from (147).*

The most common material for the magnetic core is iron oxide, a ferromagnetic material. This means it has its own permanent magnetic properties in the absence of an external magnetic field. This is in contrast to paramagnetic compounds, which become magnetic in the presence of an external magnetic field but retain no magnetism when the field is withdrawn. Iron oxide MPs display "superparamagnetism", a property of a ferromagnetic material which has been reduced in size such that it now has only a single magnetic domain. When not exposed to an external magnetic field, the domain of each particle alternates at random such that the net magnetic moment of all particles in zero. However, when exposed to a magnetic field the particles display characteristics of a paramagnetic compound, except with considerably greater magnetic susceptibility – hence, *'super*-paramagnetism' (148).

The purpose of the coating is to protect the particle from corrosion and to confer biocompatibility (147). They are commonly natural polymers, such as the carbohydrate dextran, as these are biocompatible. Indeed, dextran-coated MPs have been used in biomedical applications such as cancer treatment for some time (149). However, some natural polymers lack mechanical strength or are water-soluble and so may be unsuitable for some *in vivo* applications. Here, synthetic organic polymers such as poly-ethylene-glycol (PEG), can be used as an alternative (150). The surface of the coating can then be modified through the addition of organic linker molecules in order to facilitate coupling of functional biomolecules to the particle surface. In the instance of genes, a molecule with a strong positive charge is preferred to facilitate electrostatic binding of negatively charged DNA (147). The range of materials from which the individual components of the MP complex can

be synthesised confers a structural versatility to the particles, which can be adjusted to suit a variety of clinical applications.

In the context of gene delivery, the gene-particle complex can then be applied to cells under the influence of a magnetic field, a process known as *"magnetofection".* The most widely used application involves application of gene-particle complex to adherent monolayer cultures, which are then rested on the surface of a magnet. The magnetic field draws the particle-gene complex towards the surface of the cells, thereby increasing the likelihood of cell-particle interaction, which appears to upregulate innate phagocytotic abilities of the target cell population (151), following which the genes are expressed by the target cells.

Magnetofection protocols have been developed for the safe and efficient delivery of genes to every major neural transplant population. These have included astrocytes (152), oligodendroglial cells in both differentiated and undifferentiated forms (153), microglia (154) and NSCs cultured both as monolayers and neurospheres (155). Crucially for translation of engineered cells to the clinic, the transfection efficiencies achieved by these methodologies are often within the ranges of those reported for viral vectors. For example, in the case of astrocytes, magnetofection protocols yield a transfection efficiency of 54%, compared to a range of reported viral transduction efficiencies of 14-100% (152). Perhaps more importantly, in all cell types studied, the optimal magnetofection protocol did not show any adverse effects on cellular morphology, phenotype, or biochemical markers of cellular proliferation or viability.

In addition to their viability as transfection agents, magnetic particles possess further properties that make them ideal candidates for incorporation in to cOMC-based combinatorial strategies. For example, the formulation of coating and organic linker can be adjusted to facilitate the incorporation of additional functional biomolecules, such as drugs (147). The particles can then be directly to required site, or can be administered systemically and guided to the therapeutic target through the use of an externally applied magnetic field. For example, MP-drug complexes have been the subject of extensive investigation for targeted drug delivery to cancerous lesions (156).

Further, the high iron content of MPs means they attenuate T1 and T2 weighted magnetic resonance imaging (MRI) signals. This can be used to non-invasively image a transplant population in order to correlate neurological outcomes with cell biodistribution (157). For example, Sandvig et al recently developed protocols for efficiently labeling OECs with iron oxide MPs of 0.96 μm diameter (158). They reported a labeling efficiency of >90% after 6 h, in the absence of a magnetic field. Cell suspensions were then injected in to the vitreous of the eyes of anaesthetised rodents, which were then imaged by MRI. In this experiment, viability and proliferation analyses revealed no negative impact of magnetic particle labeling on OECs compared to un-labeled controls. Moreover, MP-labeled OECs were clearly visible on MRI for > 20 days post-transplantation.

Finally, iron oxide MPs have been FDA approved for use as contrast agents since 1996 (159), two of which are currently approved for clinical use for imaging of the liver: Endorem and Resovist (160). This illustrates their biocompatibility. The cytotoxicity of iron oxide particles *in vitro* has been the subject of extensive research (161). With regards to pre-clinical studies of safety for gene delivery, studies which applied magnetic particles to neural populations have largely shown no adverse reactions, and where cytotoxicity does occur it tends to do so in a dose-dependent manner (152,155,162). However, despite their advantages in terms of gene transfer, and their wider benefits as multimodal agents, the utility of magnetofection strategies in the delivery of genes to cOMCs has not yet been investigated.

1.3.4 There is a need to develop protective cell delivery systems for OMC administration to sites of spinal injury

Current methods of OMC administration to spinal injury foci in clinical applications rely primarily on intraspinal injection (163). When injected, cells are exposed to mechanical forces: passage from the relatively wide diameter of the syringe to the narrow-bored needle creates extensional forces. Within the needle, differing fluid flow rates between the inner and outer aspects of the lumen creates shearing forces (164). These forces cause cell death during injection, resulting in low numbers of cells being delivered to lesion sites (termed “poor stability”).

For example, in a recent trial of autologous cOMC administration to canine subjects (109), 20-22-guage 90 mm long spinal needles were used to deliver a total of 400 µL of cOMC suspension, containing a total of 2.5 million OECs, percutaneously to three sites: Two to the intervertebral space overlying the lesion epicenter, and the two adjacent intervertebral spaces. Each bolus injection was 100 µL administered over ca. 5 minutes, a flow rate of approximately 20 µL/minute. In another study, when the effects of differing flow rates and needle lengths on five independent measures of cell survival was studied, it was found that the lowest cellular viability occurred at injection rates of 20 µL/minute, and that cell death was even greater when needles of increasing length (essential for percutaneous cell injection to the spinal cord) were used, strongly suggesting this could account for the incomplete response seen in the subjects of the canine study described above (164).

Indeed, studies have correlated the therapeutic efficacy of cell transplantation with higher cellular viability post-transplantation (165), and dramatic cell loss has been identified as a major cause of neural transplant inefficacy (166). For example, it is estimated that <10% of injected NSCs survive the transplantation procedure, and only 29% of oligodendrocyte precursors (167,168). In the case of OECs, a 2007 study by Pearse identified low cell survival post-injection, which continued to fall over subsequent weeks (169). Here, OECs were transplanted in to the rodent spinal cord one week after infliction of contusion injuries. OECs were then identified at sites of injury over subsequent weeks through immunolabelling of male chromosomes in histological spinal sections. Reported survival of OECs following injection in to sites of spinal injury fell from 69.4 ± 6.0% at 3 days to 3.1 ± 1.4% at three

weeks. These studies suggest that not only does cell death occur during the injection procedure, but also injection may confer lasting detriment that continues to cause cell death at the graft site, which has been shown to worsen functional outcomes (170). Additionally, washout of cell solution from injury sites, suspension viscosity and cell clumping can result in difficulty with achieving smooth flow of cell suspensions and resultant variability in cell distribution through the lesion site. This highlights the need for development of cell transplantation tools to enhance cell viability and biodistribution of OMCs post-transplantation.

1.3.5 Hydrogels as protective cell delivery systems for neural transplantation

Hydrogels are biocompatible polymer scaffolds comprised of 3-D networks of cross-linked hydrophilic polymer chains. They are typically stored as monomers in a liquid state before the addition of cells, following which they are polymerised in to chains in response to one or more environmental cues (171). The nature of the intermolecular forces are such that the hydrogel is able to absorb 95% of its total weight in water (172). This gives hydrogels soft, tissue-mimetic mechanical properties and confers biocompatibility, allowing them to support the survival and 3-D growth of cells suspended in a mouldable matrix (171), and therefore making them suitable as cell delivery devices. Indeed they have been used for a wide variety of clinical applications, such as bone, cartilage and cardiac regeneration (173,174). A schematic representation of the structure of a hydrogel is provided in **Figure 4**.

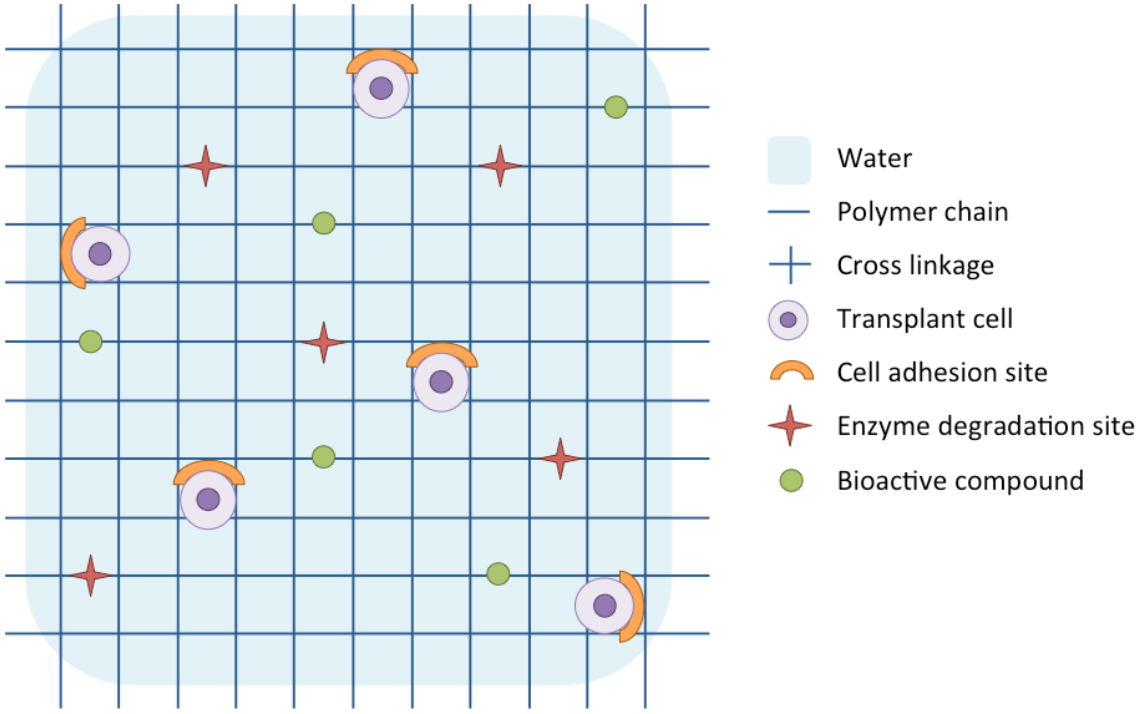

Figure 4: Schematic representation of a hydrogel. *A hydrogel is composed of a 3-D network of cross-linked, hydrophilic polymer chains. The nature of the gel construct allows it to hold around 95% of its weight in water. Its ECM-like structure makes it suitable for cell culture. Its specific properties can be adjusted through alterations to its constituent polymer, such as the addition of cell adhesion sites, enzyme degradation sites, or through the incorporation of bioactive compounds such as drugs.*

The development of a mouldable, implantable biomimetic scaffold offers significant clinical advantages. Primarily, transplant populations are encapsulated in a protective matrix during the implantation procedure, and so are not subject to the same forces that may cause lysis and clumping during injection of a liquid suspension. Moreover, cell survival and distribution within the matrix can be verified *ex vivo* before any surgical procedures. This would be useful if, for example, one aspect of a heterogeneous spinal lesion was more damaged than the other, in which case it may useful to know which aspect of the construct contained the greatest number of therapeutic cells such that the gel may be orientated accordingly. Low cellular viability post-injection is likely to result in delivery of dead cellular material to sites of injury, where cell fragments and debris would promote local inflammatory responses that would hinder the repair process.

Hydrogels also possess further properties that make them suitable for cell delivery to neural tissues:

(1) ECM-like structure: Hydrogels can be synthesised from a diverse range of synthetic or naturally occurring polymers. For example, collagen and hyaluronic acid are key components of the CNS ECM that can be isolated and formulated into hydrogels (175). Conversely, synthetic materials such as PEG can be used to synthesis hydrogels *de novo*. The polymer structure is such that nutrients from the local tissue environment can flow easily through the gel in order to support the growth of graft populations.

(2) Support of regenerating tissue: A number of studies have tested the therapeutic capacity of hydrogels to promote spinal regeneration in the absence of encapsulated cells. Recently, Tukmachev et al delivered ECM-derived hydrogels to a hemisection model of spinal injury (176). Histological analyses at 2, 4 and 8 weeks post-injection revealed that hydrogel constructs were able to integrate fully in to the lesion and support the ingrowth of regenerating spinal axons and blood vessels.

(3) Potential for incorporation of functional molecular domains: Incorporation of enzyme-specific binding domains in to the structure of the gel can be used to fine-tune the degradation rate of the structure *in situ* (177). This is particularly useful in cases where the hydrogel is intended to remain *in situ* to act as a scaffold to support the regeneration of spinal axons across the lesion site before being degraded by local enzymes. Similarly, additional therapeutic factors such as slow-release drugs can be incorporated in to their matrix (178). These drugs can be pro-regenerative, for example alginate hydrogels containing slow-release VEGF complexes have been delivered to spinal injury foci in order to both support the regeneration of axons and enhance neovascularization at the lesion site (179). Alternatively, anti-inflammatory adjuvants can be incorporated in order to suppress surrounding inflammatory responses that might otherwise hinder the repair processes (180).

(4) Immunomodulation: *In vivo* studies of implantable hydrogels have determined that they may have some inherent immunomodulatory properties. For example, implantation of

collagen hydrogels in to sites of spinal injury is associated with reductions in the size of the astrocytic scar (181).

(5) Tissue-mimetic mechanical properties: Finally, there is a known need to tissue-match implantable materials in terms of stiffness to host sites. How the precise mechanical properties of hydrogels impact the growth and survival of both grafts and donor tissues, and current methods of tissue-matching will be discussed further in the introduction section of **Chapter 3 (Section 3.1.2)**.

1.3.6 Hydrogels can improve survival of transplant populations

Due to the versatile nature of hydrogel constructs, their biocompatibility with neurological transplant populations as a potential treatment for SCI has been the subject of some research (84). However, as discussed above, hydrogel formulation can vary significantly in terms of constituent polymer (natural/synthetic), and as such direct comparisons between studies are not always possible.

Synthetic hydrogel constructs have been associated with enhanced survival of transplant populations. For example, NSCs have been successfully cultured in 3-D PEG networks and demonstrated 90% viability following ATP:DNA analysis after 24 h in culture (182). This increased to 100% following repeat measures at 16 days in culture. This finding illustrates the potential growth-supporting effects of hydrogel constructs. Moreover, early studies have

shown improved survival of cells when implanted as hydrogels. Natural polymer hydrogel formulations have been associated with enhanced biodistribution of graft cell populations. Retinal stem cells delivered to the retinal pigment epithelium (RPE; therapeutic target of macular degeneration) of rodent eyes in saline solution gave a clustered appearance. This is in contrast to the continuous banding pattern around the RPE seen when they were administered in blended hyaluronan and methylcellulose hydrogel formulations (183). This suggests that delivery of cells as part of a hydrogel construct can optimise the distribution of cells at a lesion site, which in the context of spinal injury may enhance functional outcomes.

1.3.7 The utility of hydrogels as implantable matrices for OMC therapy has not been fully investigated

Some work has involved seeding OECs onto freeze-dried pre-formed collagen-heparin sulphate matrices and conducting morphological and proliferation analyses (184). This study reported increased process length of OECs when grown on 3-D compared to 2-D substrates, and higher proliferation rates for up to 14 days, indicating biocompatibility. A 2006 study by Wang et al analysed compared the behaviour of OECs grown on 2-D collagen surfaces to those cultured on pre-formed 3-D collagen matrices (185). They reported an increased proliferation rate of OECs grown on 3-D constructs compared to 2-D, and reported that cellular apoptosis was lower after 30 days in the 3-D culture conditions than the 2-D culture conditions. Moreover, there was upregulation of genes encoding therapeutic factors such as BDNF in 3-D culture conditions as measured by semi-quantitative RT-PCR analysis, with no

differences in the expression of the OEC phenotype marker p75. This suggests that OECs are compatible with collagen scaffolds, and indeed these constructs may enhance their pro-regenerative properties. However, these studies tell us little regarding the biocompatibility of OECs within encapsulating hydrogel constructs.

Novikova et al reported on the phenotypic and regenerative profiles of OECs encapsulated in implantable hydrogels (186). Here, OECs grown in Matrigel^{TM} hydrogel formulations retained their bipolar morphologies, and normal metabolic activity, recorded by Almar-Blue assay, was reported. Further, when OEC-impregnated 3-D constructs were seeded on to collagen-coated DRG cultures, they encouraged neurite outgrowth, suggesting that this formulation of 3-D construct has therapeutic potential. However, when the same experiments were performed on OECs encapsulated in alginate constructs, OECs lost their bipolar morphologies and were not able to support the growth of DRG neurites. This highlights the need to investigate the response of transplant populations to a range of hydrogel formulations, as the responses of cells may vary depending on the precise physicochemical properties of the construct. However, there is currently limited data available relating to the biocompatibility of OMC populations derived from a clinically relevant transplant population encapsulated in implantable hydrogel matrices. Given the significant advantages that this tissue engineering strategy possesses in the context of cell delivery for neuroregeneration, there is a need to investigate the amenability of OMC populations to culture in 3-D hydrogel constructs.

1.4 Aims of experimental chapters

This introduction has identified two key domains that currently limit the translational potential of autologous OMC transplantation for spinal cord injury. These are: (i) incomplete CST regeneration in patients who receive autologous OMC grafts. (ii) Low stability of cells in injection solutions. The cells used for all of the studies detailed in the following experimental chapters **(Chapters 2 and 3)** were obtained from the same cell bank in Cambridge. These are the cells which were used in the 2012 clinical trial of autologous cOMC transplantation into companion dogs with chronic SCI discussed above **(Section 1.2.5)**. These were a *mixed* population of OECs and fibroblasts derived from the lamina propria of canine nasal olfactory mucosa, hence the term cOMC. In order to address these key limitations and optimise cOMC transplantation therapy, the experimental chapters will assess two key tissue-engineering strategies. In this regards, the aims of the experimental chapters are:

1. The broad aim of this chapter is to test the hypothesis that cOMCs can be safely genetically engineered using magnetic particles in combination with an applied magnetic field.

2. The broad aim of this chapter is to test the hypothesis that cOMCs are compatible with 3-D culture in collagen hydrogel scaffolds of two different concentrations. Moreover, I aim to determine the feasibility of generating non-invasive measurements of canine spinal cord stiffness using a clinically available imaging technique.

Chapter 2: Optimised magnetofection protocols can be used to safely and efficiently deliver genes to cOMCs

2.1 Introduction

Chapter 1 detailed the complex nature of the spinal injury process, noting that there is a consensus emerging in the field of regenerative neurology that combinatorial strategies are likely to be necessary to address multiple facets of the regenerative process simultaneously **(Section 1.3)**. OMCs are an attractive cell type for genetic engineering as they are autologously derived from minimally invasive procedures and have been proven to provide clinically detectable recovery in a clinical trial (109). However, there is a need to augment this therapy in order to enhance its regenerative potential in order to restore CST continuity across lesion sites. One method of addressing this issue may be to genetically engineer transplant populations *ex vivo* to allow them to secrete therapeutic biomolecules in order to enhance their established therapeutic potential. The clinical utility of this approach has been demonstrated in several animal studies, however methods of OEC engineering to date have overwhelmingly relied on viral vector methodologies **(Section 1.3.1)**, which cannot safely be translated to the clinic (141). The utility of MPs was highlighted in the introduction, but their utility for cOMC engineering, particularly in conjunction with magnetofection technology, has not been explored to date.

2.1.1 Oscillating magnetic fields may enhance gene delivery to cOMCs

Initial studies in to gene delivery using magnetofection strategies utilised static magnetic fields to enhance gene delivery to cells down the magnetic field gradient. In 2002, Mah et al

demonstrated that *in vitro* parvovirus-mediated transduction of HeLa cell derivatives with the reporter gene GFP could be increased to 58.9 ± 2.57% when the gene vector was reversibly linked to a microsphere before being added to cell cultures, compared to when free virus alone was added (8.48 ± 5.77%) (187), although it must be remembered that viral vector transduction studies typically report higher values using free virus. Further, when the parvoviral vector was coupled with a magnetic microsphere and the cell culture rested on the surface of a small square magnet, gene transfer efficiency increased again to 75.84 ± 2.75%. When viewed microscopically, GFP expression was seen to localise to cells in the region of the magnet. This result strongly suggests that the enhanced transduction was due to increased exposure to gene vectors which had been drawn to the cell surface down the magnetic field gradient. This was followed soon after by work from Scherer et al, who demonstrated that the use of non-viral gene vectors complexed with MPs could safely transfect cell populations within minutes, and with efficiencies in the same order of magnitude as viral vectors (188).

Subsequent work by McBain et al investigated transfection efficiencies of lung epithelial cells when luciferase reporter gene-MP complexes were applied to cells in the presence of an *oscillating* magnetic field, hypothesising that the increased energy provided by the lateral motion of the magnet would increase particle dispersion across the surface of the cells and stimulate increased particle uptake (147). The researchers found that oscillating magnetic fields outperformed static fields in terms of gene delivery by around two times (ca. 1 unit of luciferase activity versus ca. 0.5), and the conventional lipofection agent Lipofectamine by

several times (ca. 0.2). Crucially, they also reported differences in terms of gene delivery depending on the frequency at which the magnet oscillated.

Since then, this difference in transfection efficiency under fields oscillating at different frequencies (hereafter termed *"oscillo-specific variation"*) has been found to present in all cell neural cell types investigated. The precise mechanism for this increased transfection efficiency in response to oscillating fields is unknown, but may be due to: (i) increased distribution of MNPs across the surface of cells, (ii) increased endocytotic activity stimulated by movement of particles across the cell membrane. Importantly, each cell type has a specific oscillation frequency that confers optimal transfection efficiency. Subsequent work investigated the value of magnetofection in so-called "hard-to-transfect" populations such as NSCs (155). Here, transfection efficiency was 32.2% in the optimal oscillating field condition (oscillation frequency 4 Hz), compared to 18.4% in the presence of a static field and 9.4% when no magnetic field was applied. However, the optimal magnetic field conditions for gene transfer to cOMCs have not been determined. Moreover, the translation of engineered transplant populations to the clinic necessitates rigorous safety analyses in order to ensure that incorporation of novel genetic material to the graft genome does not negatively influence the safety of the graft in host sites.

2.1.2 DNA minicircles offer advantages for gene delivery over bacterial plasmids

Despite the advantages offered in terms of gene delivery by magnetofection platforms, an

inverse relationship has been reported between plasmid size and transfection efficiency using non-viral methods. For example, Pickard et al used magnetofection protocols to deliver DNA plasmids encoding the reporter gene GFP (3.5 kb), and the functional gene basic fibroblast growth factor (FGF2; 7.4 kb) to NSCs (155). Here, the researchers reported lower transfection efficiencies when NSCs were transfected with the larger functional plasmid (13.5%), compared to the smaller reporter plasmid (32.2%). In a similar experiment, Xu et al complexed plasmids encoding bone morphogenic protein-7 (OP-1; ca. 13 kb) and plasmids encoding GFP reporters (4.7 kb) to the same chitosan nanoparticle, before *in vitro* administration of this complex to adult canine chondrocytes (189). They then used fluorescence microscopy to identify GFP expression in order to determine the transfection efficiency of the cells, and enzyme-linked immunosorbent assay (ELISA) to confirm the expression of OP-1. Here, chondrocytes were able to express GFP but OP-1 was not detectable in culture supernatant at any point in the following two weeks. As both plasmids were attached to the same particle, the results imply that inability to express the functional genes was a function of plasmid size as opposed to the gross structure of the complex, particularly given that OP-1 gene functionality was confirmed by delivery using commercial lipofection agents followed by ELISA of supernatant. While the use of reporter plasmids have some value in proof-of-concept demonstrations, the incorporation of functional genes in to the construct necessitates an increase in plasmid size. As such, gene vectors capable of bypassing these size restrictions are essential if non-viral engineering of cells capable of secreting therapeutic factors are to become a clinical therapy.

In this regard, DNA minicircle vectors are an attractive alternative. These are small DNA vectors which encode essential gene expression cassettes, but, importantly, are devoid of the backbone components of conventional plasmids, significantly reducing their size. These constructs are derived from parental plasmids (PPs), larger DNA plasmids that contain the bacterial backbone components necessary for *in vivo* amplification of plasmid constructs (190). The minicircle is isolated from the PP construct through site-specific degradation, leaving behind the bacterial components. The absence of bacterial components confers further advantages to minicircles in that they are therefore less likely to undergo gene silencing events *in vitro* or immunogenic events *in vivo*, and as such their use is associated with enhanced transgene expression.

For example, a recent study performed a direct comparison of NSC transfection efficiency when optimal magnetofection protocols (oscillation frequency 4 Hz) were used to deliver either minicircles containing only essential expression cassettes encoding GFP (1.6 kb), or the PP from which this was derived (5.6 kb) (191). Here, the optimal transfection efficiency achieved using parental plasmids was 15.4%, compared to a maximal transfection efficiency of 45.4% using minicircles. Further, repeat transfection using minicircles significantly increased this transfection efficiency to a maximum of 54.4%, the highest reported non-viral transfection efficiency seen to date in NSCs, with no negative impact on cellular viability or proliferation reported. Moreover, increased gene expression was also detectable for up to four weeks post-transfection in minicircle-transfected cells versus PP-transfected cells, indicating the potential for improved transgene expression, which has also been reported by

other researchers (190). It is possible that the differences in transfection efficiencies is due a greater number of minicircles being able to bind to the surface area of a particle due to their small size, as the researchers reported increased GFP expression cassettes in minicircle-transfected cells. Similarly, it may be due to differences in the manner in which the DNA constructs bind to and are cleaved from the particle surface.

Translation of non-viral delivery of minicircle constructs to transplant populations in to the clinic requires the delivery of functional genes, as part of a combinatorial strategy. Current work from our group has determined that delivery of minicircles (4 kb) derived from a parental plasmid (8 kb) encoding human BDNF, driven by the human promotor EF1a, to NSCs using an identical protocol is feasible (192). BDNF belongs to the family of major neurotrophic factors described in Chapter 1 **(Section 1.1.4)** and acts both centrally and peripherally to support and regulate the growth of neural tissue. It has been demonstrated extensively in experimental models to promote axonal regeneration in the injured spinal cord (193). Its reported effects also include enhanced neuroplasticity and neuroprotection (194,195). As such, it has been identified as a key therapeutic target for neural regeneration research (196).

Our data has shown that maximum transfection efficiencies were significantly higher when NSCs were transfected with minicircles (28.9%), compared to parental plasmids (4.4%), facilitating an increase in BDNF secretion of 20 times in NSCs double-transfected using minicircles, compared to un-transfected controls (192). Moreover, BDNF overexpression by

NSCs resulted in significantly enhanced proliferation of the cells in culture, suggesting that the factors released are functional. Again, rigorous safety analyses for cell-specific markers of phenotype and proliferation, and cell viability markers, revealed no negative impact from the transfection protocol. These results indicate that optimised magnetofection strategies in combination with novel DNA minicircle vectors can be used to deliver genes encoding a functional key neurotrophic factor to a major neural transplant population. Despite the advantages offered by this combination of DNA minicircle vectors and oscillating magnetic fields in terms of safe and efficient non-viral gene delivery to transplant populations, their utility in gene delivery to cOMCs has not yet been investigated.

2.1.3 Objectives

The specific objectives of this chapter are:

(i) Identify the magnetic field conditions that result in optimal transfection efficiency of cOMCs using plasmids encoding the reporter gene GFP.

(ii) Evaluate the feasibility of using MPs complexed with novel DNA minicircles to engineer cOMCs capable of secreting BDNF.

(iii) Determine the effects of magnetofection protocols on cOMC proliferation and viability.

2.2 Experimental procedures

2.2.1 Materials

Cell culture reagents and culture grade plastics were from Invitrogen (Paisley, Scotland, UK), Sigma (Poole, Dorset, UK) and ThermoFisher Scientific (Loughborough, UK). Recombinant Human NRG1-beta 1 (Neuregulin) and Human BDNF Quantikine ELISA kit were from R&D Systems Europe Ltd (Abingdon, UK). Neuromag transfection-grade magnetic particles were from OZ Biosciences (Marseilles, France). The Magnefect-nano oscillating 24-magnetic array system was from nanoTherics Ltd (Stoke-On-Trent, UK). Minicircle BDNF (mcBDNF) DNA vector reagents were from System Biosciences (SBI; Mountain View, CA, USA). Minicircle vector purification kits were from Qiagen (Manchester, UK). All restriction/cloning enzymes were from Promega (Southampton, UK). pmaxGFP plasmid was from Amaxa Biosciences (Cologne, Germany). LIVE/DEAD assay kits were from Invitrogen. Click-iT® EdU Imaging Kits were from ThermoFisher Scientific (Loughborough, UK). Primary antibodies and dilutions **(Table 1)** used were: The OEC marker low-affinity nerve growth factor receptor p75 (p75), 1:200 (Chemicon, Darmstadt, Germany); the fibroblast marker fibronectin (Fn), 1:400 (Dako, Denmark); copGFP, 1:1000 (ThermoFisher Scientific); BDNF, 1:500 (Promega, UK). Secondary antibodies and dilutions used differed between Neuromag-GFP and mcBDNF transfection experiments, based on previously developed optimised protocols. For Neuromag-GFP transfection, secondaries were from ThermoFisher Scientific (1:400). For mcBDNF transfection, secondaries were from Jackson Immunoresearch Laboratories Ltd, Westgrove,

PA, USA (1:200). Details of antibodies are provided in **Table** 1. Vectashield mounting medium with the nuclear stain 4',6-diamidino-2-phenylindole (DAPI) was from Vector Laboratories (Peterborough, UK)

	P75/Fn	**BDNF/copGFP**
Primary antibodies	Mouse anti-human p75 IgG Monoclonal [clone number: 8211] (1:200)	Chicken anti-human BDNF IgY Polyclonal (1:1000)
	Rabbit anti-human fibronectin IgG Polyclonal (1:400)	Rabbit anti-copGFP IgG Polyclonal (1:500)
Secondary antibodies	Goat anti-mouse IgG Polyclonal (1:400)	Donkey anti-chicken IgG Polyclonal (1:200)
	Goat anti-rabbit IgG Polyclonal (1:400)	Donkey anti-rabbit IgG Polyclonal (1:200)

***Table 1: Details relating to the antibody formulations used for immunostaining protocols**.*

Including host species, target species, antigenic target, isoform, clonality and dilution.

2.2.2 Primary cell harvest and culture

The care and use of all animals used in the production of cell cultures were in accordance with the Animals Scientific Procedures Act of 1986 (UK).

Cell banks generated during the clinical trial for cOMC transplantation into sites of spinal injury in companion dogs **(Section 1.2.5)** were used to generate the primary cOMC cultures used for all experiments. The precise surgical procedures used to derive these cells can be found in the primary paper, a summary of which is provided here: The left frontal sinus of the skull of anaesthetised dogs with chronic SCI equivalent to ASIA A was opened to access the olfactory mucosa of the frontal sinus and caudal nasal cavity. Fragments of olfactory mucosa were dissected and transferred in a petri dish on ice to the laboratory to be processed. Cartilage, connective tissue, blood vessels and non-olfactory mucosa were removed under microscopic guidance. The remaining tissue was then finely chopped using a scalpel, and dissociated before being passed through a 40 µm filter. The resultant pellet was then re-suspended and plated in DMEM containing 10% fetal bovine serum, Forskolin (2 µM in dimethyl sulphoxide), Neuregulin-1 (20 ng/mL), penicillin and streptomycin (both at 10 mg/mL), at 37°C in 95% air:5% CO_2 to allow confluence to be reached. Cells were then passaged in order to generate sufficient numbers for transplantation to injury foci. Excess cells were then kept frozen at below -80°C for approximately 48 months before being expanded under growth factor stimulation in cOMC media, composed of DMEM containing 10% fetal bovine serum, Forskolin (2 µM in dimethyl sulphoxide), Neuregulin-1 (20 ng/mL),

penicillin and streptomycin (both at 10 mg/mL), at 37°C in 95% air:5% CO_2.

2.2.3 Determination of a safe Neuromag dose for cOMC transfection

Previous work from our lab has reported on the cell-specific differences in Neuromag dose toxicity (152,155,197). Most recently, Neuromag concentrations of 2.1 µL/mL have been used to safely engineer NSCs (155). However, obvious cell rounding and detachment was seen at this concentration during pilot experiments (n = 2, **Figure 3A**, inset). Conversely, uniform cellular morphologies with no obvious rounding or detachment were seen when cells were treated with 1.05 µL/mL Neuromag. This concentration was therefore used for all subsequent Neuromag-GFP transfection experiments.

2.2.4 DNA minicircle vector formulation

All reagents used to generate the mcBDNF were obtained from System Biosciences, CA, USA and Thermofisher Scientific, UK. The minicircle construct contains (i) an Elongation Factor 1 alpha (EF1a) promoter which is a constitutive promoter of human origin, (ii) an internal ribosomal entry site (IRES), a commonly used nucleotide sequence which enables the simultaneous expression of human BDNF and GFP (for assessment of transfection efficiency). mcBDNF was generated from the parental construct pMC.EF1a-BDNF-IRES-GFP-SV40PolyA (**Figure 1**). The minicircle induction protocol involved the production of a large volume (400

mL Terrific Broth containing kanamycin) of the parental plasmid (transformed in ZYCY10P3S2T Producer Bacterial Strain, a specifically engineered E.Coli strain which upon addition of arabinose express two enzymes that permit the generation of highly purified minicircle yields: (i) ΦC31 integrase - splits the larger parental plasmid of 8.1 kb into two circular entities: minicircle DNA (size: 4.1 kb), and the bacterial backbone containing SceI endonuclease recognition sequence (size: 4.0 kb) and (ii) SceI endonuclease which degrades the bacterial backbone sequence. mC-BDNF-GFP was subsequently extracted using an Endotoxin-free maxiprep kit (Qiagen,UK). Prior to use, this construct was sequenced (outsourced to Source Biosciences, UK) to verify that the full length BDNF was present and contained no mutations.

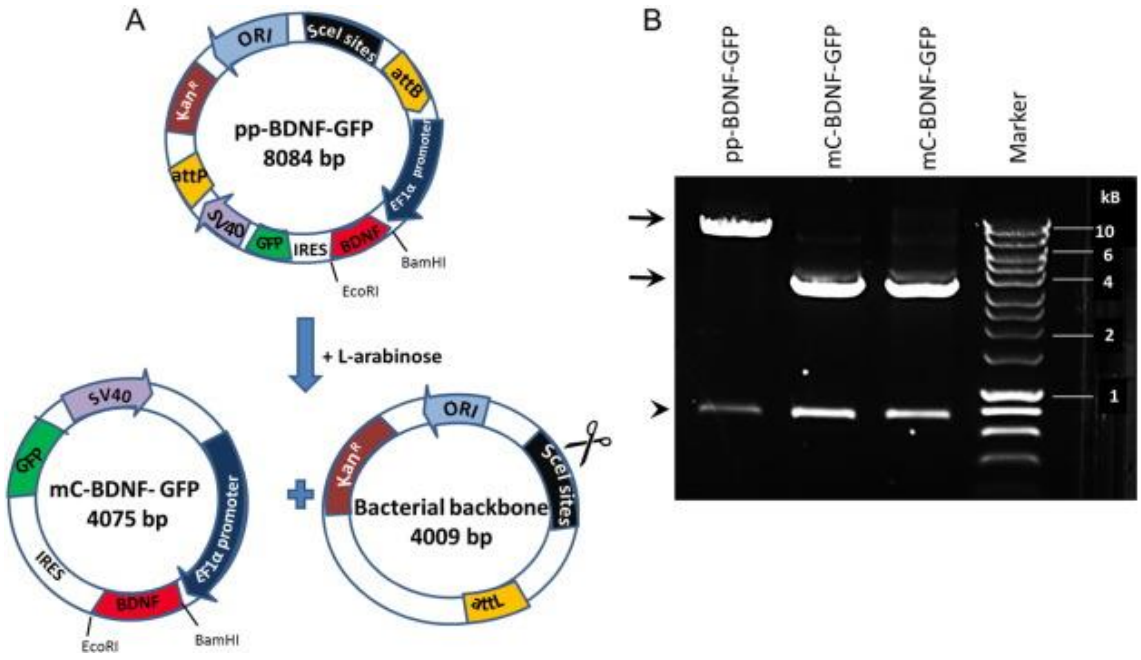

Figure 1: *Minicircle derivation, DNA vector maps and purity of vector preparations. (A) Schematic showing the generation of mC-BDNF-GFP from parental plasmid pp-BDNF-GFP following l-arabinose induced (i) recombination between attB and attP sites (present in pp-BDNF-GFP) and (ii) SceI endonuclease initiated degradation of the bacterial backbone.(B) Agarose gel electrophoresis micrograph of EcoRI and restriction BamHI digests of pp-BDNF-GFP (lane 1) and two independent preparations of mC-BDNF-GFP (lanes 2 and 3) run alongside a 10 kB DNA marker (lane 4). The DNA fragment corresponding to the DNA vector (i.e. parental plasmid or minicircle) is denoted by arrows, arrowheads denote the BDNF insert. (bp = base pairs; kB = kilobases). Taken with permission from (192).*

2.2.5 Magnetofection of cOMCs

Cells (passages 0-11) were seeded (1 x 10^5 cells/mL; 0.6 mL) on to PDL-coated coverslips in 24-well plates. After 24 h, the media in each well was replaced with fresh media (0.225 mL) and returned to the incubator for a minimum of 2 h. To prepare nanoparticle complexes, 88 ng pmaxGFP was added to 75 µL DMEM. This solution was then added to 0.31 µL Neuromag. The resultant solution was gently triturated ten times and incubated at room temperature (RT) for 20 mins. The complexes were then added drop-wise whilst gently swirling the plate to ensure even particle distribution. Control wells received the same volume of DMEM, without complexes. Plates were returned to the incubator and directly exposed to their respective experimental magnetic field conditions. These were: no field (NF), static field (F = 0Hz), and oscillating magnetic fields of frequency F = 1Hz and F = 4Hz. Control wells were not exposed to a magnetic field. Magnetic fields were applied using the Magnefect-nano oscillating magnetic array system, which comprises a 24-magnet array (NdFeB, grade N42; field strength of 421 ± 20 mT), allowing a 24-well plate to rest on the surface of the magnets such that each well covers one magnet. The frequency, amplitude and duration of each oscillation cycle were programmed using an attached computer and an amplitude of 0.2 mm was used for all experiments which has previously been shown to be optimal for a range of cell types (198,199). Cells were then removed from the magnetic array and returned to the incubator for 24 h prior to fixing. Neuromag-mcBDNF transfection was performed in an identical manner, using only a single optimum magnetic field condition and a control.

2.2.6 LIVE/DEAD staining

24 h post transfection, media was replaced with 4 µM calcein AM (green fluorescence in live cells) and 6 µM ethidium homodimer-1 (EtH; red fluorescence in dead cells) in DMEM. Cells were incubated at room 37°C for 15 mins before imaging by fluorescence microscopy. To calculate cellular viability, 3 microscopic fields per experimental condition were taken, with a minimum of 100 cells per field assessed per condition. Number of cells expressing calcein (LIVE) was expressed as a percentage of the total cells expressing either calcein or EtH (DEAD) to give the percentage cell survival per condition.

2.2.7 Immunocytochemistry

Cells were fixed in 4% paraformaldehyde (PFA) at 24 h post-transfection to assess transfection efficiency, particle uptake and measures of protocol safety. Fixed samples were blocked for 30 mins at RT. Blocking solutions differed between experiments involving pmaxGFP transfection (10% normal goat serum and 0.3% Triton-X-100 in PBS) and mcBDNF transfection (5% normal donkey serum in PBS-0.3% Triton X-100). Following this, cells were incubated with primary antibodies (p75 and Fn for Neuromag-GFP transfection; copGFP and BDNF for mcBDNF transfection) in blocking solution for 24 h at 4°C. Cells were then rinsed three times in phosphate buffer solution (PBS) before being incubated with appropriate secondary antibodies for 2 h in the dark at RT (see **Table 1** for details of antibodies). Cells were mounted on to glass slides using VectaShield mounting medium with DAPI prior to

immunofluorescence microscopy analysis.

2.2.8 Phase and fluorescence microscopy

Phase and fluorescence microscopy of all experiments was performed using an Axio Observer.Z1 equipped with an AxioCam MRm powered by Zen 2 (blue edition) software (Carl Zeiss MicroImaging GmbH, Goettingen, Germany). Images were merged and quantified using ImageJ 1.49v software (200).

2.2.9 Assessment of particle uptake and transfection efficiency in cOMCs

Fluorescence microscopy analysis was used to estimate particle uptake and transfection efficiency of cOMCs. This method was selected as it allows for detailed microscopic evaluation of key measures of overall cell health, including adherence and morphology, to be conducted at the same time. Three microscopic fields per magnetic field condition were analysed, with a minimum of 100 cells assessed for each condition. Number of cells displaying particle uptake were estimated from triple merged DAPI, phase and fluorescent MP images and numbers of GFP expressing cells were calculated from double merged DAPI and GFP images. In both instances, MP and GFP exposure levels were set using control conditions and kept constant for every experiment. To assess transfection efficiency/success of the minicircle vector, cells were stained with primary antibodies for copGFP and BDNF

(Section 2.2.7). The different copGFP was used as it has lower toxicity compared to mutated forms of GFP such as pmaxGFP (used in optimisation experiments), and as such is more relevant to translational medicine. However, it is less readily detectable via immunofluorescence microscopy and so must enhanced via immunostaining for GFP.

2.2.10 Phenotypic characterization of transfected populations

Transfected cells were classified based on immunostaining and morphology. Generally, p75+ cells displayed an elongated fusiform bipolar or tripolar morphology, a well-described OEC phenotype (89). Fn+ cells tended to display a broad, flattened morphology with a larger soma, likely to be fibroblasts. In addition, there was a population of cells which did not display phenotypes typical of either OECs of fibroblasts. For the purposes of classification, three phenotypic categories were therefore identified: (1) Strongly p75+ elongated fusiform bi- or tri-polar cells, presumed to be OECs; (2) Strongly Fn+ cells displaying flattened morphology, presumed to be fibroblasts and; (3) Uncategorised cells which did not fit either category (1) or (2), including flattened p75+ cells, unipolar Fn+ cells and small, rounded cells. It is possible that a proportion of these cells represent OECs or fibroblasts, but were placed in this category to avoid falsely high measures of OEC or fibroblast transfection. Three fields per condition were analysed (at least 100 cells per condition).

2.2.11 Assessment of cell viability and proliferation

The proportion of live cells per condition was assessed using triple merged live, dead and phase images. The proportion of pyknosis (indicating cell death, seen as nuclear shrinkage, fragmentation, and chromatin condensation) was calculated from images taken from evaluation of transfection efficiency, using double-merged DAPI and phase images. In order to examine effects of the procedures on cellular proliferation, a Click-iT® EdU assay (a nucleoside analogue of thymidine incorporated in to DNA during active DNA synthesis) was performed according to manufacturer's instructions. Here, the EdU reagent (1 µM) was added to cells 6 h prior to fixation and the cells taking up EdU (proliferating cells) were fluorescently labelled and assessed using quadruple-merged phase, DAPI, GFP and EdU images.

2.2.12 ELISA

Cell supernatants were collected 24 h post-transfection and centrifuged (6 min at 1500 rpm) to clear cells/cell debris. To determine the BDNF protein concentration in cell supernatants, an ELISA was applied using the Quantikine® ELISA Kit (R&D Systems, UK) according to the manufacturer's instructions. This assay employs the quantitative sandwich enzyme immunoassay technique. Briefly, standards and samples were added to wells pre-coated with a monoclonal antibody specific for human BDNF and incubated for 2 h followed by several washes. Horseradish peroxidase-linked monoclonal antibody specific for BDNF is added to the wells. Excess antibody-enzyme reagent was removed from the wells and washed. Colour

development occured upon addition of the substrate and then stopped before measurement of the color intensity (absorbance at 450 nm) using Glomax Multi Detection System (Promega, UK).

2.2.13 Statistical analysis

Data were analysed by a one-way ANOVA and Bonferroni's multiple comparison test (MCT), except where sets of only 2 data were compared, in which case an unpaired T-test was used. Statistical analysis was performed using Prism software (version 6.0h, Graphpad), and values are expressed as mean ± SEM. The number of experiments 'n', refers to the number of independent cultures used, each derived from a different companion dog.

2.3 Results

2.3.1 Characterising primary cOMC cultures

Primary cOMC populations from the nasal mucosa of domestic dogs were successfully cultured, with good adherence to the substrate surface **(Figure 2A)**. These cultures contained a mixed population of cell types with both strongly p75+ elongated, bi- or tri-polar cells classified as OECs **(Figure 2B)** and rounded cells strongly Fn+, classified as fibroblasts **(Figure 2C)**.

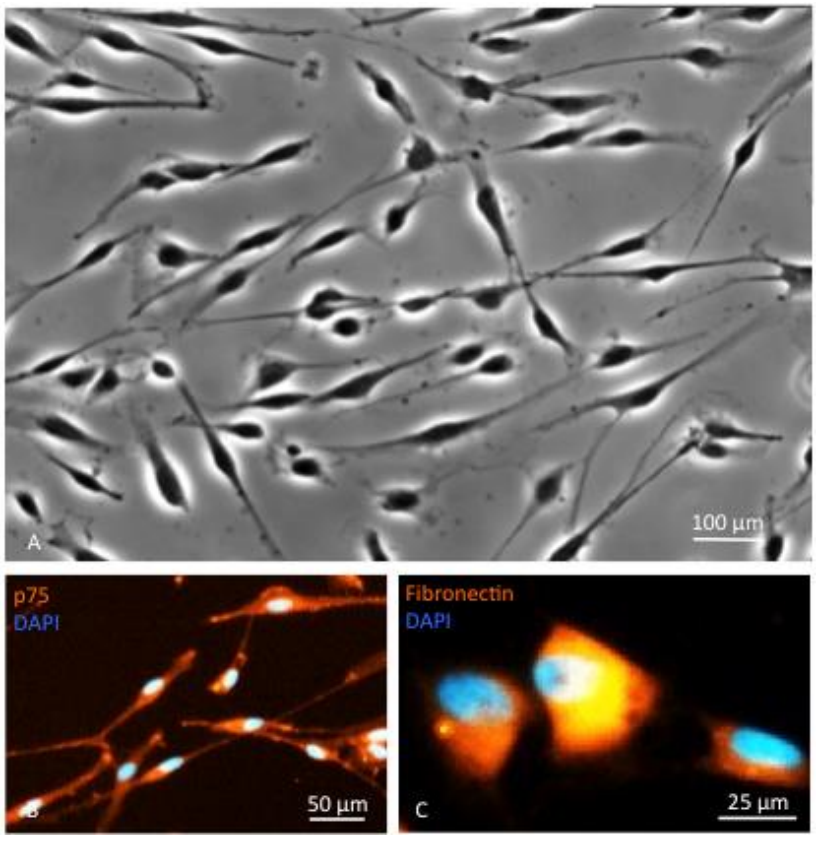

Figure 2: Classification of mixed cOMC populations. *(A) Phase image of cOMCs in culture. (B) Cells displaying fusiform morphology typical of OECs. (C) Cells displaying round morphology typical of fibroblasts.*

2.3.2 Field application enhances particle uptake in cOMCs

Next, I sought to determine the extent to which cOMCs were able to take up particles. 24 h post-transfection, cells were fixed and then viewed microscopically in order to identify what proportion of cells had taken up particles, which were fluorescently labeled so they could be visualised via fluorescence microscopy. Extensive cellular uptake of particles was observed in all experimental conditions. Particles tended to be localised in the cell body, with almost no particles visible in cell processes **(Figure 3A and B)**. The percentage of cells displaying uptake was upwards of 85% in all experimental conditions, and was greater in those conditions where magnetic fields were applied, versus those where no field was applied. Specifically, in the absence of an applied magnetic field, the "baseline" particle uptake was 86.0 ± 0.8% (NF; range 85.0-87.2%; **Figure 3A and C**), which was significantly ($P < 0.01$) increased to 94.8% ± 1.6% when a static magnetic field was applied (F = 0 Hz; Range 91.8 - 99.3%; **Figure 3B and C**). Although application of the oscillating magnetic fields significantly enhanced the numbers of cOMCs which took up particles (to 95.9 ± 0.9% and 95.0 ± 1.6% for the F = 1 Hz and F = 4 Hz, respectively) compared to when no field was applied,, there was no further enhancement in uptake over the static field condition **(Figure 3C)**.

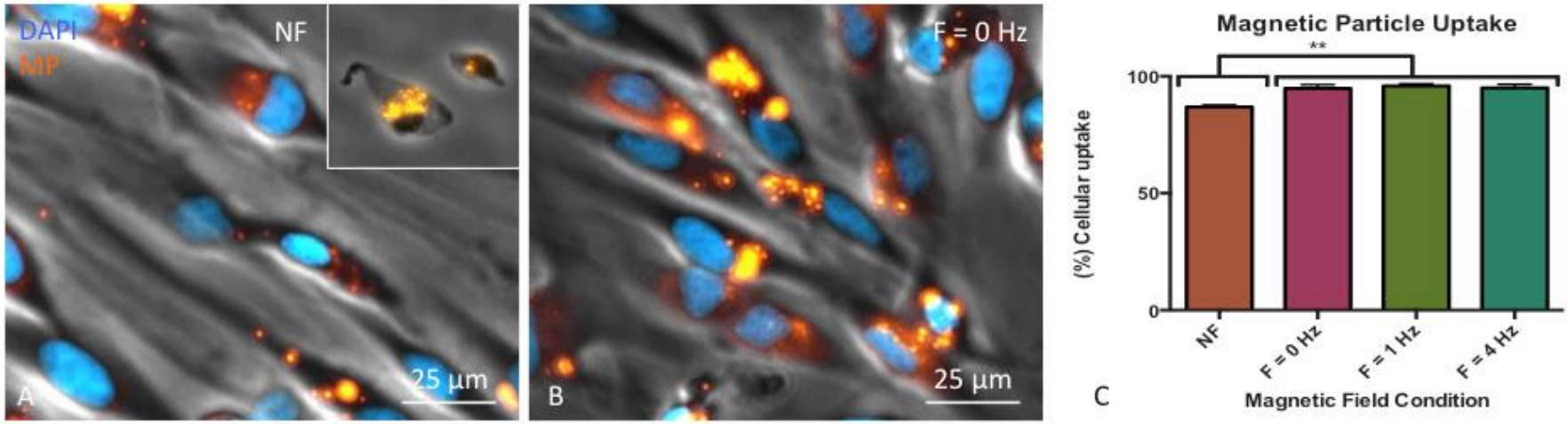

Figure 3: Magnetic fields are associated with increased particle uptake. *(A) Fluorescent Neuromag uptake in the NF condition. Inset: cellular detachment and retraction of processes in response to toxic Neuromag dose. (B) Fluorescent Neuromag uptake in the F = 0 Hz condition (C) Graph showing the percentage of cells which displayed Neuromag uptake. **P < 0.01, n = 4.*

2.3.3 Magnetic field application significantly enhances GFP expression in cOMCs

GFP expression was observed in all experimental conditions in both OEC and fibroblast-like cells **(Figure 4A and B)**. Baseline transfection efficiency, i.e. transfection efficiency when no magnetic field was applied, was 34.9 ± 2.9% (NF; range 28.8 - 42.7%; **Figure 4A and C**). When a magnetic field was applied, transfection efficiency was increased to ≤ 60% in all magnetic field conditions. Specifically, transfection efficiency in the static field condition was 57.7 ± 3.5% (F = 0 Hz; range: 48.8 - 63.9%; **Figure 4B and C**), and in the 1 Hz and 4 Hz oscillating field conditions was 56.1 ± 4.5% (F = 1 Hz; range: 47.5 - 68.6%) and 56.6 ± 6.4% (F = 4 Hz; range: 41.2 - 72.0%), respectively **(Figure 4C)**. Expression of GFP was found to be uniform throughout transfected cells. When viewed microscopically, transfected cells did not display variation in morphology or adherence when compared to controls. The intensity and pattern of immunocytochemical markers of cell phenotype did not differ between transfected and untransfected cells, nor did it differ between cells transfected under differing magnetic field conditions. Of the total number of transfected cells across all conditions, 47.6 ± 3.1% displayed a bipolar fusiform morphology and p75 staining (OEC; range: 38.8-52.6%), and were therefore considered to be transfected OECs. 29.3 ± 6.0% displayed fibroblast-like morphologies with strong Fn+ staining (Fb; range: 19.0-42.3%), and were therefore considered to be transfected fibroblasts. 23.1 ± 3.5% were defined as uncharacterised (UC; range: 15.4-30.0%), as they displayed phenotypic properties which meant they did not fit the description of OECs or fibroblasts described in **Section 2.2.10** and so could not be readily identified. The results of this phenotypic classification analysis is displayed in **Figure 4D**.

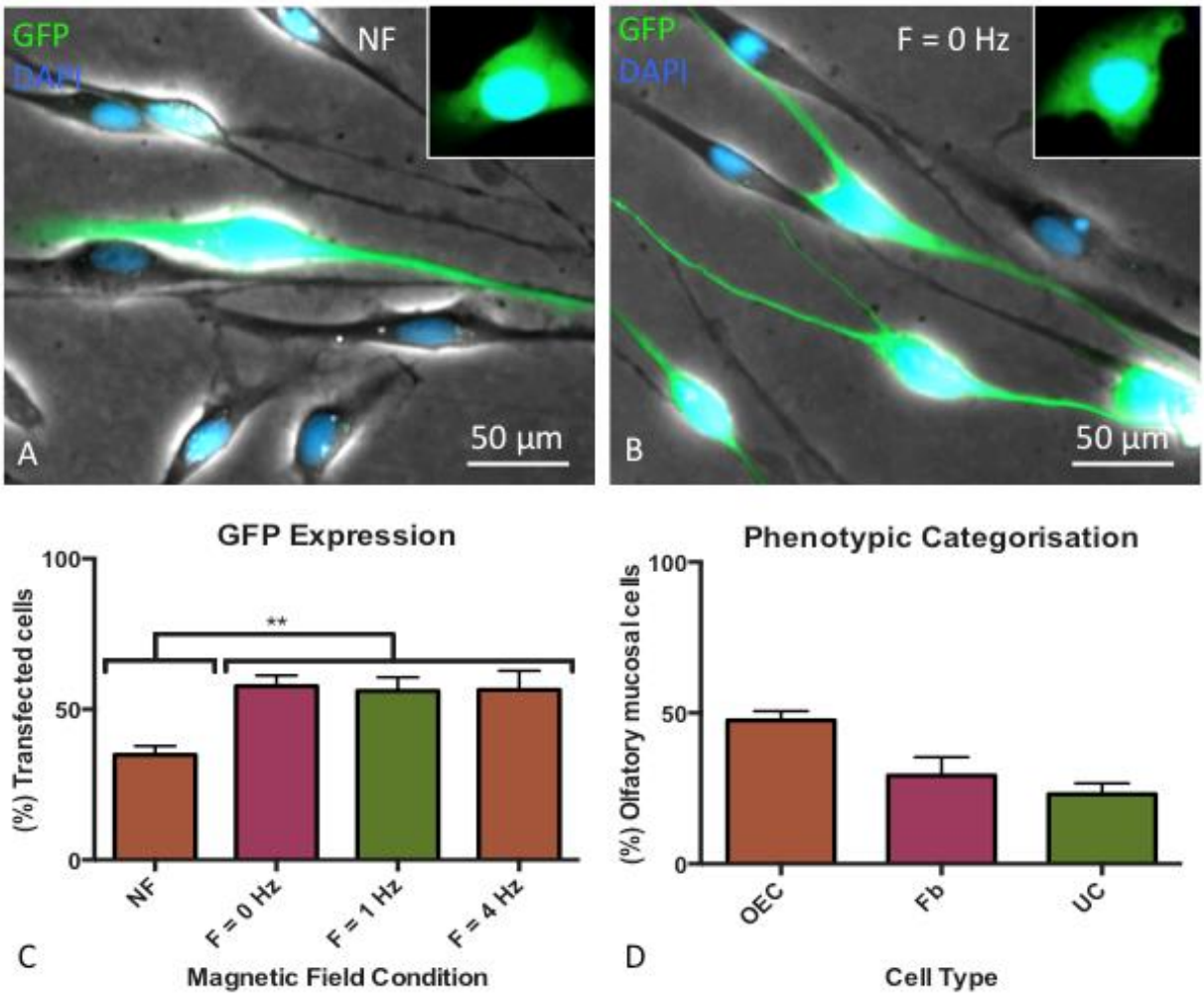

Figure 4: Magnetic fields are associated with higher transfection efficiency. *(A) GFP expression in the NF condition with GFP+ fibroblast (inset). (B) GFP expression in F = 0Hz condition with GFP+ fibroblast (inset). Note greater number of transfected cells in F = 0 Hz condition. (C) Graph showing the percentage of transfected cells in each field condition. Note greater expression in conditions where cells were exposed to a magnetic field. (D) Graph showing the percentage of transfected cells which fell in to each phenotypic category. **P < 0.01, n = 4.*

2.3.4 Magnetofection protocols had no effect on cell safety markers

Transfected cultures displayed similar numbers of proliferating cells to control conditions, as measured by Click-iT® EdU proliferation assay, with GFP expressing cells also staining positive for the proliferation marker **(Figure 5A and D)**. There was no decrease in cell survival in transfected cells compared to controls, with all conditions displaying similar viability, which was upwards of 95% as judged using by a LIVE/DEAD assay **(Figure 5B and E)**. Finally, the level of pyknosis was low and did not differ between experimental conditions, remaining below 3% in all conditions **(Figure 5C and F)**.

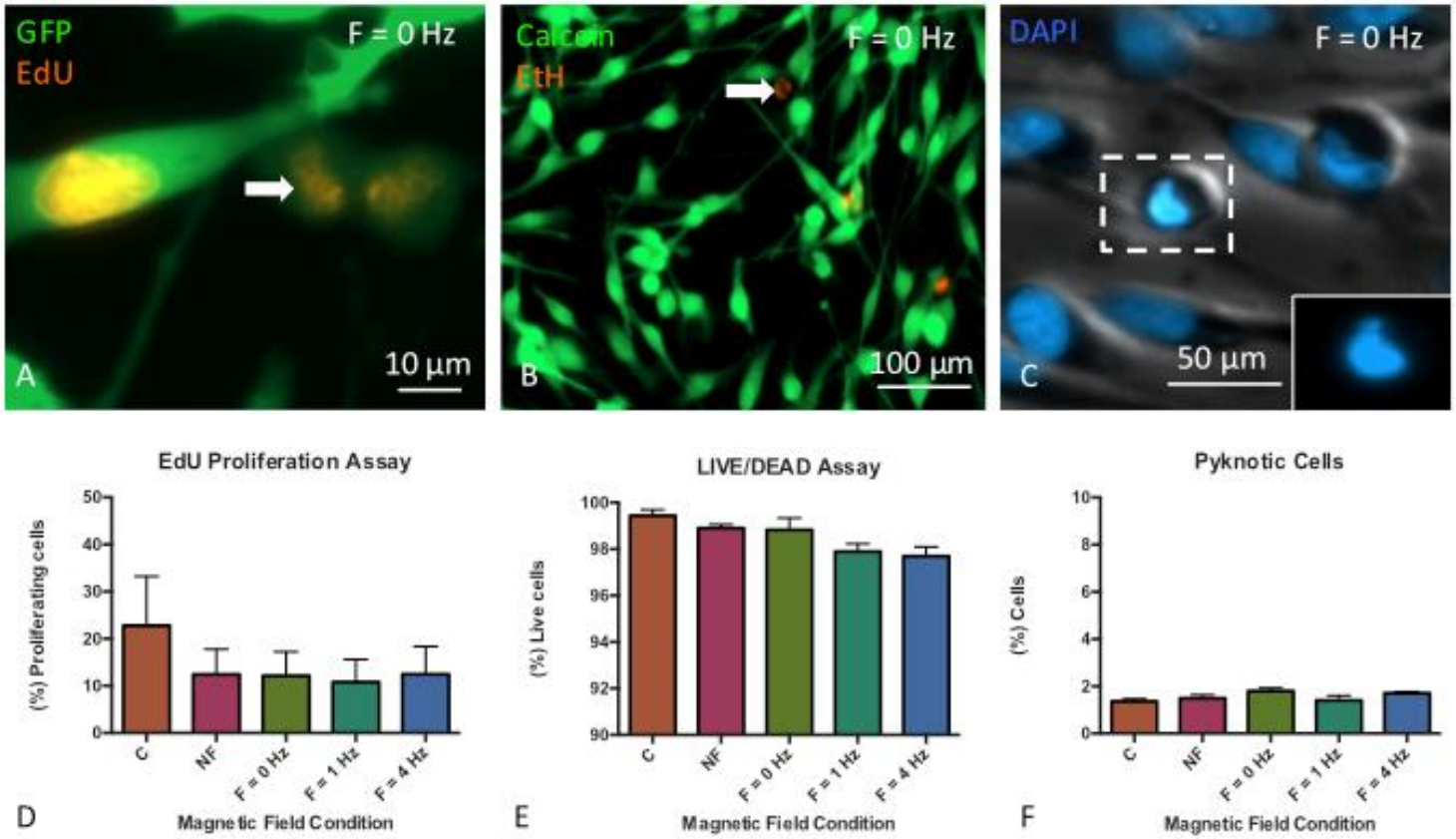

Figure 5: Cellular viability and proliferation were unaffected by magnetofection protocols. *(A) EdU+ GFP+ cells in static field (F = 0Hz) condition. EdU is a marker for cells which have undergone recent mitosis, and two transfected EdU+ cells can be seen here (arrows) in close proximity, suggesting they are daughter cells. (B) LIVE/DEAD assay showing a small proportion of dead (EtH) cells. (C) Typical pyknotic cell displaying rounded appearance and nuclear condensation. (D) Graph showing the percentage of cells per magnetic field condition which underwent mitosis within a 6h timeframe. (E) Graph showing the percentage of live cells per condition. (F) Graph showing the percentage of cells per condition which displayed pyknotic characteristics. n = 4.*

2.3.5 Optimised magnetofection protocol enables safe delivery of mcBDNF

Overall, particle uptake and GFP expression did not differ significantly between conditions exposed to a magnetic field. Additionally, there was no evidence of differences in cellular viability and proliferation between experimental conditions. However, static magnets are considerably cheaper and more readily available than oscillating magnetic arrays, and as such have a greater translational relevance to magnetofection protocols performed in a clinical setting. Therefore, the static F = 0 Hz was taken as the optimum field condition for the BDNF transfection experiments. For mcBDNF experiments, under the static field condition, transfection efficiency was estimated to be 8.1 ± 0.3% (range: 7.5 - 8.7%). Additionally, immunostaining for BDNF revealed a punctate pattern of fluorescence within copGFP+ cells suggesting that BDNF was stored within perinuclear vacuoles **(Figure 6B)**. There was also some weak BDNF staining visible within cells that did not express copGFP, suggesting endogenous BDNF expression by cOMCs. In ELISA assays, the mean concentration of BDNF in transfected cell supernatant was significantly greater (three-and-a-half-fold) versus controls **(Figure 6C).** Specifically, transfected cell supernatant contained 245.7 ± 16.0 pg/mL BDNF (T; range: 222.3-276.2 pg/mL), compared to 67.3 ± 1.87 pg/mL in controls (C; range: 64.1 - 70.1 pg/mL). Safety assays revealed that there was no difference between mcBDNF transfected and untransfected control cells in terms of the percentage of proliferating cells, cell viability or percentage of pyknotic nuclei **(Figure 6D-F)**.

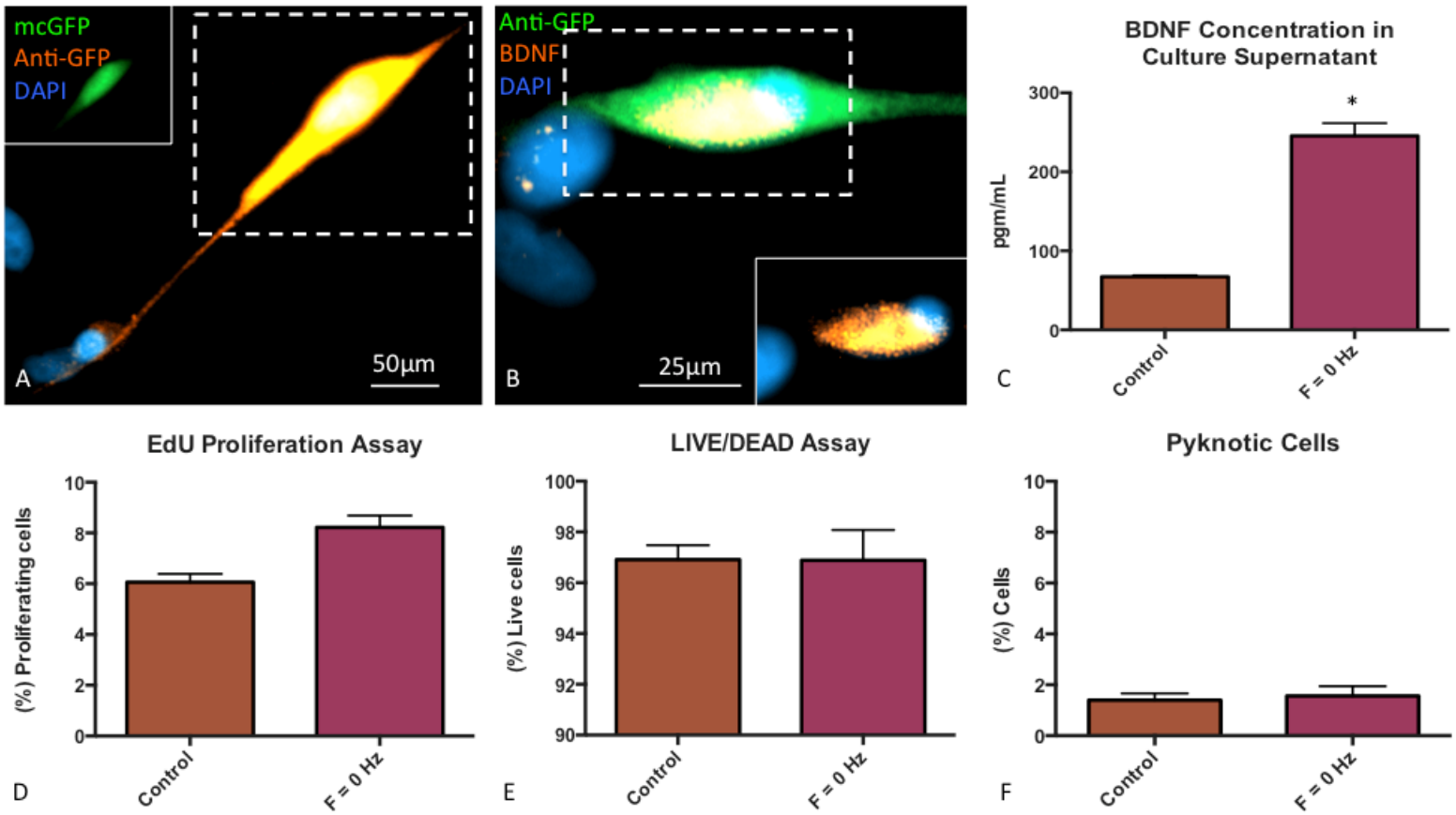

Figure 6: MPs combined with an applied static magnetic field can effectively deliver genes encoding BDNF to cOMCs, with no effect on cellular viability or proliferation. *(A) Anti-GFP staining enhanced fluorescence (inset, top left). (B) When cells were stained for intracellular BDNF, greater accumulation of BDNF was seen inside transfected cells (green) than untransfected cells. Note small quantities of BDNF inside adjacent untransfected cell. (C) Graph showing concentration of BDNF in cOMC culture supernatant of transfected versus untransfected cells.. (D) Graph showing percentage of cells which underwent mitosis in a 6h timeframe in both the transfected and the control conditions. (E) Graph showing percentage of live cells in the control conditions versus the transfected conditions. (F) Graph showing percentage of cells per condition which displayed pyknotic characteristics. *$p<0.05$, $n = 3$.*

2.4 Discussion

To the best of my knowledge, this study is the first to demonstrate that MPs in combination with an applied magnetic field can be used to safely and efficiently deliver genes to a clinically relevant transplant population. Further, combining the technology with a DNA minicircle vector enabled delivery of the major neurotherapeutic protein BDNF, potentially facilitating graft secretion of additional repair promoting molecules. As such, combining the pro-regenerative qualities of BDNF with the permissive growth environment created by OMCs may represent a highly viable therapeutic strategy, a “best of both worlds” scenario. As such, the developed protocols could represent the next steps in enhancing the therapeutic capacity of cOMCs and we consider the data offers considerable promise with regards to translating the MP platform to human application.

2.4.1 Magnetic particles to engineer cOMCs offers translational advantages

In the context of developing a safe and effective therapy for spinal injury, the combination of methodologies employed in the present study offers distinct translational advantages. OMCs are a promising clinical population due to their relatively straightforward autologous derivation and their proven potential in promoting repair after spinal injury. Further, engineering cOMCs through the magnetofection technology seems particularly advantageous given the highly efficient particle uptake of cOMCs and the lack of an effect on measures of cell health, meaning the additional benefits provided by the MP platform could potentially be

safely exploited. For example, non-invasive imaging of a high proportion of the transplant population is a desirable requirement for translating cell therapy studies into clinical trials. However, there are currently few MPs that possess the necessary characteristics for both gene delivery and non-invasive tracking. Work to develop such a multifunctional particle is currently underway (167). Future studies would have to investigate time dependent retention of the particles by OMC cultures, ability of MPs to track cOMCs using MRI and any potential long-term toxicity to examine whether this strategy could be used to track the transplant population.

2.4.2 The use of minicircles may facilitate incorporation of additional therapeutic genes

In addition to the advantages in terms of safety and functionality offered by the use of MPs as gene vectors, the minicircle constructs are entirely biocompatible as they employ a human promoter (EF1a) opposed to the widely used cytomegaloviral promoter. As discussed in **Section 1**, meaningful functional recovery is likely to require us to address multiple aspects of the regenerative process at once. The relative small size of the construct may allow for the incorporation of additional therapeutic genes that could aid this, before a reduction in transfection efficiency is encountered.

For example, lentiviral vectors have been used to deliver ChABC or a neurotrophic factor to Schwann cells, before comparing the *in vivo* responses to these cell variations both individually and in combination in rodent SCI models (28). The results indicate a synergistic

effect of combining two therapeutic biomolecules, resulting in improved outcomes in terms of number of regenerating CST axons in association with the graft and locomotor capabilities. Incorporation of a gene encoding ChABC in to the minicircle constructs described in this chapter could allow grafts to begin to degrade the glial scar as well as supporting and promoting axonal regeneration.

Similarly, NSCs retrovirally engineered to express VEGF have been shown to enhance angiogenesis when transplanted in to experimental spinal injury foci (201). Here, the pro-regenerative qualities of NSCs were enhanced by improving vascular proliferation at the site of injury, which was significantly greater in engineered NSCs than in the un-engineered group. If genes encoding VEGF were incorporated in to the minicircle structure, it is possible that similar benefits would result.

2.4.3 cOMCs are highly amenable to magnetofection strategies and do not display oscillo-specific transfection responses

The transfection levels reported are the highest achieved by our group for neural cell transplant populations, using magnetofection approaches to date **(Figure 7)**. This suggests a large proportion of the transplant population could be engineered to secrete therapeutic biomolecules, in order to achieve effective repair, whilst maintaining a high level of safety. Transfection efficiency under optimal magnetic field conditions in this experiment was ca. 57%. While this is lower than the levels of reporter gene expression reported in proof-of-

concept demonstrations of virus-mediated OEC transduction in previous work, often close to 100% (202), the drawbacks associated with these methodologies in terms of safety mean they are likely to be less relevant in terms of clinical translation. Moreover, the magnetofection strategies described here result in moderately high transfection efficiency of cOMCs within 24h, following the application of a protocol which takes no longer than 1 full hour to implement, and uses materials which can be generated in large quantities inexpensively. When this is considered in the context of OMCs, which as discussed can be derived non-invasively and amplified in culture to the numbers required for transplantation (109), the ease with which this methodology could be scaled up to the clinic becomes apparent.

As discussed in **Section 2.1.1**, neural cells display oscillo-specific differences in transfection efficiency. For example, astrocytes respond optimally to fields oscillating at 1 Hz with a transfection efficiency of ca. 55%, while NSCs respond with incrementally increasing transfection efficiencies to magnetic fields of increasing oscillatory frequencies, reaching an optimal efficiency of ca. 10% in neurospheres and ca. 30% in monolayers at an oscillatory frequency of 4 Hz. However, we report no such differences in the present study, possibly because OECs are inherently endocytotically active, as others have reported. Li et al in 2005 conducted an in-depth analysis of the specific properties of OECs *in vivo* which allow them to support the regeneration of ORNs. Here, they explain that this cell type is highly endoocytotically active throughout adult life in order to facilitate the removal of degenerating axons (203). It is possible that this property confers significant amenability to magnetic

particle uptake, and subsequent transfection, making any oscillo-enhancement effects redundant. Indeed, amenability to transfection is a quality cOMCs have in common with microglia, the main phagocytotic cell of the CNS which demonstrate magnetic particle uptake of >90% after only 4h (154), and astrocytes, which are highly metabolically active in their regulatory capacity within the CNS. This confers further advantages in terms of scaling-up procedures for clinical translation in that static magnets are significantly cheaper than oscillating magnetic arrays.

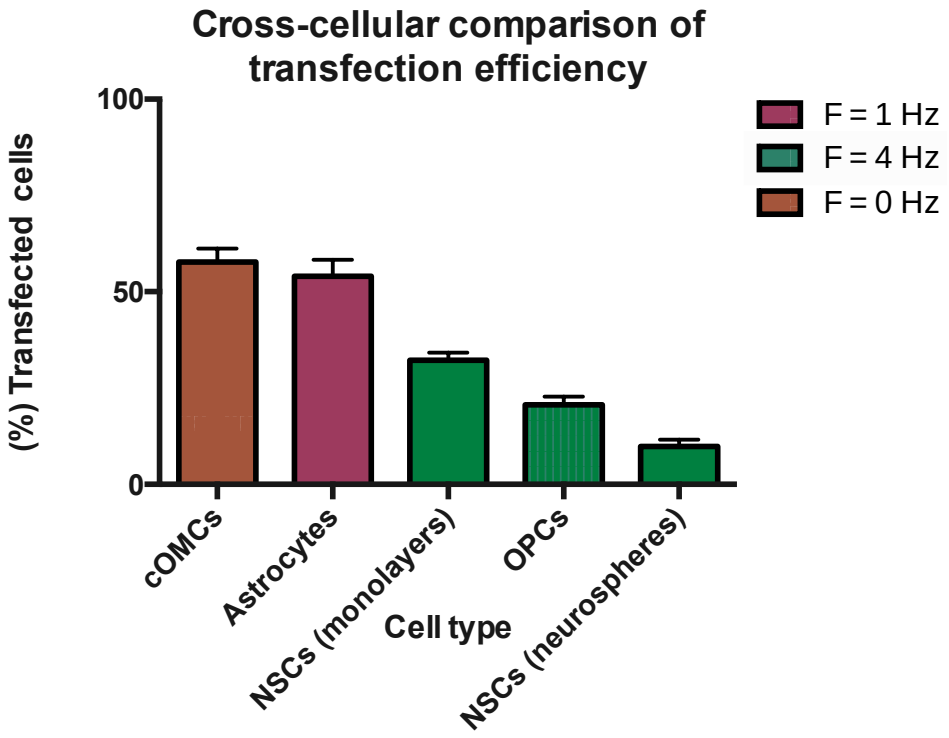

Figure 7: cOMCs show a greater permissiveness for transfection than other neural transplant populations. *Graph displaying how optimum transfection efficiency in cOMCs compares to that seen in other neural transplant populations for which optimised magnetofection protocols have been developed. Adapted from* (153,155,199).

2.4.4 Magnetofection can generate cOMCs capable of secreting neurotrophic factor

Our ELISA analysis of the transfected cell supernatants suggests that optimised magnetofection protocols can be used to engineer cOMC grafts capable of secreting BDNF. This is significant in that it could augment the potential therapeutic capacity of OMCs. While the absolute number of transfected cells, as measured by GFP-positivity, was relatively low (ca. 8%), the concentration of BDNF in cell supernatant was 3.5x higher than that of the control. This may be because fewer cells are transfected, possibly owing to differences in the promoter used in the plasmid for the optimisation experiments versus those used in minicircles for functional gene delivery, in which case a small number of cells are secreting high levels of BDNF. It may also be due to some dissociation occurring at the transcription/translation level between the gene encoding BDNF and the downstream GFP gene. In which case, cells are secreting BDNF but are not expressing GFP. In any case, future *in vivo* work such as growth bioassay using DRG cells *or in* vivo SCI models is needed to determine if the neurotrophin released by these cells is biologically active

2.4.5 Magnetofection protocols produce a mixed population of transfected cOMCs

Our phenotypic characterisation data indicate that we have engineered a mixed population of olfactory mucosa-derived cells, including OECs and fibroblasts. Analysis of transfected OECs versus fibroblasts revealed no statistically detectable difference between the relative proportions of these two populations, although it must be remembered that the

uncategorised population may represent OECs or fibroblasts displaying phenotypic variability. Similarly, they may also represent contaminant cells of one of the several phenotypes that have been identified in the olfactory mucosa, including MSCs (204) and Schwann cells (205). That said, the primary goal was to engineer a transplant population that can secrete BDNF to augment the pro-regenerative qualities of cOMCs. As such, the relevance of precisely which phenotypes act to secrete the therapeutic biomolecule is debatable, provided there are a population of OECs there to support regeneration.

Moreover, previously published data regarding transplantation of this cell population revealed no influence on functional outcomes from the relative proportions of OECs and fibroblasts in mixed grafts (109). Further, data from previous studies using experimental spinal injury models suggests that the presence of olfactory nerve fibroblasts may be beneficial to the regenerative process (107,206). As such it may be the case that the relative proportions of transfected cells will not affect functional outcomes.

However, more recent work which directly compared the therapeutic efficacy of purified OECs, purified fibroblasts and mixed olfactory cultures found that purified OECs performed best in terms of axonal regeneration, and that purified cells outperformed mixed cell populations (207). As such, further work may be needed to determine the relative therapeutic values of the cell types delivered to this particular population.

2.4.6 Conclusions and future directions

We have demonstrated that mixed cOMC populations can be engineered as biopumps for neurotrophic factors. Further, the use of novel minicircle vectors opens up the possibility that we can engineer multifunctional biopumps, which can resolve multiple barriers to spinal regeneration simultaneously, and as such the delivery of additional functional genes to cOMCs will be a focus of future research. In light of the critical advantages offered by MPs complexed to minicircle constructs and the highly efficient uptake by this clinically relevant cell population, our results suggest a strong translational potential for this therapy. Given that the safety and efficacy of autologous OMC grafts has been established, my hope is that these results will lay the groundwork for implantation of engineered grafts into canine spinal injury patients, bridging the gap from laboratory to clinic.

Chapter 3: Hydrogels can be used to generate protective cell delivery systems for cOMC administration to spinal injury foci

3.1 Introduction

Chapter 1 detailed the current limitations associated with autologous cOMC administration as a therapy for SCI. Namely, low stability of cells during the injection procedure leading to a significant reduction in numbers of viable cells administered, and clumping in injection fluid combined with irregular flow rates leading to poor biodistribution of remaining cells. There is currently limited data relating to the response of cOMCs to 3-D culture in hydrogel constructs. Further to this, the response of neural cells to hydrogels formed from the same polymer can vary due to the variability of hydrogel formulation parameters including porosity, monomer molecular weight and density (208). For example, Park et al reported significant repair following transplantation of a hyaluronic acid hydrogel with a molecular weight of 170 kDa (209), while Horn et al failed to report any recovery using hyaluronic acid hydrogels with an unspecified molecular weight (210). As such there is a clear need to evaluate the biocompatibility of the specific transplant population with the formulation of hydrogel within which they will be implanted, as the translation of this therapy to clinical studies requires rigorous safety analyses to identify any deleterious effects to transplant populations.

3.1.1 Hydrogels may offer a novel solution to the translational challenges associated with autologous cOMC administration

As discussed in **Chapter 1**, combining the therapeutic efficacy of canine olfactory mucosal

cells with 3-D hydrogel scaffolds may offer a solution to the problem of low transplant cell viability post-injection in host tissue **(Section 1.3.5)**. A variety of synthetic and natural polymers have been investigated for protected cell delivery to sites of spinal injury *in vivo* (172). Two key synthetic polymers which have been investigated are the polymethylacrates (PMA) and PEG. PMA-based hydrogels have been investigated for their neuroregenerative potential both alone and in combination with encapsulated cell populations. For example, in a compression model of chronic spinal injury in rodents, Hejcl et al (211) compared outcomes in rodents who received implants of either PMA hydrogels alone, or PMA hydrogels within which MSCs had been encapsulated. Rodents were evaluated by BBB score monthly for 6 months, before being sacrificed so that the lesions could undergo histological analysis. Both groups showed progressively improving motor scores compared to control groups who received no implants. However, those who received hydrogels seeded with MSCs demonstrated histological evidence of reduced tissue atrophy, and infiltration of blood vessels and myelinated axonal processes in to the construct, which bridged the lesion. Moreover, MSCs remained visible inside the construct up to the point of histological analysis. Further, implantable PEG hydrogels encapsulating co-cultured neural progenitor cells (NPCs) and endothelial cells demonstrated evidence of restoration of the blood spinal cord barrier and a fourfold increase in the regeneration of functional vasculature, compared to controls who received no implant, in a rodent hemisection model (212).

With regards to natural polymers, two key substrates which have undergone *in vivo* investigation as cell delivery devices are agarose and fibrin. MSCs engineered using viral

vectors to express BDNF have been successfully encapsulated into agarose hydrogel scaffolds before implantation into a rodent model of complete transecting injury (213). Here, the researchers found that motor axonal fibres regenerated in to the scaffold construct in what they described as “fascicles of highly linear configuration”, supporting the hypothesis that implantable scaffolds can support linear regrowth of axons. Fibrin matrices impregnated with MSCs have been implanted into rodent hemisection models of spinal injury (214). Here, rodents receiving the MSC-containing constructs demonstrated significantly greater recovery of motor function than those who received constructs alone or MSCs administered as liquid suspensions. Collectively, the results of these studies suggest that the combination of implantable hydrogel scaffolds and pro-regenerative cell populations have a strong regenerative potential, with regards to SCI.

Collagen is the main component of the ECM in animals, and as such culture of mammalian cells within a type I collagen matrix is unlikely to produce any deleterious effects (215). It is soft and flexible with similar mechanical properties to the spinal cord, meaning gel constructs place minimal mechanical stress on the cord when implanted. Moreover, it possesses cell adhesion domains essential for axonal growth (216), and its chemical properties such as degradation rate can be modified by the addition of protease inhibitors. The potential to encapsulate cOMCs in to implantable collagen hydrogel matrices has not been established to date.

3.1.2 The need to tissue-match implants and host tissue

The proliferation and differentiation profiles of neural transplant populations are affected by the stiffness of the substrate in which they are grown (217,218). For example, neural cell survival is greatest in substrates with mechanical properties that closely match the native tissue environment. Further, NSCs favor neuronal differentiation in soft (ca. 1 kPa) substrates (219), while harder substrates (ca. 7-10 kPa) tend to induce differentiation in to glial cell lineages (220). Designing a hydrogel for cOMC delivery for spinal regeneration may therefore require tuneable mechanical properties to support the growth of desired neural cell types: a softer gel which preferentially supports axonal extension across a transecting lesion may be preferable to a stiffer gel, which may encourage astrocyte proliferation and consequent scarring. Matching of the mechanical properties of the hydrogel to the host tissue is also important to minimise contact stresses from normal movement and the possibility of an exacerbated immune response (177). A spinal cord undergoes various degrees of twisting and bending. As such, a graft must be flexible enough to move with the cord and not provide mechanical resistance that might cause trauma. It must also be stiff enough not to collapse under the weight of surrounding tissues. There is therefore a need to tissue-match implantable hydrogel constructs in terms of stiffness to the host spinal cord.

3.1.3 USE may facilitate non-invasive measurements of spinal cord stiffness

Despite the need to match graft and host tissue, there is currently no standardised means of measuring the stiffness of the spinal cord. Taking dogs as an example, a recent review found only 2 historical studies which had reportedly measured the stiffness of the canine cord (177). The first was performed on cadaveric specimens using tensile testing (221). Here, the reported stiffness was 16.8-19.0 kPa when weight was applied to the cord in 5 g increments from 0 g to 150 g. The second was on live, anaesthetised puppies, who subsequently experienced temporary loss of sensorimotor function in the spinal segments measured (222). Here, reported values were 265 kPa when strain was applied at a rate of 0.021 mm/s. Clearly the values obtained depend on method of measurement, as similar degrees of variability are also seen in reports of measures of human cord stiffness, with no single widely accepted protocol currently employed (177). Moreover, current methods of measuring cord stiffness rely on direct access to the cord, often in prosection, and as such are highly invasive and not suitable for clinical applications.

Using a predetermined value for stiffness when designing a graft may not be entirely appropriate. There may be some variation in the mechanical properties of the cord between patients of differing ages (or breeds, in the case of dogs). It is also highly likely that heterogeneity will exist between traumatic lesions: each will have its own degrees of swelling, contusion, laceration and demyelination, determined by the precise mechanism by which the injury was sustained. All of these factors are likely to influence the mechanical

properties of the cord, and so must be considered when designing a tissue-matched neural graft. Finally, the precise mechanical properties of the cord may differ depending on precisely where in the cord it is measured, for example, the relative proportions of white and grey matter differ along the length of the cord, and the total number of neurons in regions that supply major plexi is higher than elsewhere. Therefore, if there were some means of non-invasively measuring the mechanical properties of the cord, it may be possible to produce bespoke neural grafts, precisely tissue-matched to the spinal cord of each patient.

USE is an imaging modality developed over the last few decades as a means of non-invasively characterising the elastic properties, i.e. stiffness, of tissue for diagnostic purposes. It works on the principle of inducing distortion in a tissue through the use of focused sonic forces, then measuring the response. The distortion created by these sonic forces travels through the tissue, creating what is known as a shear wave. The velocity of this shear wave (m/s) is dependent on the stiffness of the tissue: The stiffer the tissue, the greater the shear wave velocity. As such, we can infer the elasticity of the tissue from the velocity of the shear wave, as the two are directly related through a simple formula (223):

$$E = 3pc^2$$

[E = stiffness (kPa), p = density of the tissue (g/cm^3) and c = shear wave velocity (m/s)]

The value of USE in non-invasively determining the mechanical properties of lesions within tissues has been known for some time. This is because pathological lesions have different mechanical properties to the surrounding tissue (224). For example, cancerous lesions of the thyroid tend to be stiffer than surrounding parenchyma, and fibrosed livers are often stiffer than healthy livers (225). USE also shares advantages with conventional ultrasound, in that it is inexpensive (226) and not associated with a dose of radiation. However, the value of USE in the measurement of spinal cord stiffness in clinical patients (with a view to informing hydrogel stiffness for encapsulated cell delivery) has not yet been evaluated.

3.1.4 Aims of the study

In the present study, type I collagen gel FDA-approved for human applications were investigated to evaluate the 3-D growth of cOMCs, as the basis of a potential encapsulated cell delivery system. Despite the known need to tissue-match implantable constructs, which requires non-invasive imaging of the host spinal cord, methods of non-invasively imaging canine spinal cords using clinically available equipment have not yet been investigated. Therefore, the specific aims of this chapter are:

(i) Determine the feasibility of encapsulating cOMCs in implantable type I collagen hydrogel matrices.

(ii) Identify deleterious effects on cOMC survival or proliferation from 3-D culture methodologies.

(iii) Develop novel non-invasive USE measurements of spinal cord stiffness in adult canine subjects.

3.2 Methods

3.2.1 Materials

Cell culture was performed in an identical manner to that described in **Chapter 2 (Section 2.2.2)**. All cell culture, fixing and immunostaining reagents are the same as those used in **Chapter 2 (Section 2.2.1)** unless otherwise stated. Additional reagents not described previously were as follows: Type I rat tail collagen from Corning (Tewkesbury, MA, USA), powdered Gibco MEM α from Life Technologies, made into a 10x MEM α solution by combining 10.17 g with 2.2 g $NaHCO_3$ and dissolving them in 100 mL distilled water. The pH of the resultant solution was adjusted to 7.4 before filter sterilising through a 0.2 µm filter. Ultrasound readings were obtained using a Siemens ACUSON S2000 (Virtual Touch™ tissue quantification; Siemens).

3.2.2 Collagen hydrogel synthesis

The formulation of type I rat tail collagen used for this study is a heterotrimer [alpha$_1$(I)$_2$ alpha$_2$(I)] of 300 nm length being composed of two alpha$_1$(I) chains and one alpha$_2$(I) chain. This formulation is particularly suited to the encapsulation of cells within the matrix as the gelation process can be easily controlled in a temperature- and pH-dependent manner.
It is stored as a monomer in an acetic acid solvent at 4°C, in order to prevent polymerisation

prior to use. Once the solution is warmed up to RT and the pH neutralised, the collagen polymerises and forms a hydrogel. In order to culture cOMCs in the 3-D hydrogel construct, the cells were incorporated into the collagen solution during the liquid phase such that they became enmeshed within the collagen fibres as it began to set.

Gel formulation was performed by combining several reagents in sequence. These were: 10x MEM α , collagen, acetic acid and NaOH. The relative proportions of each reagent per gel were adjusted in order to vary the collagen concentration, and was calculated using the formula displayed in **Table 1**.

Formulation protocol was as follows: Collagen monomer was diluted in acetic acid to the desired concentration before addition of 10x MEMα. NaOH was then added to the mixture in order to neutralise the pH. This solution was added to the cell suspension, mixed thoroughly and 0.1 mL added to each well of a 96 well plate. Plates were incubated for 30 min at 37°C to allow the gel to set. Following gelation, 0.15 mL cOMC media was added to the wells. Details of media constituents are provided in **Chapter 2 (Section 2.2.2)**.

Reagent (concentration)	*Formula to create required volume*
10X MEMα	$V_M = V_F \times 0.1$
Collagen (C_s)	$V_C = (C_R \times V_F)/C_S$
Cells (10×10^6 cells/mL)	$V_N = V_F \times 0.1$
Acetic acid (0.02M)	$V_A = V_F - V_C - V_M - V_N$
NaOH (1M)	$V_S = (V_A + V_C) \times 0.023$

Table 1: Formula for deriving volumes of reagents to formulate collagen gels. *V_F = final volume; V_M = volume of MEMα; V_C = volume of collagen; V_N = volume of cell suspension; V_A = volume of acetic acid; V_S = volume of NaOH; C_R = required concentration of collagen; C_S = collagen stock concentration.*

3.2.3 Preliminary proof-of-principle studies were used to determine optimal culture conditions for subsequent experiments

The use of hydrogels to culture neural cells is a relatively novel approach in our laboratory, with protocols currently being refined for a range of cell populations. It was important therefore to determine how cOMCs would respond to culture in this 3-D matrix, and which tools and protocols would provide the best results. Therefore, pilot studies were conducted in order to develop cell culture protocol and perform a preliminary assessment of how cOMCs responded to 3-D culture. Based on the observations made during these initial studies, cell culture protocols would be adjusted for subsequent experiments.

When designing these initial studies, it was reasoned that the best place to start would be to use protocol developed previously for culture of NSCs in hydrogels, observe how well this worked for cOMCs, and then make alterations accordingly. Additionally, through personal communication with veterinary neurosurgeon Dr Nicolas Granger, the key properties to evaluate in hydrogel constructs designed with a view to intraspinal implantation, and for how long cells would be cultured *ex vivo* were determined. Key parameters were cell safety and capacity of gels to maintain cells in 3-D matrices, and cells are likely to be cultured in gels for one to four days prior to transplantation.

It was decided therefore that during pilot studies (n = 2), two time points would be assessed: 2 d and 4 d, to ensure that cells could survive in the gel outside of canine recipients for the requisite length of time. Previous work in our laboratory culturing NSCs in collagen hydrogels examined several incrementally increasing collagen concentrations, beginning at 0.3 mg/mL, as it was determined that this was the lowest possible concentration of collagen that could form a solid gel. It was reasoned that such dilute gels were unlikely to hold cells in suspension for any length of time, as such the next highest concentration of collagen that had previously been used to successfully culture neural cells was taken as the starting point. Additionally, the eventual requirement of tissue-matching collagen constructs was taken in to consideration, therefore 3 collagen concentrations were assessed in total during these pilot studies: 0.6 mg/mL, 1.2 mg/mL and 2.4 mg/mL, as this gave a logical progression from the starting concentration whilst providing a broad range of densities without encountering practical

limitations with the volume of collagen substrate required for the number of experiments.

3.2.4 LIVE/DEAD Staining

At two time points (2 d and 4 d) cell survival was evaluated using LIVE/DEAD assay. For details regarding the mechanism of action of LIVE/DEAD staining, see **Section 2.2.6**. Reagents used and their respective concentrations were identical to those outlined in **Chapter 3 (Section 2.2.6)**. However, the protocol was adapted slightly to the culture of cells in 3-D as opposed to on 2-D substrates, where it was important to ensure reagents penetrated the 3-D structure of the gel sufficiently. Gels first had to be removed from the well plates: A hypodermic needle point was used to gently free the gel from the side of the well plate, following which a pair of curved tweezers were used to gently lift out the gel. The gels were transferred from 96 to 24 well plates containing 1 mL of staining reagents, such that each gel was fully submerged with reagents allowed to surround the gel, and returned to the incubator for 30 minutes. The gels then immediately underwent z-stack fluorescence microscopy analysis.

3.2.5 Assessment of cellular proliferation

Capacity of cells to proliferate in 3-D hydrogel constructs was evaluated at two time points (2 d and 4 d) using Click-iT® EdU proliferation assay. For details regarding the mechanism of action of EdU, see **Section 2.2.11**. This was performed according to the manufacturer's

instructions, except with slight modifications to allow reagents to penetrate the gel. Gels were transferred as described above in to larger well plates containing 1 mL of EdU reagent solution, such that each gel was entirely submerged, before being returned to the incubator for 24 h prior to fixation.

3.2.6 Fixation

Cells were fixed for staining and microscopy at two time points (2 d and 4 d) in order to determine if the phenotypic properties and distribution of cells within the matrix differed over time in culture. Again, reagents used were identical to those described in **Chapter 2 (Section 2.2.7)**, with alterations to protocol. Gels were transferred to larger well plates as described above, containing PBS 1 mL PBS. Wash solution was removed and cells were fixed in 1 mL of 4% PFA solution for 1 h. The fixing solution was removed and the gels rinsed 3 times 10 minutes in PBS.

3.2.7 Immunocytochemistry

All antibodies and dilutions were identical to those used in **Chapter 2**, unless otherwise stated. Immunostaining was performed for p75 and Fn, and the DNA marker Hoechst was used to detect DNA (1:10 000) (ThermoFisher Scientific). Again, alterations to protocol were made. Following fixation, wash solution was removed and 1 mL of each antibody solution was

added to the gels. Here, incubation and rinse times were doubled from the previously described protocol. Again, this was to ensure antibodies adequately penetrated the gels. Additionally, it was observed that gentle trituration of the wash solutions surrounding the gels “flushed” out any remaining antibody and reduced background fluorescence during subsequent microscopy.

3.2.8 Microscopy and image analysis

Microscopy was performed using the same microscopy equipment as that described in chapter 2. The 3-D distribution of cells within the hydrogel was evaluated using the confocal “Z-stack” microscopy feature of the Axio Observer Z.1. This is a specialist feature which allows regularly spaced 2-D ‘slice’ images to be taken throughout the depth of the gel, the software then reconstitutes these images into a continuous frame-by-frame video, such that the entire depth of the gel can be “scrolled through” from top to bottom in a similar manner to manually adjusting the focus. Prior to imaging, gels were transferred on to glass slides in order to reduce movement from floating in a liquid medium and improve image quality over the plastic well plate.

In order to obtain a quantitative estimate of the 3-D distribution of cells along the Z-axis, the Z-stack software was used to obtain 2-D images from regularly spaced planes of analysis (PoA) throughout the height of the gel. To standardise the distribution of the PoA, the vertical height of the gel was first estimated as follows: Beginning in the plane immediately below the

base of the gel, the focus of the microscope was shifted upward until the first cell nucleus came in to focus. The Zen imaging software was used to register this as the base of the gel. Focus was shifted upwards through the gel until the last nucleus went out of focus. This was then brought back in to clear focus, and the software registered this as the top of the gel. The vertical position of the imaging lens was recorded at each of these two points, and the difference was considered as the height of the gel. This process was performed in the centre of each gel, identified by the lowest point of the meniscus on the superior surface, as it was determined that this would give the most consistent measure of height.

Images were acquired at 15 µm intervals throughout the height of the gel. Seven of these PoA were taken for analysis: the first PoA from the base of the gel, the final PoA from the top of the gel, and 5 PoA distributed evenly between these two points. Images were then exported, and the number of nuclei that were seen in clear focus in each PoA was counted from single channel Hoechst images.

The same protocol was repeated in order to quantify the number of live cells by LIVE/DEAD assay. Here, the percentage of live cells was determined by counting the number of calcein+ cells present in each PoA and adding this to the number of EtH+ cells in each PoA. The number of calcein+ cells was expressed as a percentage of the total number of cells counted. This was considered as an estimation of % cell survival. This analysis was performed for all gel densities at 2 d and 4 d post-construction.

The number of proliferating cells was again determined from images in seven planes of analysis in the manner described above. Here, double-staining for the EdU proliferation marker and Hoechst was applied. Hoechst stains all nuclei with blue fluorescence, while EdU detection in this case conferred green fluorescence to the nuclei of those cells which had incorporated the EdU marker in to their DNA during cellular replication. The total number of EdU+ was expressed as a percentage of the total number of nuclei counted for each experimental condition. All cell counting was performed using free ImageJ 1.49v software.

3.2.9 Preparation of cadaveric specimens for USE

I conducted preliminary readings of stiffness for canine spinal cord using cadaveric specimens derived from post mortem specimens (n = 3). All measurements were taken within 2 h of death and with informed consent from the owner. Immediately post-mortem, the spinal cord was removed by a board certified veterinary pathologist. In one instance, some segments of the cord were inaccessible to post-mortem analysis, because they were retained by the pathologist for other projects. Here measurements were taken from the available regions. The outer meningeal coverings were left in tact. A scalpel (Swann-Morton Ltd, Yorkshire, UK) was used to cut the specimen in to 5 sections based on anatomical divisions: cervical, thoracic, lumbar, low cervical/high thoracic and lumbosacral. The latter two regions are the spinal segments from which stem the brachial and lumbosacral plexi, respectively, i.e. grey matter tumescences. The greater number of lower motor neuronal soma in this region gives them a greater volume and circumference than the remainder of the spinal cord. It was

hypothesised that the differences in composition would impact on the stiffness readings taken. The spinal sections were then placed horizontally in to plastic containers of approximately 10 cm x 5 cm x 5 cm diameter and covered with 0.9% saline solution such that the specimens were submerged by at least 1 cm of fluid. Specimens were immobilised using hypodermic needles inserted laterally through the rostral and caudal aspects, and in to the base of the container **(Figure 1A and B)**. The specimens were then transported to the radiology department for imaging studies.

3.2.10 USE measurements of cadaveric specimens

The ultrasound analysis was carried out by holding the probe under the saline fluid level. The probe was applied longitudinally to the cord, and the spinal cord located on the ultrasound monitor by a veterinary neurosurgeon **(Figure 1C)**. A region of interest (RoI) of 1 cm^2 within the area of tissue identified as spinal cord was selected using the ultrasonography software, and the ultrasound probe returned a value in m/s for the velocity of the shear wave through this RoI. The distance from the probe to the RoI was 1.5 cm. A minimum of three readings were taken from each segment measured, from which a mean stiffness value was derived.

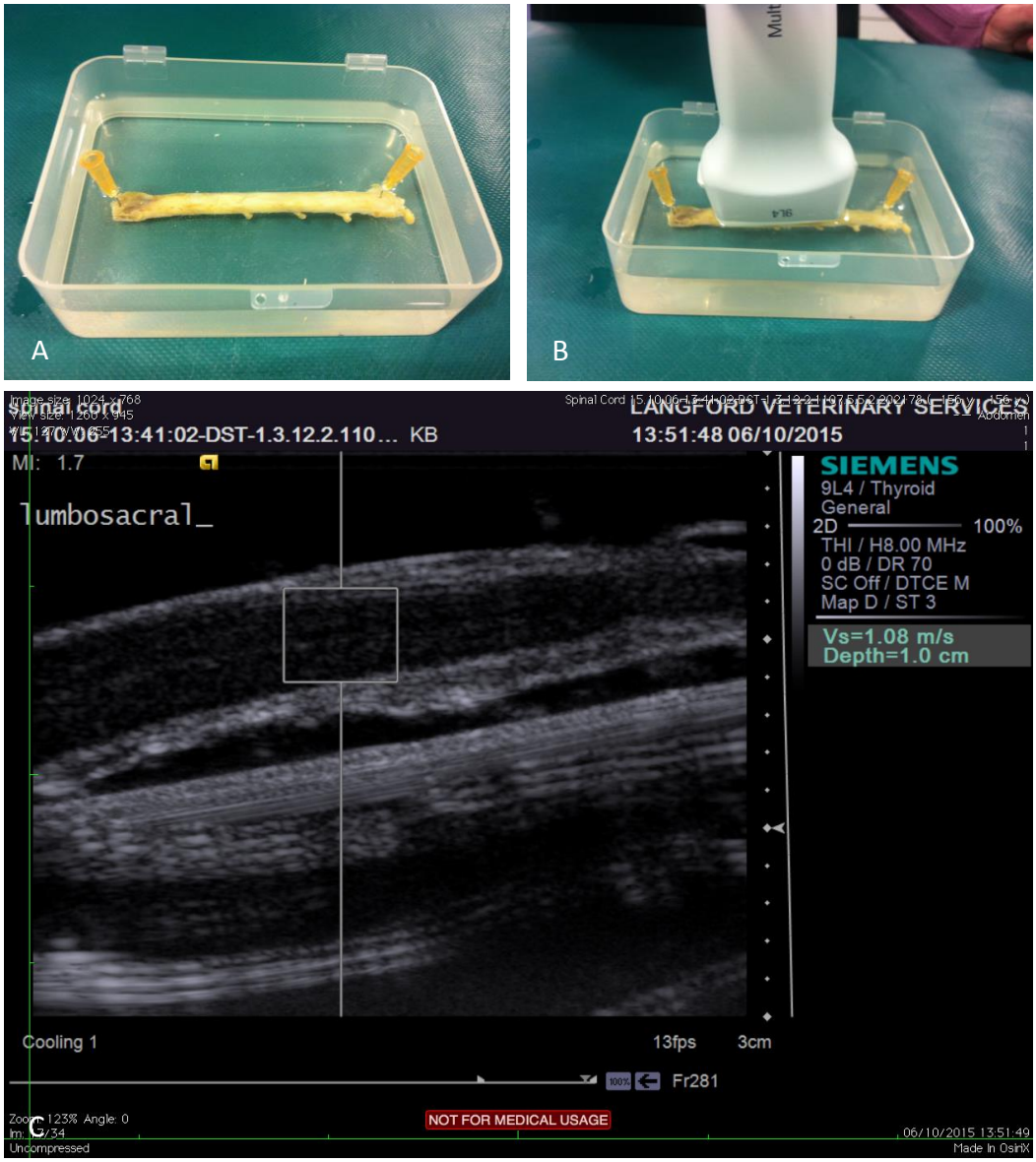

Figure 1: Preparation of cadaveric specimens for analysis and results obtained using USE protocols. *(A) Cadaveric specimens were cut in to anatomical segments before being secured to the base of a plastic container using hypodermic needles, and covered with 0.9% sterile saline solution. (B) The ultrasound probe was held longitudinally 1 cm from the cord, beneath the fluid level. (C) Image showing the appearance of the spinal cord under ultrasound. The box indicates the RoI, in this case a lumboscral cord segment. The flat surface inferior to the cord is the bottom of the container, with echo radiating beneath it.*

3.2.11 USE measurements of live canine specimens

Additionally, measurements were obtained from living canine specimens. Again, all measurements were taken with informed consent from the owner – Ethical consent (VIN VIN/15/036) obtained from the University of Bristol. Some of the measurements were taken intra-operatively during routine spinal cord decompression following disc herniation (n = 6). Here, the ultrasound equipment was transferred in to the operating theatre where client-owned dogs were undergoing hemilaminectomy for spinal decompression after type I intervertebral acute disc herniation. The precise mode of access with the probe in relation to the cord would vary depending on the conformation of the spine of each dog, it's position on the operating table and size of the surgical approach (e.g. some dogs had decompression over more than one spinal segments, therefore allowing better exposure of the spinal cord for ultrasonography), and finally mild variation in the shape of hemilaminectomy between surgeons. The given example illustrates correction of a herniated intervertebral disc. Briefly, a longitudinal incision is made along the dorsal aspect of the thoracolumbar region, ca. 2 cm lateral to the spinous processes of the vertebrae at the relevant spinal level, and overlying musculature retracted. A hemilaminectomy window was established in the spine following removal of the articular facets, through which the spinal cord could be visualised. The area was continuously flushed well with 0.9% sterile saline solution to remove any debris from the field. Anagel^{TM} ultrasound gel (Ana Wiz Ltd, Surbiton, UK) was applied to the surface of the probe before being ensheathed in a sterile plastic covering. The probe was then placed longitudinally over the hemilaminectomy window and the spinal cord identified in the

ultrasound monitor by a veterinary neurosurgeon. The distance from the probe from the RoI was standardised to 1.5-2 cm for all measurements. A minimum of three measurements were taken per dog. Where possible, measurements were taken in three regions: 1-2 vertebral segments cranial to the lesion, 1-2 vertebral segments caudal to the lesion (located through identification of vertebral transverse processes) and the lesion epicentre.

Additionally, readings were taken from one non-anaesthetised dog in the clinic, a 10 year-old male Labrador retriever, visiting due to clinical signs of chronic spinal cord compression from a thoracolumbar disc protrusion, which was under the care of the veterinary neurology department. In this instance, the dog was transported to the radiology department for imaging. Here, the dog was placed in the prone position on a couch adjacent to the ultrasound equipment. The site of the lesion was then identified by surface anatomy through the palpation of spinous processes (T13/L1 vertebral level). Anagel^{TM} ultrasound gel was applied and the probe was placed on the surface of the skin and measurements taken in exactly the same manner described for intraoperative measures. The distance from the probe to the RoI was 2.5 cm.

3.2.12 Conversion of shear wave velocity to stiffness

The Siemens ACUSON s2000 ultrasonography equipment used in the present study returns values for shear wave velocity through the RoI **(Section 3.2.10)**. As discussed in **Section 3.1.3**, shear wave velocity (m/s) and stiffness in kPa are easily relatable by the formula $E = 3pc^2$

(223,227,228), where E = stiffness (kPa), p = tissue density (g/cm^3) and c = the velocity of the shear wave (m/s). In order to compare the values obtained using USE methodology in this chapter to the values of previous studies of spinal cord stiffness that utilised different measurement equipment, the values for the velocity of the shear wave through the RoI in each measurement taken was converted to a value for stiffness. All soft tissues have approximately the density of water (1 g/cm^3) (215,216), and as such this was taken as an approximate value for the elasticity of the spinal cord.

3.2.13 Statistical analysis

All comparable data were analysed using prism software (version 6.0h, Graphpad). Data are presented as mean ± SEM and statistical differences were measured by one-way ANOVA with Bonferonni's MCT. With regards to the culture of cOMCs in hydrogels, repeat experiments ('n') are using cells derived from a different canine subject. Regarding USE measurements, repeat experiments ('n') are measurements taken from a different canine subject.

3.3 Results

3.3.1 Low density gels are not able to maintain cOMCs in 3-D matrices

Preliminary observations made during initial proof-of-principal experiments of all concentrations at the 2 d time point revealed phase bright cells with bipolar morphologies. In all conditions, cells were seen in greatest number at the base of the gel. This was most striking in the lowest gel density (0.6 mg/mL; **Figure 2**), where at 2 d, cells were seen almost entirely (>98%) to have sunk to the base, with few cells distributed within the matrix. At 4 d, no cells were seen within the 3-D matrix of the gel, indicating that sinkage and/or migration continued after the gelation phase.

Preliminary qualitative evaluations of LIVE/DEAD and EdU staining protocols revealed that these techniques can be used to estimate intraconstruct cellular survival and proliferation. Here, immunostaining reagents adequately penetrated the gels such that live, dead and proliferative cells were observed throughout the depth of the gels. Additionally, preliminary qualitative analyses of these stains revealed no immediately apparent differences in cell survival or proliferation between gels or time-points.

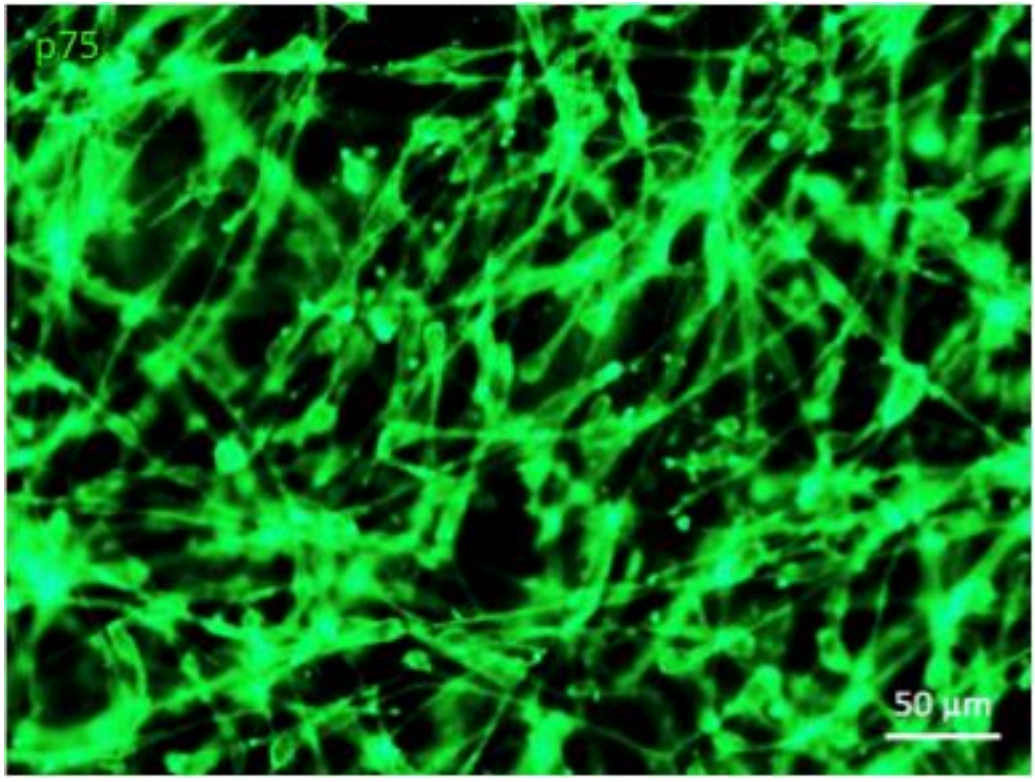

Figure 2: Low density gels cannot hold cOMCs in 3-D suspension. *Image showing accumulation of cOMCs at the base of the hydrogel construct 4 days post-construction at a collagen concentration of 0.6 mg/mL.. n = 2.*

3.3.2 Intraconstruct staining of cOMCs for fibronectin was suboptimal

Qualitative analysis of cell staining revealed no difference in staining intensity throughout the thickness of the gel, and there was no difference between gels of varying densities. Intraconstruct cells were seen to stain clearly for p75. However, the staining for Fn was consistently found to be suboptimal. Double staining revealed clearly labeled p75+ cells throughout the 3-D construct. Fn staining however was nonspecific. Attempts to stain intraconstruct cells with Fn resulted in nonspecific staining throughout the gel construct that displayed a weak, diffuse, nebulous pattern with no overlap between cells and staining. This is displayed in **Figure 3**.

In order to optimise staining, multiple parameters of the staining protocol were adjusted. Antibody dilutions were assessed at the following concentrations: 1:100, 1:200, 1:400, 1:800. Where primary antibody dilutions were adjusted, secondary antibody dilutions were kept constant (1:200). Where secondary antibody dilutions were adjusted, primary antibody dilutions were kept constant (1:200). These were applied using the volumes and incubation times outlined above. There was no visible difference in staining intensity or distribution at any of the antibody dilutions tested. Antibody potency was verified by testing on cOMCs seeded on to glass coverslips, which revealed staining profiles identical to those described in **Chapter 2 (Section 2.2.10)**. Next, incubation times were shortened (24 h for primary, 2 h for secondary; 12 h for primary, 2 h for secondary), and then increased (3 d for primary, 6 h for secondary), using antibody dilutions of 1:200. The concentration of blocking solution used

was increased from 10% to 20% and staining attempted using the protocol described in **Section 3.2.7**. Finally, the duration and number of PBS washes after each incubation was increased from 3 times 10 minutes to 5 times 30 minutes. For around 2 minutes during each wash, a pasteur pipette was placed in to the wash solution and gently triturated in order to generate mild turbulence, in an attempt to "flush" as much remaining antibody out of the gel as possible, the rationale being that this would minimise background fluorescence and potentially reveal any weak cellular staining. For each parameter adjustment described above, both single (Fn only; p75 only) and double (p75 and Fn) staining was applied.

In all optimisation experiments, no visually detectable difference was seen in the staining profiles of any 3-D construct. The reasons for this remain unclear. However, given time restrictions I was unable to spend any longer on further optimisation of the staining protocol. However, this is something that could be addressed in future work with these constructs.

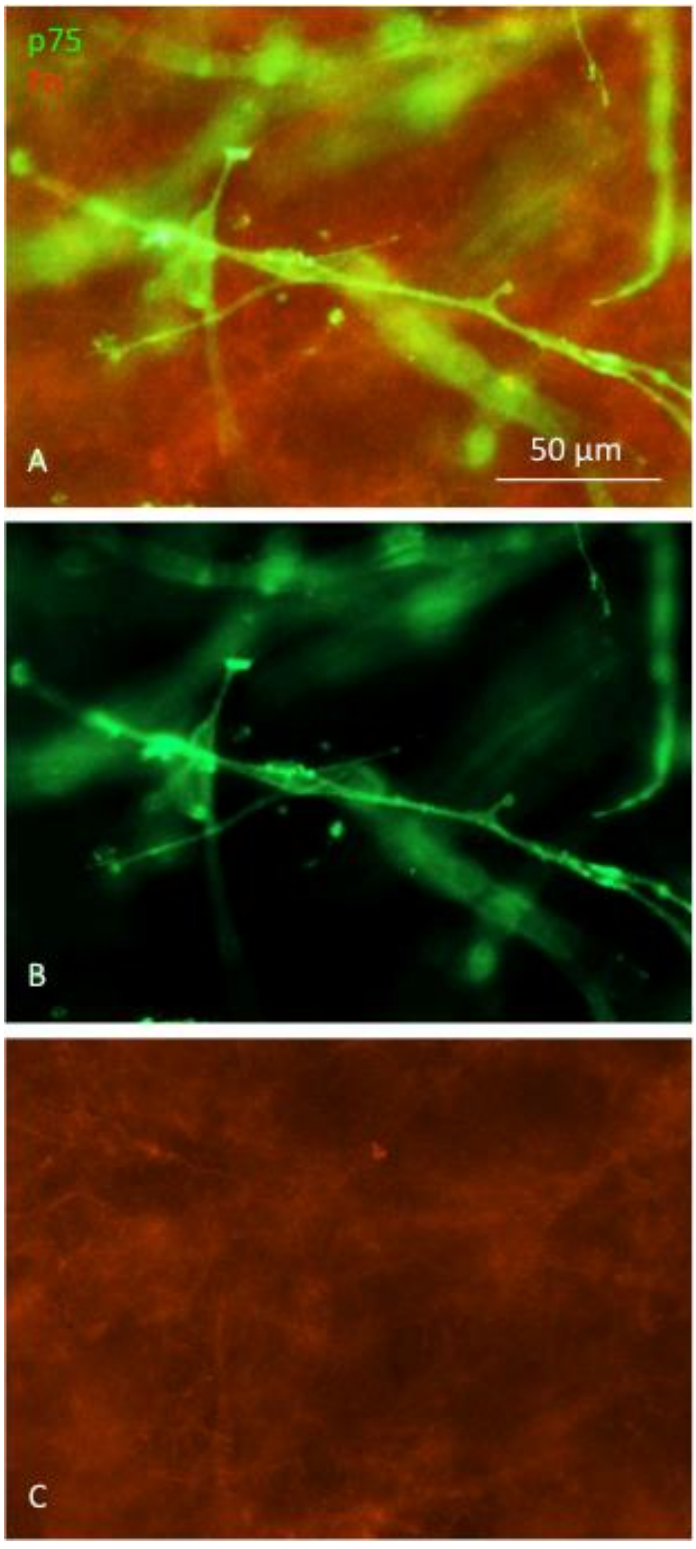

Figure 3: Intra-construct staining of cOMCs was suboptimal. *(A) Double-merged image showing intraconstruct p75 and Fn staining. Note clear p75 immunostaining, nonspecific appearance of fibronectin with high levels of background fluorescence. (B) Single-channel p75 image (C) Single-channel Fn image.*

3.3.3 cOMCs can be cultured within 3-D hydrogel constructs *ex vivo* for four days

Microscopy analysis revealed the vast (≳ 95%) majority of cells expressed a fusiform morphology. Of these, the majority (≳ 90%) were bipolar, the remainder were either tri- or unipolar. A very small proportion (< 5%) of cells displayed a rounded morphology. No cells were seen to express the flattened, multi-processed morphology typical of fibroblasts grown on glass. The vast (≳ 95%) majority of cells stained positively for p75.

Cellular processes were seen orientated in multiple dimensions and were not simply aligned parallel to the gel surface **(Figure 4a)**. Cells could be seen either alone or arranged in groups, in which case they tended to align longitudinally as "chains" of bipolar cells. There was no difference in cellular morphology between gel densities or time points. At the base of the gel, cells were aligned longitudinally in parallel in a manner comparable to that seen on glass substrates.

3.3.4 cOMCs were seen to be distributed throughout hydrogel matrix

Higher density hydrogel formulations were found to support 3-D cOMC growth **(Figure 4b)**. The mean depth of the gels was 1133 µm (range: 885 - 1434 µm). At gel density 1.2 mg/mL, at both time points mean cell number was significantly greater at the base of the gel (99.3 ± 6.7 at 2 d; 106.3 ± 24.0 at 4 d) compared to the rest of the matrix (4.6 ± 0.85 at 2 d; 3.6 ± 0.98 at 4 d). However, there was no statistically detectable difference between mean cell numbers

within the remainder of the gel. At gel density 2.4 mg/mL, at 2 d a statistically detectable increase in cell number was seen at the base (52.7 ± 19.0) compared to the upper ca. 20% of the gel matrix. At 4 d, a statistically detectable increase in mean number of cells was seen between the base (65.7 ± 29.8) and the remainder of the gel. At neither time point in gel density 2.4 mg/mL was there a statistically detectable difference between cell number within the matrix of the gel (6.7 ± 1.0 at 2d; 4.8 ± 0.8 at 4 d).

.

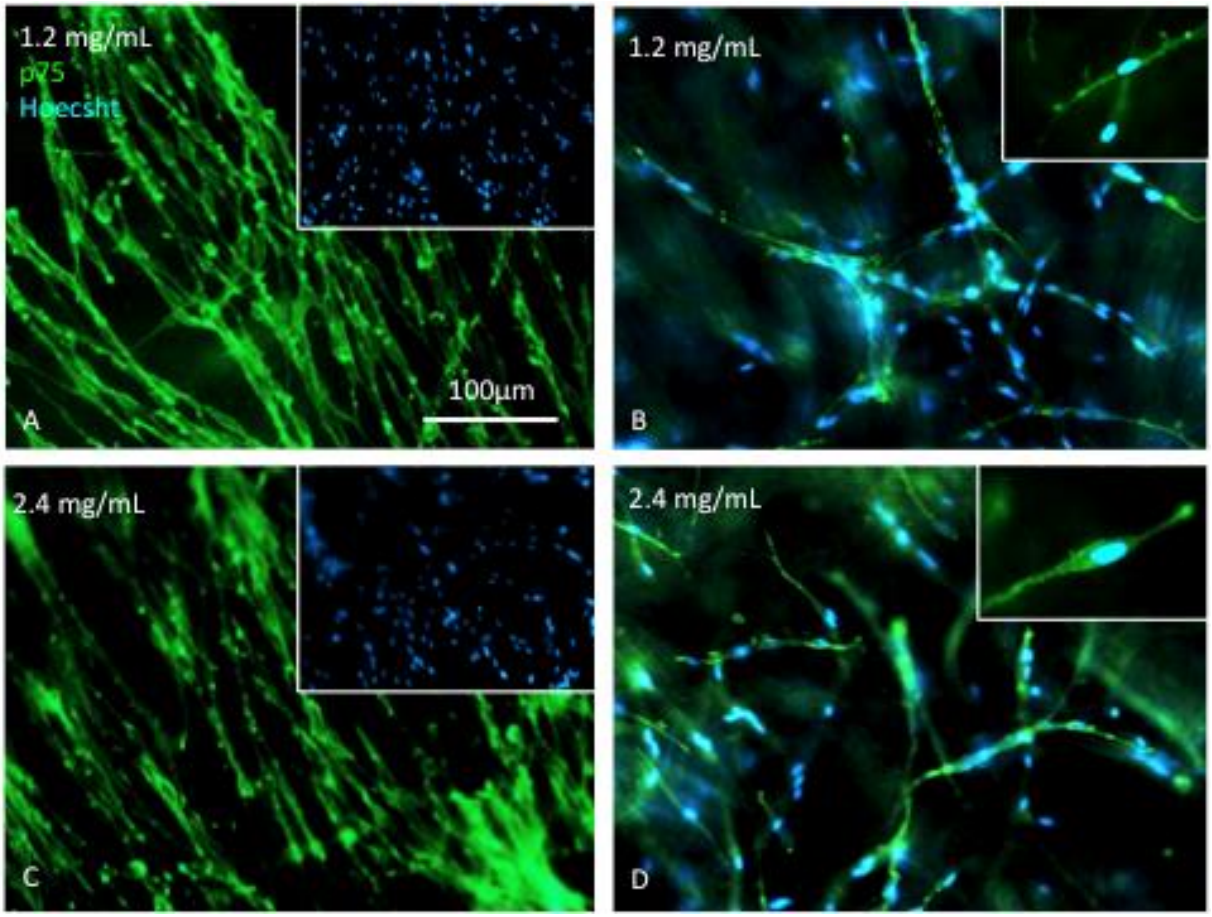

Figure 4a: cOMCs can be successfully cultured within type I collagen hydrogel constructs. *(A) Image taken at 4d at the base of a gel with a collagen density of 1.2 mg/mL (inset: single channel Hoechst image of the same cells). (B) Image taken midway through a gel with a collagen density of 1.2 mg/mL (inset: single cOMC within the collagen hydrogel matrix). (C) Image taken at 4d at the base of a gel with a collagen density of 2.4 mg/mL (inset: single channel Hoechst image of the same cells). (D) Image taken midway through a gel with a collagen density of 2.4 mg/mL (inset: single cOMC within the collagen hydrogel matrix). n = 3.*

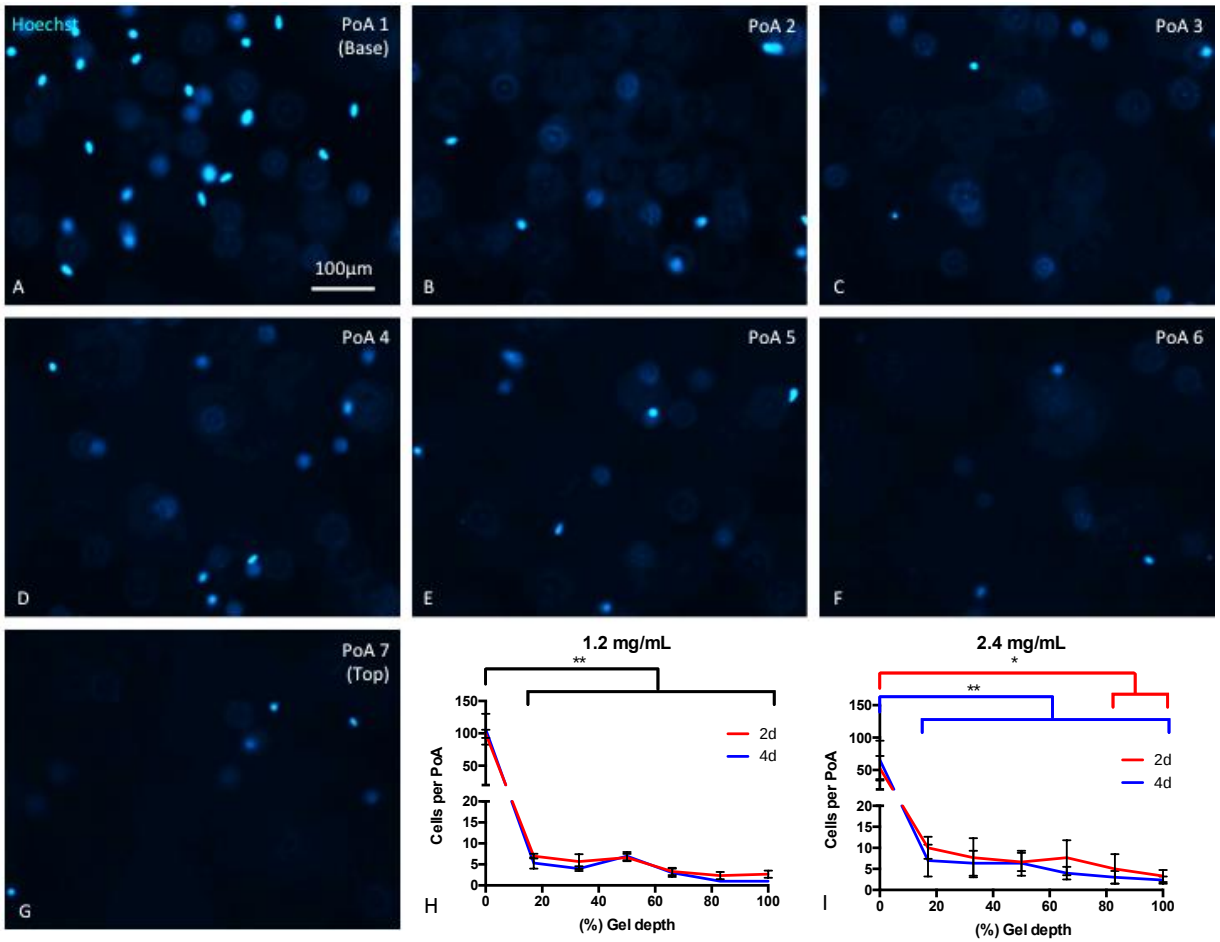

Figure 4b: Cell density was greatest at the base of the gel. *(A-G) Z-stack of gel with collagen concentration 2.4 mg/mL at 4 d, continuing upwards through the matrix at regularly spaced intervals (B-F; PoA 2-6) and ending at the last visible nucleus (G; Po7). (H) Graph showing the number of cells counted at each regularly spaced PoA throughout gels with a collagen collagen of 1.2 mg/mL, starting at the base (0%) and ending at the last visible nucleus (100%). (I) Graph showing the number of cells counted at each regularly spaced PoA throughout gels with a collagen collagen of 2.4 mg/mL, starting at the base (0%) and ending at the last visible nucleus (100%). Cell numbers were greatest at the base of the gels, homogeneous throughout the remainder of the matrix by 4d. *P<0.05, **P<0.01, n = 3.*

3.3.5 3-D culture methodologies do not impact cellular proliferation or survival

The results of cell safety assays are displayed in **Figure 5.** Analysis of gel constructs at 2 d revealed healthy, phase bright cells throughout the depth of the matrix. At this time point, LIVE/DEAD staining revealed cell viability of >85% in both gel densities. There was no statistically detectable difference in cell survival between gel densities. EdU analysis at 2 d did not reveal any statistically detectable difference in cellular proliferation profiles between gel densities. Analysis of gels constructs at 4 d again revealed healthy, phase bright cells throughout the depth of the matrix. LIVE/DEAD staining revealed viability of >85%. There was no statistically detectable difference in cell survival between gel densities at 4 d. EdU analysis did not reveal any statistically detectable differences in cellular proliferation profiles between gel densities. When all safety assays are considered together, there is no difference in terms of cell survival or proliferation rate between any of the densities or time points assessed.

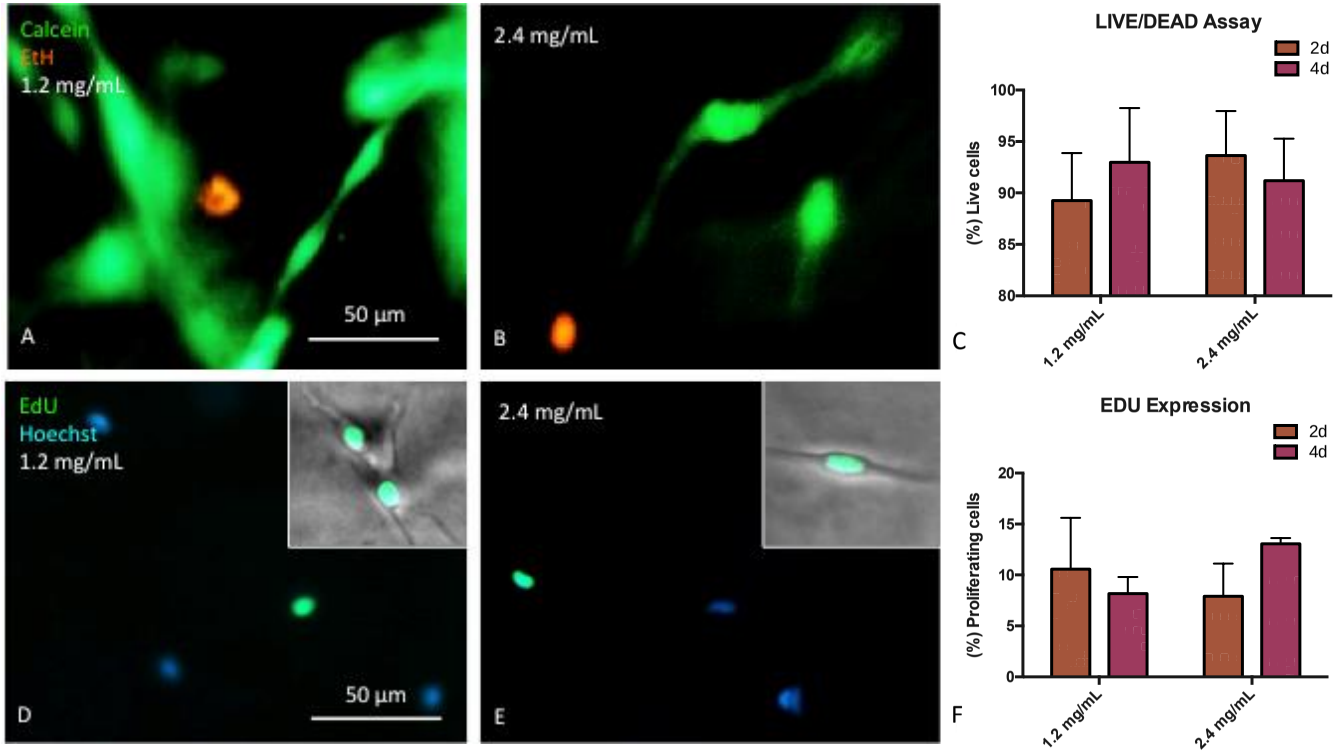

Figure 5: 3-D culture methodology does not negatively affect cell survival or proliferative capacity. *(A, B) Double-merged Calcein and EtH images taken at 4d in gels with a collagen concentration of 1.2 mg/mL and 2.4 mg/mL, respectively, showing both live (Calcein) and dead (EtH) cells. (C) Graph showing percentage of live cells at 24h at 2d and 4d, in gels with collagen concentrations of 1.2 mg/mL and 2.4 mg/mL. (D,E) Double-merged EdU and Hoechst images showing EdU+ cells within gels with a collagen concentration of 1.2 mg/mL and 2.4 mg/mL, respectively (Insets: Double-merged EdU and phase images showing EdU+ cells which have recently undergone mitosis. (F) Graph showing percentage of cells which underwent mitosis in a 24h timeframe. n = 3.*

3.3.6 USE protocols can be used to easily obtain stiffness readings from cadaveric canine spinal cord specimens.

We were able to obtain readings from all cadaveric specimens. The results of these readings are displayed in **Table 2**. On average, the standard error for each reading was lower than those acquired during intraoperative measurements. This is because the range of values obtained from each reading was significantly narrower when cadaveric specimens were used.

	Shear wave velocity *(m/s; mean mean ± SEM)* *Spinal Segment Stiffness (kPa; mean mean ± SEM)*				
Demographics	*Cervical*	*Low cervical/ high thoracic*	*Thoracic*	*Lumbar*	*Lumbosacral*
Sprocker 7 y M	**0.92 ± 0.03** *2.62 ± 0.2*	**1.33 ± 0.07** *5.51 ± 0.5*	**0.95 ± 0.03** *2.77 ± 0.2*	**0.90 ± 0.05** *2.53 ± 0.3*	**1.15 ± 0.02** *4.06 ± 0.1*
-	-	**1.75 ± 0.02** *9.43 ± 0.2*	**1.68 ± 0.03** *8.7 ± 0.3*	-	**1.45 ± 0.03** *6.50 ± 0.3*
Doberman 7 m F	**0.86 ± 0.02** *2.27 ± 0.09*	**1.47 ± 0.02** *6.71 ± 0.2*	**1.05 ± 0.01** *3.41 ± 0.08*	**1.24 ± 0.05** *4.76 ± 0.3*	**1.86 ± 0.01** *10.65 ± 0.1*

Table 2: Mean values for measurments obtained from cadaveric spinal cord specimens using USE protocols. *Values in bold represent mean shear wave velocity through the region of interest (m/s). Italicised represent mean stiffness of the tissue occupying the region of interest (kPa).*

3.3.7 USE protocols can be used to easily obtain stiffness readings from live canine spinal cord specimens.

Intraoperatively, we were able to obtain readings from every dog on which the protocol was attempted **(Figure 6)**. The results of the elastography measurements are displayed in **Table 3**. Due to time restrictions on surgical procedures or physical obstructions due to the surgical approach or equipment being used, we were not able to obtain readings from all three sites in the cord. In total, 15, 12 and 17 readings were obtained from the cranial aspect, caudal aspect and lesion epicentre, respectively. The (mean ± SEM) readings obtained were as follows: cranial to the lesion was 2.57 ± 0.3 m/s; 23.63 ± 3.6 kPa, caudal to the lesion was 3.15 ± 0.3 m/s; 33.26 ± 5.8 kPa and at the epicentre was 2.77 ± 0.4 m/s; 15.56 ± 3.4 kPa. A statistically significant difference between readings taken at the epicentre and caudal to the lesion was identified ($p<0.05$). The SEM for each measure taken ranged from 0.04-0.8 m/s; 0.2-8 kPa.

The USE measurements obtained non-invasively from a dog in the clinic gave the following reading (mean ± SEM): cranial to the lesion was 1.47 ± 0.01 m/s; 6.7 ± 0.1 kPa, caudal to the lesion was 1.46 ± 0.02 m/s; 6.6 ± 0.2 kPa and at the epicentre was 2.38 ± 0.1 m/s; 17 ± 3.4 kPa.

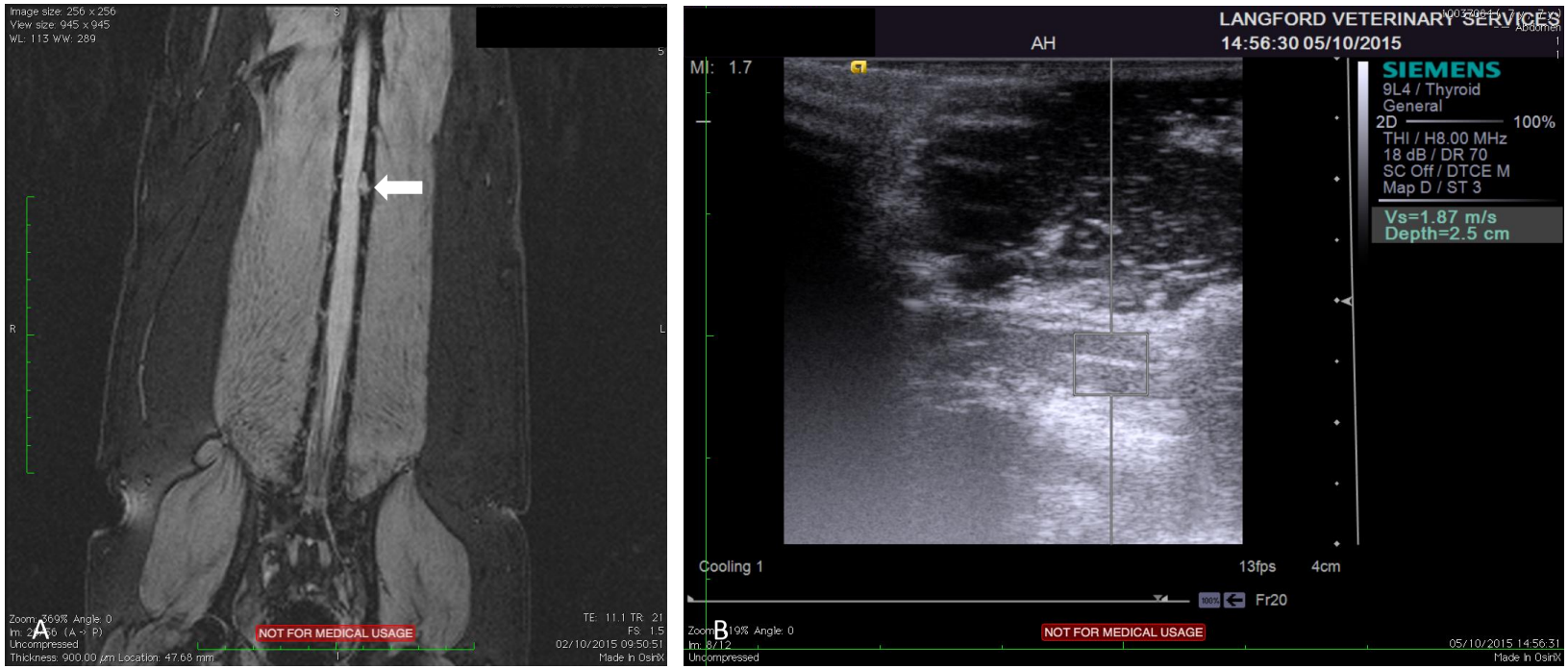

Figure 6: USE protocols can be used to obtain measurements from the acutely compressed spinal cord. *(A) Magnetic resonance image taken from a dog from which an intraoperative USE measurement was taken, it shows a herniated intervertebral disc (arrow). (B) USE measurement from the same patient, taken at the lesion epicentre. The box represents the RoI, here a longitudinal section of lumbar cord.*

Demographics	***Spinal segment***	**Shear wave velocity *(m/s; mean mean ± SEM)*** *Spinal Segment Stiffness (kPa; mean mean ± SEM)*		
		Cranial to lesion	*Caudal to lesion*	*Lesion epicentre*
Cocker Spaniel 7 years old Female	L2/L3	-	-	**1.89 ± 0.05** *11.12 ± 0.6*
Cocker Spaniel 8 years old Female	L2/L3	**2.91 ± 0.2** *26.6 ± 4.3*	**2.29 ± 0.2** *16.48 ± 3.1*	-
Dachshund 6 years old Male	T12/T13	**3.37 ± 0.3** *35.59 ± 5.7*	**4.5 ± 0.1** *63.16 ± 4.0*	**5.17 ± 0.8** *86.18 ± 23*
Beagle 4 years old Male	T12/T13	**3.33 ± 0.2** *34.48 ± 3.1*	**2.38 ± 0.04** *17.52 ± 0.7*	**2.07 ± 0.1** *13.30 ± 1.2*
CKCS* cross Pug 5 years old Male	L1/L2	**2.53 ± 0.1** *19.95 ± 2.2*	-	**1.67 ± 0.4** *9.47 ± 3.4*
Labrador 6 years old Male	L1/L2	**0.70 ± 0.05** *1.53 ± 0.2*	**3.41 ± 0.04** *35.87 ± 0.9*	**3.63 ± 0.4** *41.70 ± 8.0*

Table 3: Intraoperative measures of spinal cord stiffness taken using USE protocols from dogs undergoing decompressive surgery for acute cord compression. *Values in bold represent mean shear wave velocity through the region of interest (m/s). Italicised represent mean stiffness of the tissue occupying the region of interest (kPa).*

**Cavalier King Charles Spaniel*

3.4 Discussion

This study represents the first proof that cOMCs can be safely cultured in 3-D type I collagen hydrogel constructs. Our results support the feasibility of developing a biocompatible implantable “plug” of cOMC-impregnated type I collagen hydrogel for delivery in to sites of spinal injury. Moreover, preliminary investigations indicate the feasibility of non-invasively measuring the stiffness of the canine spinal cord.

3.4.1 3-D culture methodologies do not negatively impact cellular survival or proliferation

Cellular viability was high (>85%) in all conditions, and did not differ significantly over four days in culture. Similarly, cellular proliferation was not significantly affected by time in culture. This indicates that the 3-D culture methodologies described provide a stable environment for cOMC growth. However, further studies investigating long-term cell survival are needed. Further, cell or proliferation rates did not differ significantly between gel densities. However, further studies of stiffer gels are necessary in order to determine the upper limit of collagen density for cell survival.

3.4.2 3-D hydrogel constructs could enhance cOMC biodistribution

In both gel densities, cell numbers were greatest at the base of the gel, indicating some degree of cell sinkage. It is likely that the majority of this occurred during the liquid phase of the gelation process, however some sinkage or migration to the base may have occurred during the solid phase over the 4 d course of the experiment. Statistical analysis at 4 d revealed no significant difference between the number of cells counted at each plane within a gel when the base was excluded. This indicates that distribution throughout the remainder of the gel matrix is homogeneous.

However, there are limitations to the counting methodology employed here. Namely, it tended to give low estimates of the number of cells in each plane. This is because in order for a cell nucleus to be counted, it must be in clear focus in the 2-D image. However, many 2-D planes featured multiple cells which ranged from slightly to almost completely out-of-focus. It was reasoned that counting only cells in clear focus would avoid inconsistencies between counts, but this came at the expense of potentially underestimating the number of cells within the 3-D matrix of the gel.

From a translational standpoint, it is unclear what the significance of these “bottom-heavy” constructs would be. Indeed, it may be of some value to know where in the construct the highest numbers of cells are, such that if one region of a heterogeneous lesion was “more damaged”, the gel could be orientated accordingly. Conversely, this may be undesirable, in

which case there may be some value to investigating means of preventing cell collection at the base, such as inverting the well plates more frequently during gelation through the development of robotically-assisted automation systems, or simply removing the base of the gel pre-implantation.

3.4.3 Knowledge of the rate of degradation of hydrogel constructs is essential to inform their precise application to regenerative neurology

If collagen hydrogels are to be used therapeutically as protective cell delivery systems for human patients, their biocompatibility *in vivo* must be established. There exists a number of type I collagen-based constructs which have been FDA approved for peripheral nerve repair for some time (229). However, the immune system of the CNS differs from that of the rest of the body in that it is governed primarily by resident microglia as opposed to circulating white blood cells (166), and as such observed responses to collagen implants peripherally may not be generalisable. Collagen *per se* is unlikely to induce serious deleterious immune reactions, as it is an abundant ECM molecule (177), and Type IV collagen is a key component of the glial scar. Some researchers have even suggested that collagen may beneficial effects within the spinal cord, such as promotion of axonal regeneration and suppression of reactive astrocytosis (181).

Indeed, previous studies in to collagen grafting within the injured cord have reported no immune rejection (181,230–232). Li et al implanted chitosan tubes filled with Type I collagen

in to a transecting rodent model of spinal injury, and reported enhanced locomotor recovery in the 18 month follow-up period (231). The researchers speculated that collagen enhanced regeneration via interactions between regenerating axons and membrane binding domains on the collagen peptide.

Collagen hydrogel degradation *in vivo* occurs via hydrolysis and exposure to enzymes (233), which differ throughout the body. As such the rate of degradation will vary depending on precisely where the construct is implanted. The spinal cord has a water content of around 70%, so gels are likely to experience some degree of hydrolysis and exposure to circulating enzymes, which may react with the polymer in a manner similar to systemic collagen remodeling by matrix metalloproteases (234), whereby collagen is systematically broken to its component amino acids, which are then phagocytosed (235). However, precise data on the degradation rates of collagen constructs grafted in to spinal cords *in vivo* is lacking.

Li et al reported that intraspinal type I collagen constructs took a total of 18 months to degrade completely (231), although these were encased in chitosan tubes which may have inhibited hydrolysis and enzymatic access. Yoshii et al reported *in vivo* degradation of 20 µm diameter collagen fibrils as quickly as 12 weeks, although here the small size may have enhanced degradation rate (230). Crucially, however, neither study reported deleterious effects of the collagen breakdown products. The fate of the implant depends on the interaction between the precise formulation of collagen and the local tissue environment.

In the instance of implantable collagen gels for spinal cord repair, it may be advantageous for the gel to degrade slowly in order to support axonal regeneration through the implant. The structure of the hydrogel can be modified in order to slow or speed up the rate of removal, such as through the addition or removal of enzyme binding domains or cross-linkages. This would allow the gel to remain for sufficient time as to support regenerating axons, but not so long as to risk eliciting immune responses reported with permanent implants (236).

3.4.4 Porosity of hydrogel constructs will influence integration into host tissue

Finally, the pore size is likely to act as a determinant of the capacity of hydrogels to support ingrowth of axons. The reported average axonal diameter in the spinal cord ranges from 1-5 µm (237). As such, collagen constructs should be formulated with a pore size of equal or greater diameter. The pore size of collagen gels is reported to be inversely related to the square root of protein concentration; denser gels produce narrower pores (238). Reported pore size diameter for gels in the range we tested range from around 4 µm in gels with 1 mg/mL collagen (239), to 1 µm in gels with 2.4 mg/mL collagen (238). Therefore, the constructs we have developed are likely to support axonal ingrowth. Moreover, Yang et al report increasing pore size when type I collagen gels are exposed to lower temperatures (ca.22 C) prior to incubation at 37°C during gelation. Holding gels at this temperature for 30 minutes increased pore size to ca. 17 µm. As such, porosity is likely to be a feature which can be fine-tuned to support axonal regeneration if this is something which is found to be lacking in future studies with these constructs.

3.4.5 Hydrogel matrices may confer additional advantages as tissue-mimetic models for the study of 3-D culture

A further benefit to the culture of cOMCs in tissue-mimetic matrices composed of ECM components is that it provides a means of studying the phenotypic, survival and proliferation profiles of cells grown in a structure more closely related to the native tissue environment than conventional 2-D substrates. Traditionally, cells have been grown in 2-D cultures on glass substrates for the purpose of preliminary investigations and proof-of-concept demonstrations. However, it should be emphasised that cells within the body reside in tissues with differing stiffnesses and, as discussed, this specific property can have a profound impact on cell survival, differentiation, proliferation and motility. Tissue engineering studies across different physiological systems are currently witnessing a paradigm shift to the culture of cells in more biologically relevant tissue-mimetic 3-D structures, both for basic research (e.g. proof-of-concept biocompatibility studies) and further clinical applications (e.g. developing implantable and supportive cellular matrices). Indeed, now that the safety of 3-D cOMC culture has been established, in addition to therapeutic potential, the 3-D construct described has the potential to be used as a model for future investigations in to cOMC engineering in biologically relevant and neuromimetic constructs.

3.4.6 The advantages of implantable hydrogels must be weighed against injectable hydrogels

One advantage of the formulation of collagen used in this study is that the gelation process occurs over 30 minutes at a biological pH, at body temperature. As such, it could easily be used as a thermosetting injectable gel. A key advantage here is that the liquid gel would enter the lesion site in the liquid state and polymerise *in vivo*, conforming to the dimensions of the host cavity (240), a useful trait particularly given the heterogeneity of human and canine lesions. However, this would not necessarily result in an even distribution of cells within the lesion, another key translational barrier to cell delivery, as our results indicate some cell sinkage during the gelation. Further, injection methods can be of value in incomplete lesions where the blood-brain barrier and dura are intact, whereby there is minimal need to disrupt the dura, which may reduce reactive astrocytosis and cyst formation (24). It remains to be seen which is superior of implantable and injectable gels, it is quite possible that both have significant value, and the superiority of one is determined by the pathological features that predominate in a given lesion.

3.4.7 USE can non-invasively measure the stiffness of the injured cord

In the instance of cadaveric specimens, the intra-measurement variability was low. This may be because measurement protocols were much easier to standardise when dealing with cadaveric specimens. In instances where complete measures were taken, the greatest difference in mean stiffness readings was detected between the lumbosacral and low

cervical/high thoracic regions, and the remainder of the cord. However, measurements must be taken on more cadaveric specimens if we to determine if this difference in stiffness is statistically significant.

When measurements were taken intraoperatively, the level of intra-measurement variability differed between sites measured and between dogs. In some instances readings were very consistent with a narrow SEM, while in others the range of readings obtained were very broad. For example, in one dog a range of 30 kPa was seen between measurements taken at the epicentre, while the maximum range of craniocaudal measurements was 2 kPa. The reasons for this difference in variability are unclear. However, it may be due to adjustments to the position of the ultrasound probe when there was a need to flush the wound with saline or apply gauze to a site of bleeding. Moreover, there was often considerable variability between readings, even when taken from similar vertebral levels. Again, the reasons for this are unclear. It may be a combination of differences in position of the ultrasound probe, the properties of the spinal injury and differences between ages and breeds of dog. The variability in mean readings detected between dogs highlights the need for bespoke tissue-matched gels.

While we were only able to obtain transcutaneous readings from a single dog in the clinic, it was found to be a very straightforward process. The results indicate that this could become a highly effective means of measuring stiffness, particularly when the advantages of USE are weighed against current stiffness measures. However, if measure of spinal stiffness is to

become a widely accepted clinical application for this imaging modality, then further work is needed to build up a more extensive database of measurements, work that is ongoing in our group.

3.4.8 Tissue-matching of hydrogels necessitates precise measurements of gel stiffness

Tissue-matching of hydrogels requires a measurement of the stiffness of the hydrogel construct, and as such this is a key domain for future research in to the development of tissue-matched implantable constructs. Results from previous studies in to the stiffness of collagen hydrogels do not give consistent results. This is likely due to the range of measurement equipment and protocols available (241). Compression testing of type I collagen hydrogels yields a stiffness of ca. 250 Pa in collagen densities of 2 mg/mL (242). Oscillatory shear rheometry yields a stiffness of ca. 17 Pa for 2 mg/mL and ca. 7 Pa for 1.25 mg/mL (243). It must also be considered that cellularisation of hydrogels is likely to affect the stiffness, and that this may depend on the specific cell type delivered. Cells which actively remodel collagen may reduce the stiffness of the gel (244). In any case, if tissue matching of gels to host tissue is to become clinically relevant, then a standardised method of measuring gel stiffness is essential.

3.4.9 Conclusion and future directions

Our results show that cOMCs can be propagated *ex vivo* in 3-D type I collagen hydrogel constructs. There was no negative impact on cellular proliferation, and cells remained highly viable at 4 d post-construction. Moreover, we have demonstrated the capacity of these constructs to maintain cells in 3-D distribution, which may increase the likelihood of optimal biodistribution at lesion sites. We have also proven that USE can be used to quickly and reliably provide measures of spinal cord stiffness. These represent the accomplishment of key goals in proof-of-concept research in to the development of tissue-matched protective cell delivery systems for regenerative neurology, and as such are promising in terms of the translational potential of this therapy. Future work will continue to develop a database of spinal cord stiffness readings in an attempt to both optimise the protocol and identify trends in stiffness readings relating to the site and nature of spinal pathology.

Chapter 4: Final conclusions and future directions

4.1 Implications of findings and future research directions

When considered together, the results of the experiments detailed in this thesis support the possibility of creating an implantable plug of genetically enhanced OMCs for delivery to sites of chronic spinal injury in domestic canine patients. Moreover, the demonstration that USE can be used to non-invasively obtain values for the stiffness of the canine spinal cord suggests that future research using these constructs may be able to generate grafts which are tissue-matched to the host site. This thesis has, I hope, highlighted the importance of developing a combinatorial approach to what is a vastly complex pathological scenario, and presented some key findings that could begin to address this.

This thesis has demonstrated single gene delivery to OMC populations. However, in keeping with a combinatorial approach, future research could investigate the possibility of delivering multiple therapeutic genes to OMC populations. Indeed, work in our lab has demonstrated the possibility of engineering multifunctional biopumps, capable of expressing multiple transfected genes simultaneously (155). Indeed, the OMCs engineered here expressed both the reporter and functional gene encoded by the minicircle construct. Future work with OMCs could utilise the small size of minicircle vectors to create OMCs capable of secreting growth factors to regenerate neural tissue, ChABC to break down the glial scar and VEGF to encourage angiogenesis. In this way, multiple barriers to the regeneration of chronically injured spinal tissue could be addressed simultaneously. Further to this, work is currently on going to develop what have been termed “multifunctional nanoplatforms” (152,245). These are magnetic particles that are capable not only of delivering genes to cells, but of other

functions, such as non-invasive tracking post-implantation. Future work to develop the application of these particles In OMCs would need to test a variety of MP formulations in order to evaluate their transfection efficiency and MR contrast enhancement, as well as their cytotoxicity profiles.

This thesis has also demonstrated the 3-D growth of a key pro-regenerative transplant population in a biocompatible, tissue-mimetic implant. However, there is currently no way to ensure that OECs will integrate with regenerating axons once the construct is implanted. Significant work has been undertaken in the development of pre-formed nanotubular scaffolds, which act as conduits for the guidance of regenerating spinal axons, often seeded with guidance cues or a pro-regenerative cell type (246). However, if possible, it may be preferable to generate these conduits from native biological tissue. Work which has characterised the morphological properties of OECs and fibroblasts *in vivo* has noted that they maintain continuous channels which ensheath primary olfactory axons along their length (203). Moreover, electron microscopy studies in to the arrangement of OECs in relation to regenerating axons in both the spinal cord and optic nerve has noted a similar arrangement of OECs ensheathing regenerating axons along their length (247,248). When viewed microscopically, the OMCs grown in hydrogel here in some cases also displayed a longitudinal arrangement. It is tempting to speculate then on the possibility that these cells could be induced to align longitudinally within the 3-D constructs in order to support the growth of regenerating axons. Further work could investigate the potential of generating constructs with pre-aligned OECs. This could be done using emerging 3-D printing

technologies, whereby biological materials such as ECM components can be dispensed through the printing apparatus, including the incorporation of topographical guidance cues which influence cell orientation, on to which individual cells are then "bioprinted" (249). Alternatively, it could be done through the application of stretch forces to the construct, which has been shown to induce alignment in cell populations *in vitro* (250). However, extensive *in vivo* research would be necessary in order to determine what, if any, regenerative benefit this might have.

In addition to the culture of single cells, it may be possible to co-culture OMCs with additional regenerative cell populations may have some benefit. In this way, it may be possible to provide both support of regenerating axons and direct replacement of lost cells cells, such as neurons and oligodendrocytes. Inedeed, OECs have been successfully co-cultured with NSCs in 3-D Matrigel^{TM} constructs, and have been shown to be of benefit in promoting their differentiation, as well as inducing the expression of neuronal processes that are significantly longer than those usually seen in 3-D culture (251). Other researchers have also speculated on the possibility of a synergistic effect between these two cell types when administered in to the injured spinal cord, suggesting that it may be the case that OECs would form "bridges" across which NSCs could then establish synaptic continuity between the lesion stumps (252). Therefore, a possible future direction for this work could be to establish 3-D co-cutures of OECs with other neural cell types, such as NSCs and oligodendrocytes, and conduct morphological evaluations of how these cell types interact, as

well as phenotypic analysis of NSC differentiation profiles using cell-specific markers of differentiation.

Finally, given the safety analyses performed at each stage in the development of the engineering and culture protocols, and the fact that the safety of cOMCs in autologous transplantation in to the injured cord has already been established, there is a strong clinical potential for these treatments. With regards to MPs, several formulations are currently approved for clinical use, and genetically engineered cells have been approved for trials in the CNS (253). Moreover, hydrogel implants in the CNS in pre-clinical studies have largely validated their safety (172). Therefore, ethical approval is currently under application for the implantation of hydrogel matrices in domestic canine subjects. This is with a view to incorporation of autologously derived OMCs in the manner described in **Chapter 3**, before implantation in to the chronically injured cord to evaluate the regenerative potential of this combinatorial approach. In the future this could also involve the incorporation of genetically engineered OMCs, in to the development next-generation nanoengineered regenerative construct.

4.2 Final thoughts

What I have seen as being the purpose of this thesis is to provide an exploration of several components that might later make up a single therapy. My hope is that this work will be continued by our group and others, and that this thesis will be sufficient to lay the groundwork for the incorporation of all the techniques I have shown to be viable in to a singular therapy: an autologous sample of OMCs, safely engineered and distributed homogeneously throughout a protective and supportive matrix. The vision I have for the therapy is one where a dog (or indeed a human) with chronic SCI can have an olfactory mucosal biopsy and a spinal elastography reading taken in the outpatient clinic. The cells are then cultured, engineered and surgically implanted in to the cord in a hydrogel construct.

I do not believe that 50 years from now we will see blanket therapies in use, as we do so often in clinical medicine today. Human pathology is immensely complex, and the move towards combinatorial strategies has occurred in direct recognition of this complexity. I believe, however, that this is only a single step in the right direction. It is the first step towards designing therapies that address not just aspects of a pathology, but the specific qualities of that pathology in a particular patient. Just as cancer therapy comprises a tailored pharmacological care pathway suited to the precise features of a particular tumor, so should we in regenerative neurology seek to tailor our treatments to each injury. As we move in to the future, we must seek to develop therapies that can address the specific needs not just of populations or pathologies, but of patients.

References

1. Lee BB, Cripps R a, Fitzharris M, Wing PC. The global map for traumatic spinal cord injury epidemiology: update 2011, global incidence rate. Spinal Cord. 2013;(February 2012):1–7.
2. Christopherreeve.org. Paralysis Facts and Figures [Internet]. Paralysis Resource Center. 2016 [cited 2016 Feb 18]. Available from: https://www.christopherreeve.org/living-with-paralysis/stats-about-paralysis
3. Spinal-research.org. Facts and figures | Spinal Research [Internet]. 2016 [cited 2016 Feb 18]. Available from: http://www.spinal-research.org/research-matters/spinal-cord-injury/facts-and-figures/
4. Strauss DJ, DeVivo MJ, Paculdo DR, Shavelle RM, Mesard L, Carmody A, et al. Trends in Life Expectancy After Spinal Cord Injury. Arch Phys Med Rehabil. Elsevier; 2006 Aug;87(8):1079–85.
5. Crossman AR, Neary D (Professor of neurology), Crossman B. Neuroanatomy : an illustrated colour text. 192 p.
6. Kerstetter AE, Miller RH. Isolation and culture of spinal cord astrocytes. Methods Mol Biol. NIH Public Access; 2012;814:93–104.
7. Panayiotou E, Malas S. Adult spinal cord ependymal layer: a promising pool of quiescent stem cells to treat spinal cord injury. Front Physiol. Frontiers Media SA; 2013;4:340.
8. Kirshblum SC, Burns SP, Biering-Sorensen F, Donovan W, Graves DE, Jha A, et al.

International standards for neurological classification of spinal cord injury (Revised 2011). J Spinal Cord Med. 2011;34(6):535–46.

9. Kirshblum SC, Burns SP, Biering-Sorensen F, Donovan W, Graves DE, Jha A, et al. International standards for neurological classification of spinal cord injury (revised 2011). J Spinal Cord Med. 2011 Nov;34(6):535–46.

10. New PW, Cripps R a, Bonne Lee B. Global maps of non-traumatic spinal cord injury epidemiology: towards a living data repository. Spinal Cord. 2014;52(2):97–109.

11. Patient.co.uk. Spinal cord injury and compression [Internet]. 2016 [cited 2016 Feb 18]. Available from: http://patient.info/doctor/spinal-cord-injury-and-compression

12. Norenberg MD, Smith J, Marcillo A. The pathology of human spinal cord injury: defining the problems. J Neurotrauma. 2004;21(4):429–40.

13. Tator CH, Fehlings MG. Review of the secondary injury theory of acute spinal cord trauma with emphasis on vascular mechanisms. J Neurosurg. 1991 Jul;75(1):15–26.

14. Bunge RP, Puckett WR, Becerra JL, Marcillo A, Quencer RM. Observations on the pathology of human spinal cord injury. A review and classification of 22 new cases with details from a case of chronic cord compression with extensive focal demyelination. Adv Neurol. 1993;59:75–89.

15. Profyris C, Cheema SS, Zang D, Azari MF, Boyle K, Petratos S. Degenerative and regenerative mechanisms governing spinal cord injury. Vol. 15, Neurobiology of Disease. 2004. p. 415–36.

16. Bains M, Hall ED. Antioxidant therapies in traumatic brain and spinal cord injury. Biochim Biophys Acta - Mol Basis Dis. 2012;1822(5):675–84.

17. Martirosyan NL, Feuerstein JS, Theodore N, Cavalcanti DD, Spetzler RF, Preul MC. Blood supply and vascular reactivity of the spinal cord under normal and pathological conditions. J Neurosurg Spine. 2011 Sep;15(3):238–51.

18. Oyinbo CA. Secondary injury mechanisms in traumatic spinal cord injury: a nugget of this multiply cascade. Acta Neurobiol Exp (Wars). 2011;71(2):281–99.

19. Schanne FA, Kane AB, Young EE, Farber JL. Calcium dependence of toxic cell death: a final common pathway. Science. 1979 Nov 9;206(4419):700–2.

20. Mekhail M, Almazan G, Tabrizian M. Oligodendrocyte-protection and remyelination post-spinal cord injuries: A review. Prog Neurobiol. 2012;96(3):322–39.

21. Richardson PM, McGuinness UM, Aguayo a J. Axons from CNS neurons regenerate into PNS grafts. Vol. 284, Nature. 1980. p. 264–5.

22. Silver J, Miller JH. Regeneration beyond the glial scar. Nat Rev Neurosci. 2004;5(2):146–56.

23. Cregg JM, DePaul MA, Filous AR, Lang BT, Tran A, Silver J. Functional regeneration beyond the glial scar. Exp Neurol. 2014;253:197–207.

24. Macaya D, Spector M. Injectable hydrogel materials for spinal cord regeneration: a review. Biomed Mater. 2012;7(1):012001.

25. Kawano H, Kimura-Kuroda J, Komuta Y, Yoshioka N, Li HP, Kawamura K, et al. Role of the lesion scar in the response to damage and repair of the central nervous system. Cell Tissue Res. Springer-Verlag; 2012 Jul 25;349(1):169–80.

26. Bartus K, James ND, Bosch KD, Bradbury EJ. Chondroitin sulphate proteoglycans: Key modulators of spinal cord and brain plasticity. Exp Neurol. 2012;235(1):5–17.

27. Bradbury EJ, Moon LDF, Popat RJ, King VR, Bennett GS, Patel PN, et al. Chondroitinase ABC promotes functional recovery after spinal cord injury. Nature. 2002;416(6881):636–40.

28. Kanno H, Pressman Y, Moody A, Berg R, Muir EM, Rogers JH, et al. Combination of engineered Schwann cell grafts to secrete neurotrophin and chondroitinase promotes axonal regeneration and locomotion after spinal cord injury. J Neurosci. 2014;34(5):1838–55.

29. Alluin O, Delivet-Mongrain H, Gauthier MK, Fehlings MG, Rossignol S, Karimi-Abdolrezaee S. Examination of the combined effects of chondroitinase ABC, growth factors and locomotor training following compressive spinal cord injury on neuroanatomical plasticity and kinematics. PLoS One. 2014;9(10).

30. Jeffery N. Chondroitinase Clinical Trial [Internet]. 2016 [cited 2016 Jun 13]. Available from: https://vetmed.iastate.edu/vmc/services/clinical-trials/chondroitinase

31. Akbik F, Cafferty WBJ, Strittmatter SM. Myelin associated inhibitors: A link between injury-induced and experience-dependent plasticity. Vol. 235, Experimental Neurology. 2012. p. 43–52.

32. Vargas ME, Barres BA. Why Is Wallerian Degeneration in the CNS So Slow? Annu Rev Neurosci. 2007;30(1):153–79.

33. Chen MS, Huber a B, van der Haar ME, Frank M, Schnell L, Spillmann a a, et al. Nogo-A is a myelin-associated neurite outgrowth inhibitor and an antigen for monoclonal antibody IN-1. Nature. 2000;403(6768):434–9.

34. GrandPré T, Li S, Strittmatter SM. Nogo-66 receptor antagonist peptide promotes

axonal regeneration. Nature. 2002;417(6888):547–51.

35. Simonen M, Pedersen V, Weinmann O, Schnell L, Buss A, Ledermann B, et al. Systemic deletion of the myelin-associated outgrowth inhibitor Nogo-A improves regenerative and plastic responses after spinal cord injury. Neuron. 2003;38(2):201–11.

36. Huebner EA, Strittmatter SM. Axon regeneration in the peripheral and central nervous systems. Results Probl Cell Differ. 2009;48:339–51.

37. Clinicaltrials.gov. Acute Safety, Tolerability, Feasibility and Pharmacokinetics of Intrath. Administered ATI355 in Patients With Acute SCI [Internet]. 2016 [cited 2016 Jun 13]. Available from: https://www.clinicaltrials.gov/ct2/show/NCT00406016?term=NCT00406016&rank=1

38. Levi-montalcini R, Angeletti PU. Nerve growth factor. Physiol Rev. 1968;48(8):534–69.

39. Barde YA, Edgar D, Thoenen H. Purification of a new neurotrophic factor from mammalian brain. EMBO J. 1982;1(5):549–53.

40. Maisonpierre PC, Belluscio L, Squinto S, Ip NY, Furth ME, Lindsay RM, et al. Neurotrophin-3: a neurotrophic factor related to NGF and BDNF. Science. 1990;247(4949 Pt 1):1446–51.

41. Tsintou M, Dalamagkas K, Seifalian AM. Advances in regenerative therapies for spinal cord injury: a biomaterials approach. Neural Regen Res. 2015 May;10(5):726–42.

42. Furlan JC, Noonan V, Cadotte DW, Fehlings MG. Timing of decompressive surgery of spinal cord after traumatic spinal cord injury: an evidence-based examination of pre-clinical and clinical studies. J Neurotrauma. 2011;28(8):1371–99.

43. Fehlings MG, Vaccaro A, Wilson JR, Singh A, W. Cadotte D, Harrop JS, et al. Early versus

Delayed Decompression for Traumatic Cervical Spinal Cord Injury: Results of the Surgical Timing in Acute Spinal Cord Injury Study (STASCIS). Di Giovanni S, editor. PLoS One. Public Library of Science; 2012 Feb 23;7(2):e32037.

44. Juknis N, Cooper JM, Volshteyn O. The changing landscape of spinal cord injury. Handb Clin Neurol. 2012;109:149–66.

45. Short DJ, El Masry WS, Jones PW. High dose methylprednisolone in the management of acute spinal cord injury - a systematic review from a clinical perspective. Spinal Cord. 2000 May;38(5):273–86.

46. Nas K, Yazmalar L, Şah V, Aydın A, Öneş K. Rehabilitation of spinal cord injuries. World J Orthop. 2015;6(1):8–16.

47. Onifer SM, Smith GM, Fouad K. Plasticity After Spinal Cord Injury: Relevance to Recovery and Approaches to Facilitate It. Vol. 8, Neurotherapeutics. 2011. p. 283–93.

48. Edgerton VR, Tillakaratne NJK, Bigbee AJ, de Leon RD, Roy RR. Plasticity of the spinal neural circuitry after injury. Annu Rev Neurosci. 2004;27:145–67.

49. Curt a, Schwab ME, Dietz V. Providing the clinical basis for new interventional therapies: refined diagnosis and assessment of recovery after spinal cord injury. Spinal cord Off J Int Med Soc Paraplegia. 2004;42(1):1–6.

50. Dietz V, Fouad K. Restoration of sensorimotor functions after spinal cord injury. Vol. 137, Brain. 2014. p. 654–67.

51. Dobkin B, Apple D, Barbeau H, Basso M, Behrman A, Deforge D, et al. Weight-supported treadmill vs over-ground training for walking after acute incomplete SCI. Neurology. 2006;66(4):484–92.

52. Alexeeva N, Sames C, Jacobs PL, Hobday L, Distasio MM, Mitchell SA, et al. Comparison of training methods to improve walking in persons with chronic spinal cord injury: a randomized clinical trial. Vol. 34, Journal of Spinal Cord Medicine. 2011. p. 362–79.

53. Ying Z, Roy RR, Zhong H, Zdunowski S, Edgerton VR, Gomez-Pinilla F. BDNF-exercise interactions in the recovery of symmetrical stepping after a cervical hemisection in rats. Neuroscience. 2008;155(4):1070–8.

54. Lobel DA, Lee KH. Brain machine interface and limb reanimation technologies: Restoring function after spinal cord injury through development of a bypass system. In: Mayo Clinic Proceedings. 2014. p. 708–14.

55. Creasey GH, Craggs MD. Functional electrical stimulation for bladder, bowel, and sexual function. Handb Clin Neurol. 2012;109:247–57.

56. Fawcett JW, Curt A, Steeves JD, Coleman WP, Tuszynski MH, Lammertse D, et al. Guidelines for the conduct of clinical trials for spinal cord injury as developed by the ICCP panel: spontaneous recovery after spinal cord injury and statistical power needed for therapeutic clinical trials. Spinal Cord. Nature Publishing Group; 2007 Mar 19;45(3):190–205.

57. Ditunno PL, Patrick M, Stineman M, Ditunno JF. Who wants to walk? Preferences for recovery after SCI: a longitudinal and cross-sectional study. Spinal cord Off J Int Med Soc Paraplegia. 2008;46(7):500–6.

58. van Middendorp JJ, Hosman AJF, Pouw MH, Van de Meent H. ASIA impairment scale conversion in traumatic SCI: is it related with the ability to walk? A descriptive comparison with functional ambulation outcome measures in 273 patients. Spinal

Cord. 2009;47(7):555–60.

59. Ditunno JF, Scivoletto G, Patrick M, Biering-Sorensen F, Abel R, Marino R. Validation of the walking index for spinal cord injury in a US and European clinical population. Spinal Cord. 2008;46(3):181–8.

60. Craig a, Tran Y, Middleton J. Psychological morbidity and spinal cord injury: a systematic review. Spinal Cord. 2009;47(2):108–14.

61. Hoffman JM, Bombardier CH, Graves DE, Kalpakjian CZ, Krause JS. A longitudinal study of depression from 1 to 5 years after spinal cord injury. Arch Phys Med Rehabil. 2011;92(1532-821X (Electronic)):411–8.

62. Heinemann AW, Mamott BD, Schnoll S. Substance use by persons with recent spinal cord injuries. Rehabil Psychol. 1990;35(4):217–28.

63. Tate DG. Alcohol use among spinal cord-injured patients. Am J Phys Med Rehabil / Assoc Acad Physiatr. 1993;72(4):192–5.

64. Kim SU, de Vellis J. Stem cell-based cell therapy in neurological diseases: A review. J Neurosci Res. Wiley Subscription Services, Inc., A Wiley Company; 2009 Aug 1;87(10):2183–200.

65. Culme-Seymour EJ, Davie NL, Brindley DA, Edwards-Parton S, Mason C. A decade of cell therapy clinical trials (2000-2010). Regen Med. 2012 Jul;7(4):455–62.

66. Thomson JA, Itskovitz-Eldor J, Shapiro SS, Waknitz MA, Swiergiel JJ, Marshall VS, et al. Embryonic stem cell lines derived from human blastocysts. Science. American Association for the Advancement of Science; 1998 Nov 6;282(5391):1145–7.

67. Puri MC, Nagy A. Concise Review: Embryonic Stem Cells Versus Induced Pluripotent

Stem Cells: The Game Is On. Stem Cells. Wiley Subscription Services, Inc., A Wiley Company; 2012 Jan;30(1):10–4.

68. Vazin T, Freed WJ. Human embryonic stem cells: derivation, culture, and differentiation: a review. Restor Neurol Neurosci. 2010;28(4):589–603.

69. Antonic A, Sena ES, Lees JS, Wills TE, Skeers P, Batchelor PE, et al. Stem Cell Transplantation in Traumatic Spinal Cord Injury: A Systematic Review and Meta-Analysis of Animal Studies. Vol. 11, PLoS Biology. 2013.

70. Trounson A. Translating Stem Cell Discoveries. In: Stem Cells Handbook. New York, NY: Springer New York; 2013. p. 377–89.

71. Trounson A, McDonald C. Stem Cell Therapies in Clinical Trials: Progress and Challenges. Cell Stem Cell. 2015;17(1):11–22.

72. Oliveri RS, Bello S, Biering-Sørensen F. Mesenchymal stem cells improve locomotor recovery in traumatic spinal cord injury: Systematic review with meta-analyses of rat models. Neurobiol Dis. 2014;62:338–53.

73. Nasef A, Fouillard L, El-Taguri A, Lopez M. Human bone marrow-derived mesenchymal stem cells. Libyan J Med. 2007;2(4):190–201.

74. Squillaro T, Peluso G, Galderisi U. Clinical Trials With Mesenchymal Stem Cells: An Update. Cell Transplant. 2016;25(5):829–48.

75. Takahashi K, Yamanaka S. Induction of pluripotent stem cells from mouse embryonic and adult fibroblast cultures by defined factors. Cell. 2006 Aug 25;126(4):663–76.

76. Wang H, Fang H, Dai J, Liu G, Xu ZJ. Induced pluripotent stem cells for spinal cord injury therapy: current status and perspective. Neurol Sci. 2013;34(1):11–7.

77. Gage FH, Temple S. Neural Stem Cells: Generating and Regenerating the Brain. Neuron. 2013;80(3):588–601.

78. Lu P, Wang Y, Graham L, McHale K, Gao M, Wu D, et al. Long-distance growth and connectivity of neural stem cells after severe spinal cord injury. Cell. 2012;150(6):1264–73.

79. Drago D, Cossetti C, Iraci N, Gaude E, Musco G, Bachi A, et al. The stem cell secretome and its role in brain repair. Vol. 95, Biochimie. 2013. p. 2271–85.

80. Cao QL, Zhang YP, Howard RM, Walters WM, Tsoulfas P, Whittemore SR. Pluripotent stem cells engrafted into the normal or lesioned adult rat spinal cord are restricted to a glial lineage. Exp Neurol. 2001 Jan;167(1):48–58.

81. Mosahebi A, Fuller P, Wiberg M, Terenghi G. Effect of allogeneic Schwann cell transplantation on peripheral nerve regeneration. Exp Neurol. 2002;173(2):213–23.

82. Frostick SP, Yin Q, Kemp GJ. Schwann cells, neurotrophic factors, and peripheral nerve regeneration. Microsurgery. 1998;18:397–405.

83. Ramer LM, Ramer MS, Bradbury EJ. Restoring function after spinal cord injury: Towards clinical translation of experimental strategies. Vol. 13, The Lancet Neurology. 2014. p. 1241–56.

84. Assunção-Silva RC, Gomes ED, Sousa N, Silva NA, Salgado AJ, Silva NA, et al. Hydrogels and Cell Based Therapies in Spinal Cord Injury Regeneration. Stem Cells Int. Hindawi Publishing Corporation; 2015;2015:1–24.

85. Jesuraj NJ, Santosa KB, Macewan MR, Moore AM, Kasukurthi R, Ray WZ, et al. Schwann cells seeded in acellular nerve grafts improve functional recovery. Muscle

Nerve. 2014 Feb;49(2):267–76.

86. East E, Johns N, Georgiou M, Golding JP, Loughlin AJ, Kingham PJ, et al. A 3D in vitro model reveals differences in the astrocyte response elicited by potential stem cell therapies for CNS injury. Regen Med. 2013 Nov;8(6):739–46.

87. Ramon y Cajal S. Estudios sobre la cortexa cerebral humana. Estructura de la corteza cerebral olfativa del hombre y mamiferos. Rev Trim Microg. 1900;(5):1–150.

88. Barnett SC, Riddell JS. Olfactory ensheathing cells (OECs) and the treatment of CNS injury: advantages and possible caveats. J Anat. Wiley-Blackwell; 2004 Jan;204(1):57–67.

89. Gladwin K, Choi D. Olfactory ensheathing cells: Part i - Current concepts and experimental laboratory models. Vol. 83, World Neurosurgery. 2015. p. 114–9.

90. Au E, Roskams AJ. Olfactory ensheathing cells of the lamina propria in vivo and in vitro. Glia. 2003;41(3):224–36.

91. Doucette R, Words KEY. Glial influences on axonal growth in the primary olfactory system. Glia. 1990;3(6):433–49.

92. Gasser HS. Olfactory nerve fibers. J Gen Physiol. 1956;39(4):473–96.

93. De Lorenzo AJ. Electron microscopic observations of the olfactory mucosa and olfactory nerve. Biophys Biochem Cytol. 1957;3(6):839–50.

94. Barber PC, Lindsay RM. Schwann cells of the olfactory nerves contain glial fibrillary acidic protein and resemble astrocytes. Neuroscience. 1982;7(12):3077–90.

95. Doucette JR. The glial cells in the nerve fiber layer of the rat olfactory bulb. Anat Rec. 1984 Oct;210(2):385–91.

96. Pixley SK. The olfactory nerve contains two populations of glia, identified both in vivo and in vitro. Glia. 1992;5:269–84.

97. Franceschini I a, Barnett SC. Low-affinity NGF-receptor and E-N-CAM expression define two types of olfactory nerve ensheathing cells that share a common lineage. Dev Biol. 1996;173(1):327–43.

98. Barraud P, Seferiadis AA, Tyson LD, Zwart MF, Szabo-Rogers HL, Ruhrberg C, et al. Neural crest origin of olfactory ensheathing glia. Proc Natl Acad Sci U S A. 2010 Dec 7;107(49):21040–5.

99. Higginson JR, Barnett SC. The culture of olfactory ensheathing cells (OECs)—a distinct glial cell type. Exp Neurol. 2011;229(1):2–9.

100. Ramón-Cueto A, Nieto-Sampedro M. Regeneration into the spinal cord of transected dorsal root axons is promoted by ensheathing glia transplants. Exp Neurol. 1994 Jun;127(2):232–44.

101. Navarro X, Valero A, Gudiño G, Forés J, Rodríguez FJ, Verdú E, et al. Ensheathing glia transplants promote dorsal root regeneration and spinal reflex restitution after multiple lumbar rhizotomy. Ann Neurol. 1999 Feb;45(2):207–15.

102. Pascual JI, Gudiño-Cabrera G, Insausti R, Nieto-Sampedro M. Spinal implants of olfactory ensheathing cells promote axon regeneration and bladder activity after bilateral lumbosacral dorsal rhizotomy in the adult rat. J Urol. 2002 Mar;167(3):1522–6.

103. Ibrahim AG, Kirkwood PA, Raisman G, Li Y. Restoration of hand function in a rat model of repair of brachial plexus injury. Brain. 2009;132(5):1268–76.

104. Plant GW, Christensen CL, Oudega M, Bunge MB. Delayed transplantation of olfactory ensheathing glia promotes sparing/regeneration of supraspinal axons in the contused adult rat spinal cord. J Neurotrauma. 2003;20(1):1–16.

105. Resnick DK, Cechvala CF, Yan Y, Witwer BP, Sun D, Zhang S. Adult olfactory ensheathing cell transplantation for acute spinal cord injury. J Neurotrauma. 2003 Mar;20(3):279–85.

106. Ramón-Cueto A, Cordero MI, Santos-Benito FF, Avila J. Functional recovery of paraplegic rats and motor axon regeneration in their spinal cords by olfactory ensheathing glia. Neuron. 2000 Feb;25(2):425–35.

107. Li Y, Decherchi P, Raisman G. Transplantation of olfactory ensheathing cells into spinal cord lesions restores breathing and climbing. J Neurosci. 2003;23(3):727–31.

108. Raisman G, Li Y. Repair of neural pathways by olfactory ensheathing cells. Nat Rev Neurosci. 2007;8(4):312–9.

109. Granger N, Blamires H, Franklin RJM, Jeffery ND. Autologous olfactory mucosal cell transplants in clinical spinal cord injury: A randomized double-blinded trial in a canine translational model. Brain. 2012;135(11):3227–37.

110. Lowenstein PR, Castro MG. Uncertainty in the translation of preclinical experiments to clinical trials. Why do most phase III clinical trials fail? Curr Gene Ther. 2009 Oct;9(5):368–74.

111. Jeffrey N, Granger N, Franklin R. Using Naturally Occurring Spinal Cord Injury in Domestic Dogs to Explore Novel Therapeutic Options. In: Aldskogius H, editor. Animal Models of Spinal Cord Repair. 1st ed. Totowa, NJ: Humana Press; 2013. p. 185–205.

(Neuromethods; vol. 76).

112. Millis DL, Ciuperca IA. Evidence for Canine Rehabilitation and Physical Therapy. Vol. 45, Veterinary Clinics of North America - Small Animal Practice. 2015. p. 1–27.

113. Féron F, Perry C, Cochrane J, Licina P, Nowitzke A, Urquhart S, et al. Autologous olfactory ensheathing cell transplantation in human spinal cord injury. Brain. Oxford University Press; 2005 Dec;128(Pt 12):2951–60.

114. Mackay-Sim A, Feron F, Cochrane J, Bassingthwaighte L, Bayliss C, Davies W, et al. Autologous olfactory ensheathing cell transplantation in human paraplegia: A 3-year clinical trial. Brain. 2008;131(9):2376–86.

115. Chhabra HS., Lima C., Sachdeva S., Mittal A., Nigam V., Chaturvedi D., et al. Autologous mucosal transplant in chronic spinal cord injury: An Indian Pilot Study. Spinal Cord. 2009;47(12):887–95.

116. Lima C, Escada P, Pratas-Vital J, Branco C, Arcangeli CA, Lazzeri G, et al. Olfactory mucosal autografts and rehabilitation for chronic traumatic spinal cord injury. Neurorehabil Neural Repair. 2010;24(1):10–22.

117. Senior K. Olfactory ensheathing cells to be used in spinal-cord repair trial. Vol. 1, The Lancet Neurology. 2002.

118. Huang H, Xi H, Chen L, Zhang F, Liu Y. Long-term outcome of olfactory ensheathing cell therapy for patients with complete chronic spinal cord injury. Cell Transplant. 2012;21(SUPPL. 1):S23–31.

119. Tabakow P, Jarmundowicz W, Czapiga B, Fortuna W, Miedzybrodzki R, Czyz M, et al. Transplantation of autologous olfactory ensheathing cells in complete human spinal

cord injury. Cell Transplant. 2013;22(9):1591–612.

120. Chuah MI, Hale DM, West AK. Interaction of olfactory ensheathing cells with other cell types in vitro and after transplantation: Glial scars and inflammation. Vol. 229, Experimental Neurology. 2011. p. 46–53.

121. Richter MW, Fletcher PA, Liu J, Tetzlaff W, Roskams AJ. Lamina Propria and Olfactory Bulb Ensheathing Cells Exhibit Differential Integration and Migration and Promote Differential Axon Sprouting in the Lesioned Spinal Cord. J Neurosci. 2005 Nov 16;25(46):10700–11.

122. Dlouhy BJ, Awe O, Rao RC, Kirby P a, Hitchon PW. Autograft-derived spinal cord mass following olfactory mucosal cell transplantation in a spinal cord injury patient. J Neurosurg Spine. 2014;21(October):1–5.

123. Liu F, Chen T, Zhang J, Chen Z. [Comparison of competence of olfactory globular nerve layer gliocytes, olfactory epithelial gliacytes and SC in repairing nerve defect]. Zhongguo Xiu Fu Chong Jian Wai Ke Za Zhi. 2009;23(1):1–7.

124. Lu P, Yang H, Culbertson M, Graham L, Roskams AJ, Tuszynski MH. Olfactory Ensheathing Cells Do Not Exhibit Unique Migratory or Axonal Growth-Promoting Properties after Spinal Cord Injury. J Neurosci. 2006 Oct 25;26(43):11120–30.

125. Steward O, Sharp K, Selvan G, Hadden A, Hofstadter M, Au E, et al. A re-assessment of the consequences of delayed transplantation of olfactory lamina propria following complete spinal cord transection in rats. Exp Neurol. 2006;198(2):483–99.

126. Centenaro LA, Jaeger M da C, Ilha J, de Souza MA, Kalil-Gaspar PI, Cunha NB, et al. Olfactory and respiratory lamina propria transplantation after spinal cord transection

in rats: effects on functional recovery and axonal regeneration. Brain Res. 2011 Dec 2;1426:54–72.

127. Franklin RJM. Obtaining olfactory ensheathing cells from extra-cranial sources a step closer to clinical transplant-mediated repair of the CNS? Brain. 2002 Jan;125(Pt 1):2–3.

128. Lu J, Féron F, Mackay-Sim A, Waite PME. Olfactory ensheathing cells promote locomotor recovery after delayed transplantation into transected spinal cord. Brain. 2002;125(1):14–21.

129. Li Y, Field PM, Raisman G, Vidal-Sanz M, Neuberger TJ, Cornbrooks CJ, et al. Repair of adult rat corticospinal tract by transplants of olfactory ensheathing cells. Science. American Association for the Advancement of Science; 1997 Sep 26;277(5334):2000–2.

130. Keyvan-Fouladi N, Raisman G, Li Y. Functional repair of the corticospinal tract by delayed transplantation of olfactory ensheathing cells in adult rats. J Neurosci. 2003 Oct 15;23(28):9428–34.

131. Yamamoto M, Raisman G, Li D, Li Y. Transplanted olfactory mucosal cells restore paw reaching function without regeneration of severed corticospinal tract fibres across the lesion. Brain Res. 2009;1303:26–31.

132. Anderson KD. Targeting recovery: priorities of the spinal cord-injured population. J Neurotrauma. 2004 Oct;21(10):1371–83.

133. Mayeur A, Duclos C, Honoré A, Gauberti M, Drouot L, do Rego J-C, et al. Potential of olfactory ensheathing cells from different sources for spinal cord repair. PLoS One. 2013;8(4):e62860.

134. Yang H, Jin WL, Wang CT, You SW, Ju G. [Expression and biological activity of human neurotrophin-3 in olfactory ensheathing cells mediated by retroviral vector]. Shi Yan Sheng Wu Xue Bao. 2003 Feb;36(1):5–12.

135. Cao L, Liu L, Chen Z-Y, Wang L-M, Ye J-L, Qiu H-Y, et al. Olfactory ensheathing cells genetically modified to secrete GDNF to promote spinal cord repair. Brain. 2004 Mar;127(Pt 3):535–49.

136. Ruitenberg MJ, Plant GW, Hamers FPT, Wortel J, Blits B, Dijkhuizen PA, et al. Ex vivo adenoviral vector-mediated neurotrophin gene transfer to olfactory ensheathing glia: effects on rubrospinal tract regeneration, lesion size, and functional recovery after implantation in the injured rat spinal cord. J Neurosci. 2003 Aug 6;23(18):7045–58.

137. Ruitenberg MJ, Levison DB, Lee SV, Verhaagen J, Harvey AR, Plant GW. NT-3 expression from engineered olfactory ensheathing glia promotes spinal sparing and regeneration. Brain. Oxford University Press; 2005 Apr;128(Pt 4):839–53.

138. Wu J, Sun T-S, Ren J-X, Wang X-Z. Ex vivo non-viral vector-mediated neurotrophin-3 gene transfer to olfactory ensheathing glia: effects on axonal regeneration and functional recovery after implantation in rats with spinal cord injury. Neurosci Bull. Shanghai Institutes for Biological Sciences, Chinese Academy of Sciences; 2008 Apr 22;24(2):57–65.

139. Giacca M, Zacchigna S. Virus-mediated gene delivery for human gene therapy. J Control Release. 2012;161(2):377–88.

140. Rothe M, Modlich U, Schambach A. Biosafety challenges for use of lentiviral vectors in gene therapy. Curr Gene Ther. 2013;13(6):453–68.

141. Ojala DS, Amara DP, Schaffer D V. Adeno-Associated Virus Vectors and Neurological Gene Therapy. Neuroscientist. 2015;21(1):84–98.

142. Wu Z, Yang H, Colosi P. Effect of genome size on AAV vector packaging. Mol Ther. 2010 Jan;18(1):80–6.

143. Rogers M-L, Rush RA. Non-viral gene therapy for neurological diseases, with an emphasis on targeted gene delivery. J Control Release. 2012;157(2):183–9.

144. Nayerossadat N, Ali P, Maedeh T. Viral and nonviral delivery systems for gene delivery. Adv Biomed Res. 2012;1(1):27.

145. Mali S. Delivery systems for gene therapy. Indian J Hum Genet. 2013 Jan;19(1):3–8.

146. Ramamoorth M, Narvekar A. Non viral vectors in gene therapy- an overview. J Clin Diagn Res. 2015 Jan;9(1):GE01–6.

147. McBain SC, Yiu HHP, Dobson J. Magnetic nanoparticles for gene and drug delivery. Vol. 3, International Journal of Nanomedicine. 2008. p. 169–80.

148. Benz M. Superparamagnetism : Theory and Applications. 1st ed. 2012. 3-6 p.

149. Subramani K. Applications of nanotechnology in drug delivery systems for the treatment of cancer and diabetes. Int J Nanotechnol. 2006;3(4):557.

150. Nitin N, LaConte LEW, Zurkiya O, Hu X, Bao G. Functionalization and peptide-based delivery of magnetic nanoparticles as an intracellular MRI contrast agent. J Biol Inorg Chem. 2004 Sep;9(6):706–12.

151. Huth S, Lausier J, Gersting SW, Rudolph C, Plank C, Welsch U, et al. Insights into the mechanism of magnetofection using PEI-based magnetofectins for gene transfer. J Gene Med. 2004;6(8):923–36.

152. Pickard M, Chari D. Enhancement of magnetic nanoparticle-mediated gene transfer to astrocytes by “magnetofection”: effects of static and oscillating fields. Nanomedicine (Lond). 2010;5:217–32.

153. Jenkins SI, Pickard MR, Chari DM. Magnetic nanoparticle mediated gene delivery in oligodendroglial cells: A comparison of differentiated cells versus precursor forms. Nano Life. 2013;3(02):1243001.

154. Pickard MR, Chari DM. Robust uptake of magnetic nanoparticles (MNPs) by central nervous system (CNS) microglia: Implications for particle uptake in mixed neural cell populations. Int J Mol Sci. 2010;11(3):967–81.

155. Pickard M, Adams C, Barraud P, Chari D. Using Magnetic Nanoparticles for Gene Transfer to Neural Stem Cells: Stem Cell Propagation Method Influences Outcomes. J Funct Biomater. 2015;6(2):259–76.

156. Mody V V., Cox A, Shah S, Singh A, Bevins W, Parihar H. Magnetic nanoparticle drug delivery systems for targeting tumor. Appl Nanosci. Springer Berlin Heidelberg; 2014 Apr 4;4(4):385–92.

157. Frank JA, Miller BR, Arbab AS, Zywicke HA, Jordan EK, Lewis BK, et al. Clinically applicable labeling of mammalian and stem cells by combining superparamagnetic iron oxides and transfection agents. Radiology. 2003 Aug;228(2):480–7.

158. Sandvig I, Hoang L, Sardella TCP, Barnett SC, Brekken C, Tvedt K, et al. Labelling of olfactory ensheathing cells with micron-sized particles of iron oxide and detection by MRI. Contrast Media Mol Imaging. 7(4):403–10.

159. Valdiglesias V, Fernández-Bertólez N, Kiliç G, Costa C, Costa S, Fraga S, et al. Are iron

oxide nanoparticles safe? Current knowledge and future perspectives. J Trace Elem Med Biol. 2016;

160. Wang Y-XJ. Superparamagnetic iron oxide based MRI contrast agents: Current status of clinical application. Quant Imaging Med Surg. 2011 Dec;1(1):35–40.

161. Soenen SJH, De Cuyper M. Assessing iron oxide nanoparticle toxicity in vitro: current status and future prospects. Nanomedicine (Lond). 2010 Oct;5(8):1261–75.

162. Pickard MR, Barraud P, Chari DM. The transfection of multipotent neural precursor/stem cell transplant populations with magnetic nanoparticles. Biomaterials. 2011;32(9):2274–84.

163. Li L, Adnan H, Xu B, Wang J, Wang C, Li F, et al. Effects of transplantation of olfactory ensheathing cells in chronic spinal cord injury: a systematic review and meta-analysis. Eur Spine J. 2015 May;24(5):919–30.

164. Amer MH, White LJ, Shakesheff KM. The effect of injection using narrow-bore needles on mammalian cells: Administration and formulation considerations for cell therapies. J Pharm Pharmacol. 2015;67(5):640–50.

165. Bjorklund a, Lindvall O. Cell replacement therapies for central nervous system disorders. Nat Neurosci. 2000;3(6):537–44.

166. Aurand ER, Wagner J, Lanning C, Bjugstad KB. Building biocompatible hydrogels for tissue engineering of the brain and spinal cord. J Funct Biomater. 2012;3(4):839–63.

167. Jenkins SI, Yiu HHP, Rosseinsky MJ, Chari DM, Münzel EJ, Williams A, et al. Magnetic nanoparticles for oligodendrocyte precursor cell transplantation therapies: progress and challenges. Mol Cell Ther. BioMed Central; 2014;2(1):23.

168. Führmann T, Tam RY, Ballarin B, Coles B, Elliott Donaghue I, van der Kooy D, et al. Injectable hydrogel promotes early survival of induced pluripotent stem cell-derived oligodendrocytes and attenuates longterm teratoma formation in a spinal cord injury model. Biomaterials. 2016 Mar;83:23–36.

169. Pearse DD, Sanchez AR, Pereira FC, Andrade CM, Puzis R, Pressman Y, et al. Transplantation of Schwann cells and/or olfactory ensheathing glia into the contused spinal cord: Survival, migration, axon association, and functional recovery. Glia. 2007;55(9):976–1000.

170. Modo M, Stroemer RP, Tang E, Patel S, Hodges H. Effects of implantation site of dead stem cells in rats with stroke damage. Neuroreport. 2003 Jan 20;14(1):39–42.

171. Ahmed EM. Hydrogel: Preparation, characterization, and applications: A review. J Adv Res. 2015;6(2):105–21.

172. Perale G, Rossi F, Sundstrom E, Bacchiega S, Masi M, Forloni G, et al. Hydrogels in spinal cord injury repair strategies. Vol. 2, ACS Chemical Neuroscience. 2011. p. 336–45.

173. Burdick JA, Prestwich GD. Hyaluronic acid hydrogels for biomedical applications. Adv Mater. 2011;23(12).

174. Li Y, Rodrigues J, Tomás H. Injectable and biodegradable hydrogels: gelation, biodegradation and biomedical applications. Chem Soc Rev. 2012;41(6):2193–221.

175. Calderon L, Collin E, Velasco-Bayon D, Murphy M, O'Halloran D, Pandit A. Type II collagen-hyaluronan hydrogel--a step towards a scaffold for intervertebral disc tissue engineering. Eur Cell Mater. 2010;20:134–48.

176. Tukmachev D, Forostyak S, Koci Z, Zaviskova K, Vackova I, Vyborny K, et al. Injectable Extracellular Matrix Hydrogels as Scaffolds for Spinal Cord Injury Repair. Tissue Eng Part A. 2016 Feb;22(3-4):306–17.

177. Aurand ER, Lampe KJ, Bjugstad KB. Defining and designing polymers and hydrogels for neural tissue engineering. Vol. 72, Neuroscience Research. 2012. p. 199–213.

178. Ischakov R, Adler-Abramovich L, Buzhansky L, Shekhter T, Gazit E. Peptide-based hydrogel nanoparticles as effective drug delivery agents. Bioorganic Med Chem. 2013;21(12):3517–22.

179. Matsusaki M, Sakaguchi H, Serizawa T, Akashi M. Controlled release of vascular endothelial growth factor from alginate hydrogels nano-coated with polyelectrolyte multilayer films. J Biomater Sci Polym Ed. 2007;18(6):775–83.

180. Singh A, Peppas NA. Hydrogels and scaffolds for immunomodulation. Adv Mater. 2014 Oct;26(38):6530–41.

181. Joosten EA, Bär PR, Gispen WH. Collagen implants and cortico-spinal axonal growth after mid-thoracic spinal cord lesion in the adult rat. J Neurosci Res. 1995 Jul 1;41(4):481–90.

182. Mahoney MJ, Anseth KS. Three-dimensional growth and function of neural tissue in degradable polyethylene glycol hydrogels. Biomaterials. 2006;27(10):2265–74.

183. Ballios BG, Cooke MJ, van der Kooy D, Shoichet MS. A hydrogel-based stem cell delivery system to treat retinal degenerative diseases. Biomaterials. 2010 Mar;31(9):2555–64.

184. Liu N, Tang Z, Yu Z, Xie M, Zhang Y, Yang E, et al. Morphological properties and

proliferation analysis of olfactory ensheathing cells seeded onto three-dimensional collagen-heparan sulfate biological scaffolds. Neural Regen Res. 2012;7(16):1213–9.

185. Wang B, Zhao Y, Lin H, Chen B, Zhang J, Zhang J, et al. Phenotypical analysis of adult rat olfactory ensheathing cells on 3-D collagen scaffolds. Neurosci Lett. 2006 Jun 19;401(1-2):65–70.

186. Novikova LN, Mosahebi A, Wiberg M, Terenghi G, Kellerth J-O, Novikov LN. Alginate hydrogel and matrigel as potential cell carriers for neurotransplantation. J Biomed Mater Res Part A. Wiley Subscription Services, Inc., A Wiley Company; 2006 May;77A(2):242–52.

187. Mah C, Fraites TJ, Zolotukhin I, Song S, Flotte TR, Dobson J, et al. Improved Method of Recombinant AAV2 Delivery for Systemic Targeted Gene Therapy. Mol Ther. Nature Publishing Group; 2002 Jul;6(1):106–12.

188. Scherer F, Anton M, Schillinger U, Henke J, Bergemann C, Krüger A, et al. Magnetofection: enhancing and targeting gene delivery by magnetic force in vitro and in vivo. Gene Ther. 2002 Jan;9(2):102–9.

189. Xu X, Capito RM, Spector M. Plasmid size influences chitosan nanoparticle mediated gene transfer to chondrocytes. J Biomed Mater Res Part A. Wiley Subscription Services, Inc., A Wiley Company; 2008 Mar 15;84A(4):1038–48.

190. Munye MM, Tagalakis AD, Barnes JL, Brown RE, McAnulty RJ, Howe SJ, et al. Minicircle DNA Provides Enhanced and Prolonged Transgene Expression Following Airway Gene Transfer. Sci Rep. 2016;6:23125.

191. Fernandes AR, Chari DM. Part I: Minicircle vector technology limits DNA size

restrictions on ex vivo gene delivery using nanoparticle vectors: Overcoming a translational barrier in neural stem cell therapy. J Control Release. 2016;

192. Fernandes AR, Chari DM. Part II: Functional delivery of a neurotherapeutic gene to neural stem cells using minicircle DNA and nanoparticles: Translational advantages for regenerative neurology. J Control Release. 2016;

193. Weishaupt N, Blesch A, Fouad K. BDNF: The career of a multifaceted neurotrophin in spinal cord injury. Vol. 238, Experimental Neurology. 2012. p. 254–64.

194. Brock JH, Rosenzweig ES, Blesch A, Moseanko R, Havton LA, Edgerton VR, et al. Local and remote growth factor effects after primate spinal cord injury. J Neurosci. 2010;30(29):9728–37.

195. Bonner JF, Connors TM, Silverman WF, Kowalski DP, Lemay M a, Fischer I. Grafted neural progenitors integrate and restore synaptic connectivity across the injured spinal cord. J Neurosci. 2011;31(12):4675–86.

196. Nagahara AH, Tuszynski MH. Potential therapeutic uses of BDNF in neurological and psychiatric disorders. Nat Rev Drug Discov. 2011;10(3):209–19.

197. Jenkins SI, Pickard MR, Granger N, Chari DM. Magnetic nanoparticle-mediated gene transfer to oligodendrocyte precursor cell transplant populations is enhanced by magnetofection strategies. ACS Nano. 2011;5(8):6527–38.

198. McBain SC, Griesenbach U, Xenariou S, Keramane A, Batich CD, Alton EWFW, et al. Magnetic nanoparticles as gene delivery agents: enhanced transfection in the presence of oscillating magnet arrays. Nanotechnology. IOP Publishing; 2008 Oct 8;19(40):405102.

199. Tickle J a., Jenkins SI, Pickard MR, Chari DM. Influence of Amplitude of Oscillating Magnetic Fields on Magnetic Nanoparticle-Mediated Gene Transfer to Astrocytes. Nano Life. 2014;5(1):1450006.

200. Schneider CA, Rasband WS, Eliceiri KW. NIH Image to ImageJ: 25 years of image analysis. Nat Methods. Nature Research; 2012 Jun 28;9(7):671–5.

201. Kim HM, Hwang DH, Lee JE, Kim SU, Kim BG. Ex Vivo VEGF Delivery by Neural Stem Cells Enhances Proliferation of Glial Progenitors, Angiogenesis, and Tissue Sparing after Spinal Cord Injury. Combs C, editor. PLoS One. Public Library of Science; 2009 Mar 25;4(3):e4987.

202. Ruitenberg M, Plant G, Christensen C, Blits B, Niclou S, Harvey A, et al. Viral vector-mediated gene expression in olfactory ensheathing glia implants in the lesioned rat spinal cord. Gene Ther. 2002;9:135–46.

203. Li Y, Field PM, Raisman G. Olfactory ensheathing cells and olfactory nerve fibroblasts maintain continuous open channels for regrowth of olfactory nerve fibres. Glia. 2005;52(3):245–51.

204. Tomé M, Lindsay SL, Riddell JS, Barnett SC. Identification of Nonepithelial Multipotent Cells in the Embryonic Olfactory Mucosa. Stem Cells. Wiley Subscription Services, Inc., A Wiley Company; 2009 Sep;27(9):2196–208.

205. Roloff F, Ziege S, Baumgärtner W, Wewetzer K, Bicker G, Bradbury E, et al. Schwann cell-free adult canine olfactory ensheathing cell preparations from olfactory bulb and mucosa display differential migratory and neurite growth-promoting properties in vitro. BMC Neurosci. BioMed Central; 2013;14(1):141.

206. Barnett SC, Chang L. Olfactory ensheathing cells and CNS repair: Going solo or in need of a friend? Vol. 27, Trends in Neurosciences. 2004. p. 54–60.

207. Toft A, Tome M, Barnett SC, Riddell JS. A comparative study of glial and non-neural cell properties for transplant-mediated repair of the injured spinal cord. Glia. Wiley Subscription Services, Inc., A Wiley Company; 2013 Apr;61(4):513–28.

208. Aurand ER, Wagner JL, Shandas R, Bjugstad KB. Hydrogel formulation determines cell fate of fetal and adult neural progenitor cells. Stem Cell Res. 2014 Jan;12(1):11–23.

209. Park J, Lim E, Back S, Na H, Park Y, Sun K. Nerve regeneration following spinal cord injury using matrix metalloproteinase-sensitive, hyaluronic acid-based biomimetic hydrogel scaffold containing brain-derived neurotrophic factor. J Biomed Mater Res A. 2010 Jun 1;93(3):1091–9.

210. Horn EM, Beaumont M, Shu XZ, Harvey A, Prestwich GD, Horn KM, et al. Influence of cross-linked hyaluronic acid hydrogels on neurite outgrowth and recovery from spinal cord injury. J Neurosurg Spine. 2007 Feb;6(2):133–40.

211. Hejcl A, Sedý J, Kapcalová M, Toro DA, Amemori T, Lesný P, et al. HPMA-RGD hydrogels seeded with mesenchymal stem cells improve functional outcome in chronic spinal cord injury. Stem Cells Dev. 2010 Oct;19(10):1535–46.

212. Rauch MF, Hynes SR, Bertram J, Redmond A, Robinson R, Williams C, et al. Engineering angiogenesis following spinal cord injury: a coculture of neural progenitor and endothelial cells in a degradable polymer implant leads to an increase in vessel density and formation of the blood-spinal cord barrier. Eur J Neurosci. 2009 Jan;29(1):132–45.

213. Gao M, Lu P, Bednark B, Lynam D, Conner JM, Sakamoto J, et al. Templated agarose

scaffolds for the support of motor axon regeneration into sites of complete spinal cord transection. Biomaterials. 2013 Feb;34(5):1529–36.

214. Itosaka H, Kuroda S, Shichinohe H, Yasuda H, Yano S, Kamei S, et al. Fibrin matrix provides a suitable scaffold for bone marrow stromal cells transplanted into injured spinal cord: A novel material for CNS tissue engineering. Neuropathology. Blackwell Publishing Asia; 2009 Jun;29(3):248–57.

215. Palsson B, Bhatia S. Tissue Engineering. 1st ed. Prentice Hall; 2003.

216. Seyedhassantehrani N, Li Y, Yao L. Dynamic behaviors of astrocytes in chemically modified fibrin and collagen hydrogels. Integr Biol (Camb). 2016 May 16;8(5):624–34.

217. Georges PC, Miller WJ, Meaney DF, Sawyer ES, Janmey P a. Matrices with compliance comparable to that of brain tissue select neuronal over glial growth in mixed cortical cultures. Biophys J. 2006;90(8):3012–8.

218. Seidlits SK, Khaing ZZ, Petersen RR, Nickels JD, Vanscoy JE, Shear JB, et al. The effects of hyaluronic acid hydrogels with tunable mechanical properties on neural progenitor cell differentiation. Biomaterials. 2010 May;31(14):3930–40.

219. Saha K, Keung AJ, Irwin EF, Li Y, Little L, Schaffer D V, et al. Substrate modulus directs neural stem cell behavior. Biophys J. 2008;95(9):4426–38.

220. Leipzig ND, Shoichet MS. The effect of substrate stiffness on adult neural stem cell behavior. Biomaterials. 2009;30(36):6867–78.

221. Tunturi a R. Elasticity of the spinal cord, pia, and denticulate ligament in the dog. J Neurosurg. 1978;48(6):975–9.

222. Hung TK, Chang GL. Biomechanical and neurological response of the spinal cord of a

puppy to uniaxial tension. J Biomech Eng. 1981;103(1):43–7.

223. Bhatia K. Thyroid Elastography. In: Sofferman R, Ahuja A, editors. Ultrasound of the Thyroid and Parathyroid Glands. 1st ed. Springer Science & Business Media; 2012. p. 277.

224. Wells PNT, Liang H-D. Medical ultrasound: imaging of soft tissue strain and elasticity. J R Soc Interface. 2011;8(64):1521–49.

225. Parker KJ, Doyley MM, Rubens DJ. Imaging the elastic properties of tissue: the 20 year perspective. Phys Med Biol. 2012;57:5359–60.

226. Fenster a, Downey DB, Cardinal HN. Three-dimensional ultrasound imaging. Phys Med Biol. 2001;46(5):R67–99.

227. Choi YJ, Lee JH, Baek JH. Ultrasound elastography for evaluation of cervical lymph nodes. Ultrason (Seoul, Korea). 2015 Jul;34(3):157–64.

228. Youk JH, Son EJ, Park AY, Kim J-A. Shear-wave elastography for breast masses: local shear wave speed (m/sec) versus Young modulus (kPa). Ultrason (Seoul, Korea). 2014 Jan;33(1):34–9.

229. Arslantunali D, Dursun T, Yucel D, Hasirci N, Hasirci V. Peripheral nerve conduits: technology update. Med Devices (Auckl). 2014;7:405–24.

230. Yoshii S, Oka M, Shima M, Akagi M, Taniguchi A. Bridging a spinal cord defect using collagen filament. Spine (Phila Pa 1976). 2003 Oct 15;28(20):2346–51.

231. Li X, Yang Z, Zhang A, Wang T, Chen W. Repair of thoracic spinal cord injury by chitosan tube implantation in adult rats. Biomaterials. 2009 Feb;30(6):1121–32.

232. Yao L, Daly W, Newland B, Yao S, Wang W, Chen BKK, et al. Improved axonal

regeneration of transected spinal cord mediated by multichannel collagen conduits functionalized with neurotrophin-3 gene. Gene Ther. 2013 Dec;20(12):1149–57.

233. Göpferich A. Mechanisms of polymer degradation and erosion. Biomaterials. 1996;17(2):103–14.

234. Zhu J, Marchant RE. Design properties of hydrogel tissue-engineering scaffolds. Expert Rev Med Devices. 2011;8(5):607–26.

235. Bailey AJ. Molecular mechanisms of ageing in connective tissues. Vol. 122, Mechanisms of Ageing and Development. 2001. p. 735–55.

236. Polikov VS, Tresco PA, Reichert WM. Response of brain tissue to chronically implanted neural electrodes. J Neurosci Methods. 2005;148:1–18.

237. Komlosh ME, Özarslan E, Lizak MJ, Horkayne-Szakaly I, Freidlin RZ, Horkay F, et al. Mapping average axon diameters in porcine spinal cord white matter and rat corpus callosum using d-PFG MRI. Neuroimage. 2013 Sep;78:210–6.

238. Lang NR, Münster S, Metzner C, Krauss P, Schürmann S, Lange J, et al. Estimating the 3D pore size distribution of biopolymer networks from directionally biased data. Biophys J. 2013 Nov 5;105(9):1967–75.

239. Yang Y, Motte S, Kaufman LJ. Pore size variable type I collagen gels and their interaction with glioma cells. Biomaterials. 2010 Jul;31(21):5678–88.

240. Thonhoff JR, Lou DI, Jordan PM, Zhao X, Wu P. Compatibility of human fetal neural stem cells with hydrogel biomaterials in vitro. Brain Res. 2008;1187:42–51.

241. Shen ZL, Kahn H, Ballarini R, Eppell SJ. Viscoelastic properties of isolated collagen fibrils. Biophys J. 2011 Jun 22;100(12):3008–15.

242. Busby GA, Grant MH, MacKay SP, Riches PE. Confined compression of collagen hydrogels. J Biomech. 2013;46(4):837–40.

243. Willits RK, Skornia SL. Effect of collagen gel stiffness on neurite extension. J Biomater Sci Polym Ed. 2004;15(12):1521–31.

244. Raub CB, Putnam AJ, Tromberg BJ, George SC. Predicting bulk mechanical properties of cellularized collagen gels using multiphoton microscopy. Acta Biomater. 2010 Dec;6(12):4657–65.

245. Zhou F, Zheng T, Abdel-Halim ES, Jiang L, Zhu J-J, Dreaden EC, et al. A multifunctional core–shell nanoplatform for enhanced cancer cell apoptosis and targeted chemotherapy. J Mater Chem B. 2016;4(17):2887–94.

246. Sakiyama-Elbert S, Johnson PJ, Hodgetts SI, Plant GW, Harvey AR. Scaffolds to promote spinal cord regeneration. Handb Clin Neurol. 2012;109:575–94.

247. Li Y, Sauvé Y, Li D, Lund RD, Raisman G. Transplanted olfactory ensheathing cells promote regeneration of cut adult rat optic nerve axons. J Neurosci. 2003 Aug 27;23(21):7783–8.

248. Li Y, Field PM, Raisman G. Regeneration of adult rat corticospinal axons induced by transplanted olfactory ensheathing cells. J Neurosci. 1998 Dec 15;18(24):10514–24.

249. Bhuthalingam R, Lim PQ, Irvine S, Agrawal A, Mhaisalkar P, An J, et al. A novel 3D printing method for cell alignment and differentiation. Int J Bioprinting. 2015 Jul 2;1(1).

250. Li Y, Huang G, Zhang X, Wang L, Du Y, Lu TJ, et al. Engineering cell alignment in vitro. Biotechnol Adv. 2014;32(2):347–65.

251. Sethi R, Sethi R, Redmond A, Lavik E. Olfactory ensheathing cells promote differentiation of neural stem cells and robust neurite extension. Stem Cell Rev. NIH Public Access; 2014 Dec;10(6):772–85.

252. Ao Q, Wang AJ, Chen GQ, Wang SJ, Zuo HC, Zhang XF. Combined transplantation of neural stem cells and olfactory ensheathing cells for the repair of spinal cord injuries. Med Hypotheses. 2007;69(6):1234–7.

253. Aboody K, Capela A, Niazi N, Stern JH, Temple S. Translating stem cell studies to the clinic for CNS repair: current state of the art and the need for a Rosetta stone. Neuron. 2011 May 26;70(4):597–613.